

**A COMPREHENSIVE LITERATURE REVIEW OF LINER
FAILURES AND LONGEVITY**

Submitted

to

**Florida Center for Solid and Hazardous Waste Management
University of Florida**

By

**Dr. D.V. Reddy
(Principal Investigator)**

and

**Boris Butul
(Research Assistant)**

**Center for Marine Structures and Geotechnique
Department of Ocean Engineering
Florida Atlantic University**

July 12, 1999

U.S. NUCLEAR REGULATORY COMMISSION
In the Matter of LOUISIANA ENERGY SERVICES, LP
Docket No. 70-3103-M2 Official Exhibit No. 45
OFFERED by: Applicant/Licensee NREAS/PC Intervenor NREAS/PC
NRC Staff _____ Other _____
IDENTIFIED on 2/7/95 Witness/Panel G. Rice
Action Taken: ADMITTED REJECTED WITHDRAWN
Reporter/Clerk Bethany Engel

DOCKETED
USNRC

2005 MAR -3 PM 4:18

OFFICE OF THE SECRETARY

ADMINISTRATIVE STAFF

ABSTRACT

A comprehensive review of landfill liner failures, the causes and consequences, and design methodology to avoid failures are presented.

In Chapter 1 the types of liner are reviewed. The different materials, types of liners, and manufacturing procedure are explained in detail, providing a base for a better understanding of the problems associated with liners. Currently used liners are comprised of composite structures of clay and geosynthetic materials. The commonly used geosynthetic materials are HDPE (High Density Polyethylene), PVC (Polyvinyl Chloride), and PP (Polypropylene); they are produced in the form of geomembranes (impermeable) and geonets (permeable) of different thickness.

Chapter 2 deals with the properties of polymeric geomembranes as well as those of geosynthetic clay liners. The physical, mechanical, hydraulic, and endurance properties are listed and explained, referencing the different standards associated with each properties.

Chapter 3 addresses the different modes of failures and liner degradation.

Creep is the deformation of a material over a prolonged period of time and under constant pressure. This phenomenon is mainly a function of the temperature, load, and time; and is of primary importance since geosynthetics are very sensitive to creep. Under sustained constant loading, the material will elongate and break. This problem can be eliminated by using a resin that is not affected by creep, and by a proper design that limits the high stress in the geomembrane.

Stress cracking is the brittle fracture of a geosynthetic material under significantly lower stress than the material yield strength. The factors influencing this phenomenon are: UV (Ultraviolet) radiation, temperature, temperature gradient, chemical agent, and stress (particularly fatigue). Stress Cracking leads to small cracks and even holes in the geomembrane, that allow leakage through the membrane. This can be prevented by using a UV and chemical resistant resin and by limiting high stress in the liner.

Damage caused by puncture will plastically deform the material up to failure and cause leaks. Static puncture is due to contact of stones on the geosynthetic under high static load (weight of the waste), while dynamic puncture is due to the fall of objects mainly occurring during installation. Static puncture may be eliminated by using protective layers made of geonets and rounded soil particles, as well as stiff and thick geomembranes. Dynamic puncture can be eliminated by considerable care in construction (skilled workmanship is required).

Seams are the weakest points of a liner. Many problems encountered in landfill originate at seam locations. Seams are regions of high stress concentration due to defects in seaming operations and residual stresses. Also, stress cracking and brittle fractures can

deteriorate and even break seams. It is possible to reduce damage considerably at seams by using proper equipment, workmanship, quality construction, and proper inspection.

Shear properties of liners are very important for the stability of the landfill, particularly earthquakes. The materials comprising the liners, their roughness, their stiffness, the normal load; and the temperature are factors influencing interface shear strength.

Aging of geomembranes is also an important problem, since environmental conditions such as temperature, UV, oxidation, and chemical agent tend to deteriorate the liners. The modes of failure are as follows: a) softening and loss of physical properties due to depolymerization and molecular scission, b) stiffening and embrittlement due to loss of plasticizers and additives, c) reduction of mechanical properties and increase of permeability, and d) failure of membrane seams. In the majority of cases there are combinations of these factors, which can cause damage to the liner system.

Chapter 4 deals with the design and construction methods currently used, as well as quality assurance/control criteria required to ensure long term performance of the liners. It is pointed out that a good design taking into account all the problems outlined in this report will yield a theoretically flawless liner. This has to be followed by reasonable "flawless" construction, with quality assurance and control.

Finally, methods for the life prediction of geosynthetics are reviewed in Chapter 5. The four methods are the time-temperature (WLF) superposition, the Arrhenius equation, the rate process method, and the bidirectional shifting method.

It is concluded that with proper design, construction, and inspection, the safe performance life of landfill liners can be considerably increased, with significant cost-benefit ratios.

INTRODUCTION

Landfills continue to be the most predominant method of waste disposal. Due to the public resistance to landfill construction and operation, the Environment Protection Agency (EPA) has established the Resource Conservation and Recovery Act (RCRA) Subtitle D program. The program requires a landfill lining system, which is composed of primary and secondary liners, leakage detection and leakage collection systems, to be used in the construction of new landfills.

The liners are composed of High Density Polyethylene (HDPE), Polyvinylchloride (PVC), and Polypropylene (PP). These materials are used for their high values of chemical resistance, elastic modulus, yield and puncture strength, and weathering resistance. The primary function of the liner is to create an impermeable barrier, which is the last line of defense in protecting the groundwater. The groundwater is in constant danger of becoming contaminated from leachate, which is liquid that migrates through the landfill, either from precipitation, or already present in the waste.

There are many steps in the construction of the liner, or of the landfill, during which the liner may become damaged. These flaws cause the material to prematurely fail and significantly increase the cost of the project. Quality Assurance and Quality Control are the methods being used to prevent damage during construction and installation. Questions are still being raised about how long the material can perform. Research to predict the service life of the material, with and without installation damage, is of paramount importance. Work on a project of the Principal Investigator, entitled "Life Prediction of HDPE Geomembranes in Solid Waste Landfills", sponsored by Florida Center for Solid and Hazardous Waste Management (FCSHWM), identified the need for an extensive state-of-the art literature review of liner failures and longevity.

TABLE OF CONTENTS

1	DIFFERENT TECHNOLOGIES OF LANDFILL LINERS.....	1
1.1	DIFFERENT MATERIALS	1
1.1.1	Compacted Clay.....	1
1.1.2	Modified Soils	1
1.1.3	Geomembranes (Synthetic liners)	1
1.2	TYPES OF LINERS	3
1.2.1	Single liner.....	3
1.2.2	Single composite	3
1.2.3	Double liner.....	5
1.2.4	Double composite liner	5
1.3	MANUFACTURING CONSIDERATIONS	5
1.4	REFERENCES	6
2	PROPERTIES OF GEOMEMBRANES	7
2.1	POLYMERIC GEOMEMBRANES	7
2.1.1	Physical properties.....	7
2.1.2	Mechanical properties.....	8
2.1.3	Endurance properties	10
2.2	GEOSYNTHETIC CLAY LINERS (GCLs).....	11
2.2.1	Physical properties.....	11
2.2.2	Hydraulic properties	11
2.2.3	Mechanical Properties	12
2.3	EXAMPLE OF GEOMEMBRANE PROPERTIES	12
2.4	REFERENCES	17
3	LINER FAILURE AND PREDICTION.....	18
3.1	CREEP.....	19
3.1.1	Definition.....	19
3.1.2	Different phases of creep response	20
3.1.3	Tensile creep behavior	20
3.1.4	Multi-axial tensile creep.....	20
3.1.5	Creep rupture envelope.....	21
3.1.6	Compressive creep	22
3.1.7	References.....	24
3.2	STRESS CRACKING.....	25
3.2.1	Definition.....	25
3.2.2	Different types of failure	25
3.2.3	Mechanism of Stress Cracking.....	26
3.2.4	Microscopic aspects of SC.....	27
3.2.5	Reasons for SC.....	29
3.2.6	Different factors affecting the SC behavior of geomembranes.....	30
3.2.7	Repair of crack.....	31
3.2.8	Study of Geogrids.....	31
3.2.9	Field investigation.....	32
3.2.10	Brittle cracking.....	32
3.2.11	Review of the Stress Cracking Evaluation Test	33
3.2.12	How to prevent SC.....	36
3.2.13	Method of prediction.....	36

3.2.14	References.....	37
3.3	PUNCTURE/INSTALLATION DAMAGE.....	39
3.3.1	Introduction	39
3.3.2	Methods of prediction.....	39
3.3.3	Laboratory tests	43
3.3.4	Full-scale tests	47
3.3.5	Parameters influencing puncture resistance and installation damages	51
3.3.6	Design and construction of the protecting layer	51
3.3.7	Values of tests results	53
3.3.8	Conclusions.....	57
3.3.9	References.....	59
3.4	SEAMS	61
3.4.1	Different seaming technologies	61
3.4.2	Tests of double track fusion seams and effect of wedge geometry and roller pressure	64
3.4.3	Peel and shear tests.....	64
3.4.4	Impact resistance test.....	66
3.4.5	Effect of temperature and freeze-thaw cycles.....	68
3.4.6	Residual stresses in geomembrane sheets and seams	69
3.4.7	Strain concentrations adjacent to the seams	69
3.4.8	Stress cracking in the seams	71
3.4.9	Brittle fracture in seams	72
3.4.10	Seam inspection	72
3.4.11	Difficulties associated with seaming and the mode of failure	73
3.4.12	References.....	76
3.5	SEISMIC RESPONSE AND INTERFACE STRENGTH.....	78
3.5.1	Introduction	78
3.5.2	Monotonic tests	78
3.5.3	Seismic Response/dynamic shear tests	82
3.5.4	Influence of material roughness.....	86
3.5.5	A theoretical evaluation of interface stability.....	87
3.5.6	Conclusions.....	89
3.5.7	References.....	90
3.6	EFFECT OF NATURAL PARAMETERS ON GEOSYNTHETIC AGING	93
3.6.1	Introduction	93
3.6.2	Conditions at the liner level	93
3.6.3	Different stresses to which the liner is subjected.....	94
3.6.4	Environmental effects during construction	95
3.6.5	Environmental effect during service life	95
3.6.6	Degradation processes	96
3.6.7	Assessment of long term aging through tests.....	107
3.6.8	Summary	108
3.6.9	References.....	110
3.7	OTHER PROBLEMS AFFECTING GEOMEMBRANES LIFE.....	112
3.7.1	Contaminated lifespan and stochastic analysis.....	112
3.7.2	Residual stresses	112
3.7.3	Geomembrane uplift by wind.....	112
3.7.4	Rate of leakage through membranes.....	114
3.7.5	References.....	119
4	DESIGN, CONSTRUCTION, AND QUALITY PROGRAM.....	121
4.1	DESIGN	121
4.2	SAFETY ANALYSIS	122
4.3	CONSTRUCTION/INSTALLATION.....	124
4.4	QUALITY CONTROL	127

4.5	COST OF QUALITY CONTROL.....	133
4.6	REFERENCES	134
5	LIFE PREDICTION.....	136
5.1	VISCOELASTICITY.....	136
5.2	LIFE PREDICTION.....	140
5.2.1	WLF Method	141
5.2.2	Arrhenius equation.....	142
5.2.3	Rate Process Method (RPM).....	143
5.2.4	Bi-directional shifting method (BSM)	144
5.3	REFERENCES.....	145
6	CONCLUSIONS.....	146

LIST OF FIGURES

Figure 1: Cross section of different liner systems	4
Figure 2: Typical creep curves (3)	19
Figure 3: Creep Rupture Envelope (2)	21
Figure 4: Typical compressive creep curves (8)	23
Figure 5: Different faces of the specimen. Left: Ductile, Center: Brittle, Right: Quasi Brittle	25
Figure 6: Crack and craze formation in HDPE geomembranes (3)	26
Figure 7: Conceptualization of ductile and brittle failure mechanisms in semi-crystalline polymer materials, after Lustigier and Rosenberg (4).	28
Figure 8: Strain gage rosette for hole drilling method (9)	30
Figure 9: Effect of different factor on stress cracking behavior (5)	31
Figure 10: Behavior of HDPE Material in a NCTL Test (3)	34
Figure 11: Seam test SCTL specimens (3)	36
Figure 12: Mechanical puncture parameters (2)	40
Figure 13: Graph providing the stress at the geomembrane level (left) and its thickness (right) (2)	40
Figure 14: Model of a gravel puncturing a geomembrane (3)	41
Figure 15: Configuration of a pressurized geomembrane placed on a uniform layer of stone (4)	42
Figure 16: Stone contact on a geomembrane (4)	43
Figure 17: Setting of the pressure chamber used during the first part of this project (5)	44
Figure 18: Pressure plate apparatus (6)	45
Figure 19: Profile of the sheet plate by laser scanning (6)	45
Figure 20: Pyramid piston apparatus (6)	45
Figure 21: Puncture resistance summation of two different components of a liner (7)	47
Figure 22: Cross section of single composite and double composite liners (9)	53
Figure 23: Different techniques of seaming (16)	63
Figure 24: Shear (a) and peel (b) tests (4)	65
Figure 25: Notch location on a double track fusion seams for a notched stress rupture test (11)	68
Figure 26: Sheet alignment due to tensile forces (12)	70
Figure 27: Strains in an air exposed geomembrane (12)	70
Figure 28: Failure occurs in the lower sheet (12)	71
Figure 29: Ring shear test apparatus (5)	79
Figure 30: Inclined friction test apparatus (15)	81
Figure 31: Test apparatus for dynamic shear properties (16)	83
Figure 32: Dynamic response of geomembrane/sand interface (left) and geomembrane/geotextile interface (right) (16)	84
Figure 33: Definition of roughness parameter by Dove and Frost (21).	86
Figure 34: Definition of t_A , t_B , and $t_{10\sigma}$ (22)	88
Figure 35: Influence of geomembrane coating on thermal properties (5)	98
Figure 36: Topography of waves induced by UV radiation (6)	100
Figure 37: Wavelength Spectrum of UV radiation (12)	101
Figure 38: Burst test in presence of different chemicals (11)	103
Figure 39: Geomembrane uplift (3)	113
Figure 40: Pressure distribution on the surface of a cylinder (3)	113
Figure 41: Wind blowing over an empty reservoir (3)	114
Figure 42: Schematic of a tilt-table (6)	117
Figure 43: Horizontal flow between the soil and the geomembrane (4)	117
Figure 44: Pipe penetration (13)	126
Figure 45: Roll spreader bar (13)	126
Figure 46: Anchor trench (13)	127
Figure 47: Structural organization of MQC/MQA and CQC/CQA (14)	128
Figure 48: Model of viscoelastic behavior	137

<i>Figure 49: Viscoelastic response, creep (constant load)</i>	<i>138</i>
<i>Figure 50: Viscoelastic response, stress relaxation (constant deformation)</i>	<i>138</i>
<i>Figure 51: Constant stress-strain time coordinates (1)</i>	<i>138</i>
<i>Figure 52: Schematic of the viscoelastic behavior of polymers</i>	<i>139</i>
<i>Figure 53: Creep-rupture behavior for semi-crystalline polymers (2)</i>	<i>140</i>
<i>Figure 54: Master curve from experimentally measured modulus-time curves various temperatures (3)</i>	<i>141</i>
<i>Figure 55: Master curves at different load levels</i>	<i>142</i>
<i>Figure 56: Generalized Arrhenius, for a specified stress level, used for life prediction from super-ambient temperature experimental data (7)</i>	<i>143</i>

LIST OF TABLES

<i>Table 1: Mechanical Properties of Different Geomembranes</i>	13
<i>Table 2: Water Vapor Transmission Values (2)</i>	14
<i>Table 3: Values for Geomembranes Tensile Test on Sheets and Shear Test on Seams (1)</i>	14
<i>Table 4: Tensile Behavior Properties of 60-mil HDPE, 40-mil VLDPE, 30-mil PVC, and 36-mil CSPE-R (1)</i>	15
<i>Table 5: Impact Resistance of Different Geomembranes (1)</i>	15
<i>Table 6: Friction Values and Efficiencies for Soil to Geomembrane Interfaces (3)</i>	16
<i>Table 7: Friction Values and Efficiencies of Geotextile/Geomembrane Interfaces (3)</i>	16
<i>Table 8: Coefficients of Linear Thermal Expansion for Different Polymeric Materials (1)</i>	16
<i>Table 9: Fracture Toughness (K) Values of Different Polymers (4)</i>	27
<i>Table 10: Survivability Levels for Slope and Wall Application (15)</i>	54
<i>Table 11: Partial Factors of Safety to Account for Installation Damage (15)</i>	55
<i>Table 12: Effect of Installation Damage on Strength, Strain, and Modulus (15)</i>	55
<i>Table 13: Survivability Level for Separation and Embankment Application (15)</i>	57
<i>Table 14: Compatibility Between Seam Techniques and Resins (17)</i>	63
<i>Table 15: Nondestructive Geomembrane Seam Testing (17)</i>	73
<i>Table 16: Different Possibilities of Failure for Dual Wedge-Weld Seams (19)</i>	74
<i>Table 17: Different Possibilities of Failure in an Extrusion Fillet-Wedge Seam (19)</i>	75
<i>Table 18: Summary of Tests Results (5)</i>	80
<i>Table 19: Results of Inclined Friction Tests (15)</i>	82
<i>Table 20: Explanation of Terms in the Factor of Safety by Giroud et al. (22)</i>	88
<i>Table 21: Typical Chemicals in a Landfill Environment</i>	93
<i>Table 22: Coefficient of Thermal Expansion of HDPE and PVC (5)</i>	97
<i>Table 23: Average Temperature in Black and White Geomembrane (6)</i>	99
<i>Table 24: Effect of Geomembrane Exposure to Weathering and Waste (1)</i>	108
<i>Table 25: Problems Associated with Liner Design (2)</i>	121
<i>Table 26: Requirement of a Safe Liner System (4)</i>	122
<i>Table 27: Typical Range of Quality Costs (12)</i>	133

1 Different Technologies of Landfill Liners

This chapter deals with the technologies used in the different types of landfill liners currently used in Municipal Solid Waste Landfills.

1.1 Different Materials

1.1.1 Compacted Clay

Compacted clays find applications as both primary and underlying components of liners in waste containment systems. When properly compacted, clay liners have a permeability of 10^{-7} cm/s or less due to the small particles, and plastic characteristics of clay. Thus clay is considered a highly effective and economical liner material. (1)

Long-term performance of clay liners is a function of properties, such as low permeability, low diffusivity, ductility, internal and interface shear strengths, chemical compatibility, chemical retardation, minimum of preferential flow paths, and good constructability. Factors such as soil composition, placement and construction conditions, post-construction changes, and chemical compatibility affect these properties.

1.1.2 Modified Soils

When the local soil is not suitable for use as a liner, current practice is to add commercially produced bentonites or other clay minerals in the in-situ soil to lower the permeability. Since bentonite is an expansive material (resulting mainly from its sodium-montmorillonite component), only a small quantity needs to be mixed to improve the soil's permeability.

The efficiency of the modified soil depends on many characteristics such as the form of bentonite used (granular or powdered), mineralogy (percentage of sodium and/or calcium-montmorillonite), the rate of application, the characteristics of the soil (lift thickness, moisture content, and the size, type, and operation of the roller), and the use of good quality control operations (1)

1.1.3 Geomembranes (Synthetic liners)

The recent years have seen a dramatic increase in the utilization of synthetic liners, mainly due to their easy availability and low volume consumption. Geomembranes are manufactured with thicknesses ranging from 1 to 3 mm (30 to 120 mils). Landfill liners generally require geomembranes having a thickness at least equal to 80-mil (1). However, certain states as Florida, allow the use of 60-mil geomembrane when the membrane is made of HDPE material.

To assess the geomembrane's chemical compatibility with the site-specific leachate, laboratory testing is highly recommended before the installation of the membranes in the site.

The main materials used in the United States for the manufacturing of geomembranes are described below.

*** Polyethylene (PE):**

The most commonly used polyethylene is HDPE (High Density Polyethylene). Effectively, the semicrystalline (40-50%) microstructure of HDPE is responsible for the material's high strength, and excellent chemical resistance to many chemicals. Sealing membranes can also be made of CPE (Chlorinated Polyethylene). CPE powder is obtained by PE chlorination in the wet phase. The properties depend mainly on the quality of the PE and the degree of chlorination; moreover polyester fabric or sheet can improve the structural properties of CPE (2).

*** Polyvinylchloride (PVC):**

PVC is the chain assemblage of the basic raw material vinylchloride (VC), which is a reaction product from ethylene and chlorine or ethylene, air and hydrochloric acid. Many designers choose HDPE for its greater resistance to chemicals, and ignore many of PVC's advantages. Plain PVC geomembranes are quite stiff materials and cannot, therefore, be used for landfills. Loss of plasticizers is such an important problem that the state of Florida does not allow the use of PVC for liner material. However, various studies comparing the chemical resistance of HDPE and PVC have shown that the landfill leachate has virtually no effect on PVC after 16 months (3). Moreover, plasticizers increase the material's flexible characteristics. Therefore Florida should lead some studies to determine whether or not PVC materials are suitable for application as liner materials.

An interesting advantage of PVC is its fabrication into large sheets requiring less field seaming than HDPE membranes. Nevertheless, in the case of fire, highly toxic fumes of hydrochloric acid are formed (2).

*** Polypropylene (PP):**

New materials for liners are as follow: a reactor blended PP, and a fully cross-linked elastomere alloy of PP and EPDM. PP has many properties similar to PE; this similarity is explained by the fact that PP and PE are part of the same polyolefin family. PP crystallinity is generally slightly lower than PE, and even with a high value of crystallinity, stress cracking has little influence on this material. Chemical resistance of PP is less than that for HDPE, but it has better seaming behavior than HDPE: it can easily be seamed by hot air equipment at low ambient temperature (the PP/EPDM alloy has been successfully seamed at a temperature of -9°C in strong wind and snow). PP has lower UV resistance than HDPE, even though thermoplastic alloy has better UV resistance (3).

*** Ethylenecopolymer Bitumen (ECB):**

Landfill engineering uses ECB membranes as sealing materials that have been developed for the roofing industry. ECB is the assembly of raw materials composed of ethylene, butyle acrylate (50-60%), and special bitumen (40-50%). The role of the bitumen material is to soften, give a thermoplastic character, and lightly stabilize the mix (2).

** Other materials in current use are as follows:*

- Chlorosulfonated polyethylene-reinforced (CSPE-R)
- Ethylene interpolymer alloy-reinforced (EIA-R)
- Linear low-density polyethylene (LLDPE)
- Chlorinated polyethylene-reinforced (CPE-R)
- Fully cross-linked elastomeric alloy (FCEA)
- Polyisobutylene and butyl rubber
- Polychloroprene (neoprene)
- Ethylene vinyl acetate (EVA)
- Block copolymers of styrene and butadiene such as SBS rubber
- Ethylene propylene diene monomer (EPDM)

** Additives:*

Most polymers need certain additives to improve processing as well as end-use properties. For instance additives, such as lead salts and organic derived of Ba, Ca, Cd, Zn, and Sn, are added to PVC to improve the heat and light stability. Lubricating additives, such as stearates or palmitates, are added to the polymer to improve the material's manufacturing. Plastizicers in PVC and HDPE improve membrane flexibility. Moreover, to increase chemical and UV resistance, antioxidants and additives are melted into the polymer (2).

1.2 Types of liners

The different types of architecture used for landfill liners are as follows: single liner (clay or geomembrane), single composite (with or without leak control), double liner, and double composite liner (4).

1.2.1 Single liner

A single liner system includes only one liner, which can be either a natural material (usually clay), *Fig 1a*, or a single geomembrane, *Fig 1b*. This configuration is the simplest, but there is no safety guarantee against the leakage, so a single liner may be used only under completely safe hydrogeological situations. A leachate collection system, termed LCS (soil or geosynthetic drainage material), may be placed above the liner to collect the leachate and thus decrease the risk of leakage.

1.2.2 Single composite

A single composite liner system, *Fig 1c*, includes two or more different low-permeability materials in direct contact with each other. Clayey soil with a geomembrane is the most widely recommended liner.

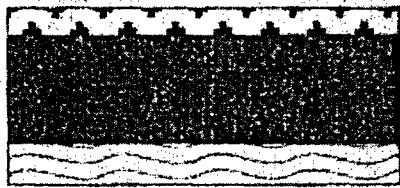


Figure 1a



Figure 1b

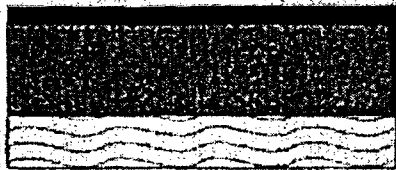


Figure 1c



Figure 1d

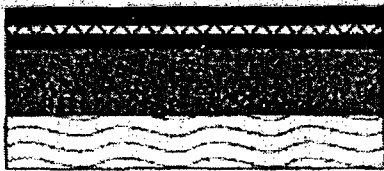


Figure 1e



Figure 1f



Soil



Leakage Detection



Mineral



Leakage Collection



Geomembrane

Figure 1: Cross section of different liner systems

Geotextile-bentonite composites are often used as substitutes for mineral liners (liners using stones or rocks as material) for application along slopes, even though many engineers prefer clay.

One of the main advantages of composite liners over single liners is the low amount of leakage through the liner, even in the presence of damage, such as holes in the geomembranes. Controversial points of view are expressed concerning the placement of draining materials between the clay and the geomembrane, also called the leakage detection system (LDS), the role of which is to detect, collect, and remove liquids between the two liners. The presence of a LDS separates the two low-permeability

materials which form two single liners separated by a layer of permeable material; for some engineers this configuration is two single liners separated by a LDS and for other it is still a composite liner. The opinion of the author of this report is that since two different materials are used this configuration forms a composite liner.

Some engineers point out that to maximize the advantages of composite liners, geomembranes should be positioned with direct contact on the top of the mineral liner, while others refute this idea and recommend placing a collecting system between the two components. The latter practice is to cope with the possibility of the geomembrane being pierced; the leachate can be evacuated outside the composite to decrease the possibility of leakage through the clay. It is always possible to place a leachate collecting system above the membrane.

1.2.3 Double liner

A double liner system, *Fig 1d*, is composed of two liners, separated by a drainage layer called the leakage detection system. A collection system may also be placed above the top liner. Double liner systems may include either single or composite liners. Nowadays, regulations in several states require double liner systems for MSW landfills. A clay layer may be placed under a double liner made of membranes as shown in *Fig 1e*.

1.2.4 Double composite liner

Double composite liners are systems made of two composite liners, placed one above the other, *Fig 1f*. They can include a LCS above the top liner and an LDS between the liners. Obviously, the more components in the liner system, the more efficient is the system against leakage.

1.3 Manufacturing considerations

Different technologies are employed to fabricate geomembranes, among those extrusion is used for HDPE, calendaring for PVC, and spraying for urethane. Even though geomembranes are quality products now, some problems may appear, such as creasing of polyethylene membrane due to the manufacturing process causing stress fractures; moreover abrasion process will add damage to the crease (5).

For HDPE materials, the resin is melted and forced through a die forming sheets; three different techniques are used:

- Horizontal cast index extrusion shapes a long strip (25mm width), then the different strips are assembled into a continuous sheet. This technique allows the fabrication of wide sheet, up to 11 meters.
- Horizontal continuous flat extrusion produces a full width from sheet feeding through counter-rotating calenders in a continuous manner (6). Five-meter wide sheets can be used.
- Vertical continuous circular extrusion produces a blown film that is stabilized, sized, and lifted by air both inside and outside the cylinder.

1.4 References

1. M. P. Rollings, P.E., and Raymond S. Rollings, JR., P.E.: Geotechnical Materials in Construction, McGraw-Hill, 1996, p. 450, 457-459.
2. G. Van Santvoort: Geotextiles and Geomembranes in Civil Engineering, 1994, p. 517, 518.
3. I.D. Peggs: "Geomembranes for Landfill Liners and Covers: Is There a Choice?", Proceedings Sardinia 93, Fourth International Landfill Symposium, p.325-332.
4. M. Shivashankar: Improved Design Methods for Evaluating the Performance of Landfill Double Liner Systems, M.S. Thesis (Dr.D.V. Reddy and J.G. Fluett-advisors) Florida Atlantic University, 1995, p. 5-8.
5. U.S. Environmental Protection Agency: "How to Meet Requirements for Hazardous Waste Landfill Design, Construction and Closure", Pollution Technology Review No. 185, 1990, pp. 29.
6. Lord Jr. A.E., Koerner R.M, Wayne M.H.: "Residual Stress Measurements in Geomembrane Sheets and Seams", Geosynthetics' 91, Conference Proceedings, Atlanta, USA, pp. 333-349.

2 Properties of geomembranes

This chapter reviews geomembrane properties and the test methods used for their assessment. Although there are a number of different types of membranes, the review is restricted to polymeric geomembrane, and geosynthetic clay liners. These properties characterize the material and help the designer to choose among the various geomembranes the most appropriate one for a special application (each landfill is unique). The properties can be classified into different groups: physical, mechanical, and endurance properties.

2.1 Polymeric geomembranes

2.1.1 Physical properties

Physical properties are assessed for the final product (not during manufacturing), and allow the proper identification of the geomembrane.

**** Thickness:***

The test method ASTM D 5199 uses an enlarged-area micrometer under a specific pressure (20 kPa) to determine the geomembrane thickness. Today's membranes are 20 mils (0.5 mm) thick or greater, and the current regulation recommends a thickness of at least 30 mils (0.75 mm) for hazardous waste material pond liners.

**** Density:***

The density or specific gravity depends on the base material forming the geomembrane. For polymer materials, values may range from 0.85 to 1.5 g/cc, with an ASTM classification requiring a density at least equal to 0.941 g/cc. One method used is ASTM D 792, based on specific gravity. Another and more accurate method, is ASTM D 1505 commonly used for material with specific gravity less than 1.

**** Melt flow index:***

Manufacturers use this property to control the polymer uniformity referring to ASTM D 1238. This test is very important for quality control and quality assurance of polyethylene resins and geomembranes.

**** Mass per unit area (weight):***

The weight is measured for unit area of a representative specimen (ASTM D 1910).

**** Water Vapor Transmission:***

This test is important since it assesses a very critical characteristic of geomembrane: its impermeability. The water vapor transmission test consists of a sealed specimen over an aluminum cup with either water or a desiccant in it, while a controlled relative humidity difference is maintained (ASTM E 96). The required test time varies from 3 to 30 days. From the results of this test, the water vapor transmission, permeance, and permeability are calculated. The results differ depending on the material: for a PVC geomembrane (30

mils of thickness) the water vapor transmission is 1.8 g/m²-day, and for a HDPE membrane (31 mils of thickness) 0.017 g/m²-day.

*** Solvent vapor transmission:**

In the presence of liquids other than water it is important to consider the concept of permselectivity. The values of vapor transmission through the membrane are most of the time different for the solvent compared to water, due to the molecular size and attraction of the liquid vis-a-vis the polymeric liner material. The test is identical to the water vapor transmission test (ASTM D 96), except that the water is replaced by solvents, which can range from methyl alcohol to chloroform.

*** Coating over fabric:**

The assessment of the property is not covered by any ASTM test but can be carried out by an optical method (5).

2.1.2 Mechanical properties

Many tests developed to assess the mechanical properties of polymeric sheet materials can be used to evaluate geomembranes.

*** Tensile behavior:**

Tensile tests, covered in ASTM D 638, D 882, D 751, are commonly used to evaluate simple samples for quality control and quality assurance of manufactured sheet materials. The curve (stress versus strain) shows a pronounced yield point, then the curve goes slightly downward, and finally extends to approximately 1000% strain, when failure occurs. Curves for VLDPE and PVC geomembranes are relatively smooth; the stresses increase gradually until failure at 700% and 450% strain.

Other types of tests can also be carried out: a) using wider specimens (8", 200 mm) to prevent the contraction in the central region giving one-dimensional behavior not conforming to the field configurations (ASTM D 4885), here the width remains uniform; b) using axisymmetric tensile test behavior when the membrane is submitted to out-of-plane stresses (GRI test method GM4).

*** Seam behavior:**

The joints between the geomembranes can be weaker than the membranes due to some imperfection in the field seaming. Several tests were developed to evaluate the strength of a seam: typical shear tests are ASTM D 4437, D 3083, and D 751; typical peel tests are ASTM D 4437 and D 413. In the peel test a specimen is taken across the seam and tested in a tensile mode. For shear testing, the specimen is separated by pulling-out, in an in-plane motion, two different points creating shear stress and strain in the seam appear.

*** Tear resistance:**

Different methods can be used to evaluate the tear resistance: ASTM D 2263, D 1004, D 751, D 1424, D 2261, and D 1938. Nevertheless the trapezoidal tear test (D 2263) is often recommended. A notched specimen is tested in a tensile machine. The tear resistance value corresponds to the maximum load. For certain membranes such as thin, non-reinforced geomembranes, the tear resistance is low, from 4 to 30 lb (18 to 130 N). Low values are problematic, especially during geomembrane handling and installation since the membrane can be pierced or damaged by sharpen objects. However, this problem is overcome when the thickness increases. The values of tear resistance for scrim-reinforced geomembranes are significantly higher, and can fit the range of 20 to 100 lb. (90 to 450 N).

*** Impact resistance:**

This property is important, since during installation the geomembrane may be damaged by falling objects that may propagate tears and consequent leaks. The test methods used are ASTM D 1709, D 3029, D 1822, D 746, D 3998, and D 1424. These tests are carried out by a free-falling dart, a falling weight or pendulum impact; all impact resistance varies greatly depending of the thickness and type of geomembrane tested.

*** Puncture resistance:**

Stones, sticks, or other debris can cause punctures to geomembranes during installation as well as during the membrane's service life. These punctures create points of tearing or leakage. The test method, ASTM D5494, consists of a geomembrane clamped over a cylindrical mold that is compressed. A rod is pushed into the geomembrane to cause puncture. The value at the breaking point is called the puncture resistance. Puncture resistance ranges from 10 to 100 lb. (45 to 450 N) for thin, non-reinforced geomembranes, and can go up to 50 to 500 lb. (220 to 2200 N) for reinforced ones. The values for puncture resistance, like other properties such as impact or tear resistance, are functions of the geomembrane thickness. The GRI test method, GM3, also addresses membrane puncture resistance.

*** Geomembrane friction:**

Soil-to-membrane friction is a critical parameter since numerous side slope failures have occurred. The ASTM D5321 test method consists of a split shear box with the geomembrane/soil interface. The friction angles of soil/geomembrane interfaces are always less than those for soil/soil ones. Smoother, harder geomembranes have the lowest values, while the rougher, softer geomembranes have higher friction values.

*** *Geomembrane anchorage:***

In some liners, the geomembrane is sandwiched between two materials and is stressed by an external force, possibly creating membrane failure. This phenomenon can be modeled in the laboratory by sandwiching the membrane between suitably anchored channels back-to-back. The channels are compressed with a hydraulic jack, and the exposed geomembrane end is pulled by grips in a tension machine (GRI test method GM2).

*** *Stress-cracking:***

ASTM D1693 can be used to test polyethylene materials: a notch is introduced in small specimens, which are then bent into a U shape, placed within the flanges of a channel holder with the notches at the bottom, and immersed in a surface wetting agent at an elevated temperature. No external loading is applied. The test records the proportion of the total number of failures in a specific time.

A more efficient test method is ASTM D5397, placing dumbbell-shaped specimens with a notch under constant tensile load in a surface wetting agent at an elevated temperature.

A ductile-to-brittle behavior is observed while tensile testing specimens at different percentages of their yield stress. The transition time varies from 10 to 5000 hours depending on the material tested. The current recommendation for HDPE is 100 hours.

Other properties may be evaluated, such as the modulus of elasticity (ASTM D882), the hardness (ASTM D2240), and ply adhesion (ASTM D413) (5).

2.1.3 Endurance properties

*** *Ultraviolet:***

Ultraviolet light can cause chain reactions and bond breaking of polymeric material due to the penetration of short wavelength energy. Accelerated tests can be carried out in the laboratory, ASTM G26 and G53, but it may be more efficient and accurate to carry out outdoor tests as described in ASTM D1453 and D4364. Nevertheless, CSPE-R and HDPE geomembranes are able to withstand UV up to 20 years thanks to additives. Other geomembranes must be buried in soil.

*** *Radioactive degradation:***

Radioactivity, higher than 10^6 and 10^7 rads, causes polymer degradation due to chain scission. Thus geomembranes must not be placed in high-level radioactive waste, but can be used to contain low-level radioactive waste.

*** *Biological degradation:***

Soil contains a tremendous number of living organisms, such as small animals, which burrow through the membrane, fungi (yeast, molds, and mushroom), and bacteria. ASTM G21 deals with the resistance of plastics to fungi, while G22 deals with the resistance of plastics to bacteria. The main concern here is not the polymeric degradation, but the fouling and clogging of the drainage system.

*** Chemical degradation:**

Chemical resistance is a very important and critical parameter since the geomembrane is in direct contact with the waste most of the time. To insure proper resistance, it is recommended to assess its behavior with the leachate or waste, the membrane will contain. The testing should be as similar (leachate, temperature) as possible to the exposure in the landfill. From test methods, EPA 9090 and ASTM D 5322, the response curves should be plotted indicating the percent change in the measured property from the original versus the duration of incubation.

*** Thermal degradation:**

Polymeric geomembranes are sensitive to changes in both warm and cold temperatures, each causing its own effects. ASTM D 794 is used to assess the consequences of hot temperature on polymeric geomembranes. Cold temperatures have less critical effects than warm ones, nevertheless the membrane's flexibility decreases and seams are more difficult to make. ASTM D 2102 and D 2259 characterize the contractions of the membrane, while D 1042 and D 1204 characterize the expansion and changes of dimensions.

Appendix VII gives the coefficients of liner thermal expansion.

2.2 Geosynthetic clay liners (GCLs)

GCLs are composite liners comprising a layer of clay under a geomembrane sheet.

2.2.1 Physical properties

*** Clay type:**

The composition of the clay can be determined by X-ray diffraction, which is an accurate but expensive method. An easier method is the American Petroleum Institute (API) methylene blue analysis.

*** Thickness:**

The determination of GCL's thickness can be problematic for certain materials. However, ASTM D1777 can be used but with maximum care.

*** Mass per unit area:**

ASTM D3776 allows the determination of a composite GCL's mass per unit area. Another method is to assess the overall mass per unit area of the complete GCL roll, which is mainly used by manufacturers for quality control check, even though the results will not be as accurate as the D3776 method since the roll weight exceeds 3000 lb.

*** Moisture content:**

Moisture content is measured by the ASTM D4643 test method and can be defined as the water content divided by the oven-dry weight of the specimen, expressed as a percentage. Bentonite clay is a very hydrophilic material, and its moisture content can be as high as 20% in humid areas.

2.2.2 Hydraulic properties

*** Hydration:**

The hydrating property of bentonite clay varies depending on the nature of the hydrating liquid, and on the applied normal stress. The assessment of this property is important since it provides the low-permeability characteristic to a CGL liner system.

** Free swell:*

This test assesses the amount of swelling of the bentonite under zero normal stress. Two tests methods are used: a) NF-XVII from the United States Pharmacological Society which consists of a cylinder filled with water (100 ml) and bentonite (2 g). After 24 hours, the volume occupied by the clay is determined; b) ASTM D 35.04: The clay is placed in a mold, then a stress of 14 lb/ft² is applied on the test specimen immersed in water, and deflections are measured for 24 hours

** Permeability:*

The test method ASTM D 35.04 evaluates the permeability (or hydraulic conductivity) of GCL with the help of a permeameter under field-simulated conditions. The values of the permeability range between 6×10^{-9} to 3×10^{-10} cm/sec.

2.2.3 Mechanical Properties

** Tensile strength:*

Three different kinds of tensile strengths of importance need to be evaluated: Wide-width tensile behavior, confined wide-width tensile behavior, and axisymmetric tensile behavior. The tensile behavior of CGL is almost similar to the tensile behavior of the geomembrane since clay property is low. Moreover, the test should be done with dry clay. The wide-width tensile behavior is determined with the test method ASTM D4595. The second test is similar to the first one, except for the confined environment. The axisymmetric tensile behavior is a very important characteristic of CGL, but unfortunately no tests have been developed to assess this property.

** Direct shear behavior:*

The test is similar to that for polymeric geomembranes; the specimen is tested in a shear box where constant strain is applied.

** Puncture resistance:*

Different tests can assess the puncture resistance of CGL: ASTM D 3787, FTM 101C-M2065, and ASTM D 5494. They use either a puncturing or pyramidal probe. One interesting property of bentonite is its capacity to self-cure after puncture, which is unfortunately not the case for polymeric material.

Endurance tests can be carried out to determine the longevity of CGL. These tests are similar to the ones used for polymeric material; obviously the results are not the same.

2.3 Example of geomembrane properties

The properties of two different geomembranes are listed in Table 1. Obviously, the properties vary as a function of the thickness.

The first geomembrane is UltraFlex manufactured by the SLT Corporation, the second one is a smooth HDPE geomembrane manufactured by the Poly-Flex Corporation.

Table 1: Mechanical Properties of Different Geomembranes

	SLT mil		Poly-Flex	
Thickness	60 mil	80 mil	60 mil	80 mil
Density (g/cc)	0.931	0.931	0.95	0.95
Melt Flow Index (g/10 min.)	≤ 1	≤ 1	0.2	0.2
Carbon Black Content	2.5 %	2.5 %	2.5 %	2.5 %
Tensile Strength at Break (ppi)	300	400	285	380
Elongation at Break (psi)	1000	1000	900	900
Tear Resistance (lbs)	45	60	50	66
Puncture Resistance (lbs)	90	120	96	128
Low Temperature Brittleness (°F)	< 120	< 120	< 112	< 112
Environmental Stress Crack (hrs)	> 5000	> 5000	> 2000	> 2000
Dimensional Stability	± 1	± 1	± 0.5	± 0.5

The following tables list some properties of different geotextile materials. Table 2 provides water vapor transmission values, Table 3 lists tensile strength values of membrane sheets and seams, Table 4 presents the tensile behavior properties values of HDPE, VLDPE, PVC, and CSPE-R membranes, Table 5 shows the impact resistance, Table 6 lists the interface friction angles of different geotextiles with different types of soil, Table 7 lists the angles of friction of geotextile/geomembrane interfaces, and Table 8 lists the coefficients of linear expansion for different polymeric materials.

Table 2: Water Vapor Transmission Values (2)

Geomembrane Type	Thickness		WVT Results	
	Mil	mm	$\text{g/m}^2\text{-day}$	perm-cm
PVC	11	0.28	4.4	1.2×10^{-2}
	20	0.52	2.9	1.4×10^{-2}
	30	0.76	1.8	1.3×10^{-2}
CPE	21	0.53	0.64	0.32×10^{-2}
	31	0.79	0.32	0.24×10^{-2}
	38	0.97	0.56	0.51×10^{-2}
CSPE	35	0.89	0.44	0.84×10^{-2}
EPDM	20	0.51	0.27	0.13×10^{-2}
	48	1.23	0.31	0.37×10^{-2}
HDPE	31	0.8	0.017	0.013×10^{-2}
	96	2.44	0.006	0.014×10^{-2}

**Table 3: Values for Geomembranes Tensile Test on Sheets and Shear Test on Seams
(1)**

Type of test	HDPE	VLDPE	PVC	CSPE-R	EIA-R
Tensile test on sheet					
ASTM test method	D638	D638	D882	D751	D751
Specimen shape	Dumbbell	Dumbbell	Strip	Grab	Grab
Specimen width (in.)	0.25	0.25	1	4 (1 grab)	4 (1 grab)
Specimen length (in.)	4.5	4.5	6	6	6
Gege length (in.)	1.3	1.3	2	3	3

Table 4: Tensile Behavior Properties of 60-mil HDPE, 40-mil VLDPE, 30-mil PVC, and 36-mil CSPE-R (1)

a) Index tension tests:

Test property	HDPE	VLDPE	PVC	CSPE-R
Maximum stress (MPa)	19	8	21	55
Corresponding strain (%)	17	500	480	19
Modulus (MPa)	330	76	31	330
Ultimate stress (MPa)	14	8	21	6
Corresponding strain (%)	500	500	480	110

b) Wide-width tension tests:

Test property	HDPE	VLDPE	PVC	CSPE-R
Maximum stress (MPa)	16	8	14	31
Corresponding strain (%)	15	400	210	23
Modulus (MPa)	450	69	20	300
Ultimate stress (MPa)	11	8	14	3
Corresponding strain (%)	400	400	210	79

c) Axisymmetric tension tests:

Test property	HDPE	VLDPE	PVC	CSPE-R
Maximum stress (MPa)	23	10	15	31
Corresponding strain (%)	12	75	100	13
Modulus (MPa)	720	170	100	350
Ultimate stress (MPa)	23	10	15	31
Corresponding strain (%)	25	75	100	13

Table 5: Impact Resistance of Different Geomembranes (1)

Geomembrane	Point Geometry Angle				
	15 deg.	30 deg.	45 deg.	60 deg.	90 deg.
PVC (20 mil)	4.8	6.6	11	> 15.6	> 15.6
PVC (30 mil)	6.8	10	13.5	> 15.6	> 15.6
HDPE (40 mil) reinforced	5.6	6.9	8.3	8.3	6.4
CSPE (36 mil) reinforced	9	9.4	10.3	14.2	> 15.6

Table 6: Friction Values and Efficiencies for Soil to Geomembrane Interfaces (3)

Geomembrane	Soil Type		
	Concrete Sand ($\phi = 30^\circ$)	Ottawa Sand ($\phi = 28^\circ$)	Micha Schist Sand ($\phi = 26^\circ$)
EPDM-R	24° (0.77)	20° (0.68)	24° (0.91)
PVC <i>rough</i>	27° (0.88)	-	25° (0.96)
PVC <i>smooth</i>	25° (0.81)	-	21° (0.79)
CSPE-R	25° (0.81)	21° (0.72)	23° (0.87)
HDPE	18° (0.56)	18° (0.61)	17° (0.63)

Table 7: Friction Values and Efficiencies of Geotextile/Geomembrane Interfaces (3)

Geotextile	Geomembrane				
	EPDM-R	PVC <i>rough</i>	PVC <i>smooth</i>	CSPE-R	HDPE
Nonwoven, needle punched	23°	23°	21°	15°	8°
Nonwoven, heat bond	18°	20°	18°	21°	11°
Woven, monofilament	17°	11°	10°	9°	6°
Woven, slit film	21°	28°	24°	13°	10°

Table 8: Coefficients of Linear Thermal Expansion for Different Polymeric Materials (1).

Polymer type	Thermal linear expansivity x 10 ⁻⁵	
	per 1°F	per 1°C
Polyethylene		
High density	6-7	11-13
Medium density	8-9	14-16
Low density	6-7	10-12
Very low density	8-14	15-25
Polypropylene	3-5	5-9
PVC		
Unplasticized	3-6	5-10
35% plasticizer	4-14	7-25
Polystyrene	2-4	3-7
Polyester	3-5	9-9

2.4 References

1. M. P. Rollings, and R. S. Rollings, Jr.: Geotechnical Materials in Construction, McGraw-Hill, 1996, p.: 450, 457-459.
2. Haxo, H. E., Jr., Miedema, J. A., and Nelson, N. A., "Permeability of Polymeric Membrane Lining Materials," Proc. Int. Conf. on Geomembranes. Denver: IFAI, 1984, pp. 151-156.
3. Martin, J. P., Koerner, R. M., and Whitty, J. E., "Experimental Friction Evaluation of Slippage Between Geomembranes, Geotextiles and Soils," Proc. Int. Conf. on Geomembranes. Denver: IFAI, 1984, pp. 191-196.

3 Liner Failure and Prediction

The failure modes can be divided into two categories: leaking and liner destruction (1):

- * Leaking is the liner's failure to ensure the containment of waste. Leachate or even waste leak from the containment to the in-situ soil, through the liner through holes or the loss of material permeability.

- * The liner destruction mainly corresponds to a loss of mechanical properties or extensive membrane movements caused by phenomena such as creep, membrane uplift by excessive wind, puncture, etc.

The phenomena can be coupled; for instance puncture creates a hole that causes a leak followed by tear propagation.

3.1 Creep

3.1.1 Definition

The physical phenomenon occurring in most material, and particularly in plastics, termed creep is the deformation of the material over a prolonged period of time under constant pressure (1). Creep is a material, load, temperature, and time-dependent phenomenon. It is associated with all the mechanical deformations: tensile, compression, torsion, and flexure (2). However, tensile and compressive creeps are the only deformations that matter for landfill liners since geomembranes are flexible materials.

The tensile creep test is carried out by applying in-plane stress while the compressive creep test is realized by applying normal loading. Creep and creep-rupture data must be taken into consideration for the determination of the creep modulus and strength of the material for long-term behavior (3).

The creep test measures the dimensional changes of a specimen submitted to a constant load during a certain period of time, while the creep rupture test measures the time taken for rupture to occur under constant load. (2).

Creep behavior is commonly assessed at constant times and temperatures, and is shown in the graph (see Fig 2): either strain versus time (or log time) or strain rate versus time.

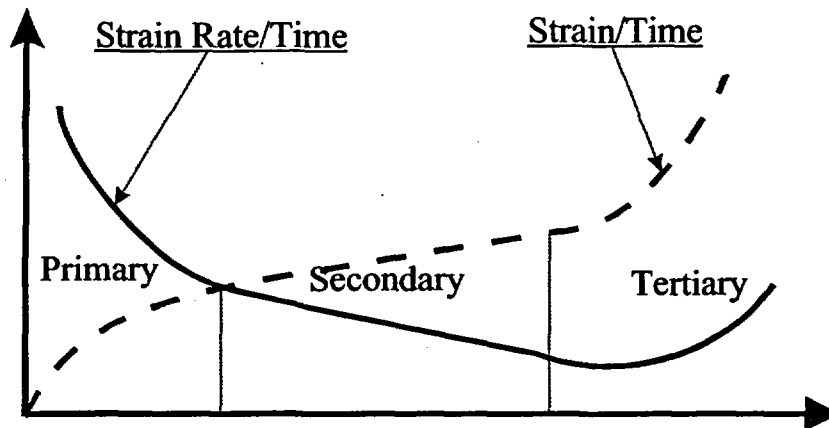


Figure 2: Typical creep curves (3)

3.1.2 Different phases of creep response

The creep behavior of a constant polymeric material can be divided into three phases called primary, secondary, and tertiary creep. During the primary phase the strain increases but the strain rate decreases, in the secondary phase (also called steady state) both the strain and strain rate are constant, and the tertiary phase is characterized by a rapid increase of strain and strain rate leading to the specimen's rupture.

For polymeric materials, tertiary creep is the dominating phase for polyethylene and polypropylene, while in geosynthetics made of polyester, primary creep is the dominating phase, thus some materials do not show strain and strain rate increases before rupture.

Long-term performance is a function of polymer type, grade, manufacturing techniques (since they influence the orientation and length of molecules), and the percent of crystallinity. Macrostructure affects creep behavior, since debonded fibers can straighten and thus increase creep strains, postponing the creep-rupture limit. Even though several studies show that temperature has little influence on creep behavior, time-temperature superposition principles are used to estimate the long-term properties of polymeric materials. Moreover, for HDPE, increasing the molecular weight can reduce the temperature influence (4). However, the effect of load is many times greater than the effect of temperature (3).

Torsion and flexural creep behavior pose no problems for flexible geomembranes that emphasizes the importance of tensile and compressive creep testing.

3.1.3 Tensile creep behavior

Cazzuffi et al. (3) evaluated the tensile creep behavior of high-strength geosynthetics, using the CEN European Method in order to compare the European and American methods. Twelve specimens were placed in a load frame, and tested at a constant temperature and humidity (controlled air-conditioned room). HDPE extruded geogrids, PET woven geogrids, and PP/PET woven/nonwoven composite geotextile were trimmed to conform to the CEN Standard (European Standard), and tensile creep tests were performed. Comparing the CEN and ASTM methods, no major differences in the procedures were observed, although parameters such as specimen sizes and loading time differed slightly.

The test temperature was 20°C and the humidity 65%; three different loads were applied, 20%, 30%, and 50% of the wide-width tensile strength. Strain versus time and strain rate versus time graphs were plotted for each load and material. The testing time extended to 10000 min. Only one specimen posed a problem: the HDPE extruded geogrid approached failure for a load equal to 50% of the wide-width tensile strength; other specimens remained acceptable for this small period of time.

3.1.4 Multi-axial tensile creep

Merry and Bray (5) tested geomembranes for multi-axial tensile creep. Specimens were made of extruded HDPE produced by two different manufacturers. The objective of this study was to evaluate the stress-dependent creep of HDPE geomembranes at different

temperatures ranging from 2°C to 53°C. Specimens were exposed to a constant stress ranging from 2 MPa to 15 MPa for a period of 36 hours.

The test results proved that when the temperature increases, the response softens significantly. When loaded to the same stress level, a geomembrane exposed to a higher temperature will fail sooner than a geomembrane exposed to a cooler temperature.

This test contradicts the common thought that creep behavior is poorly affected by temperature, and implies that other studies should address exposing specimens to longer time periods. An interesting conclusion of this test is that the behavior of membranes tested in a multi-axial mode can be modeled by an adaptation of the Singh-Mitchell (9) creep model, originally developed for soil.

3.1.5 Creep rupture envelope

While characterizing the creep behavior of a material, it is interesting to evaluate the creep rupture envelope (2), which is the curve connecting the rupture points of several tensile creep-rupture test curves, Fig. 3. The creep-rupture tests are carried out for different temperatures and loads. The envelope curves are of primary importance for designing with geomembranes.

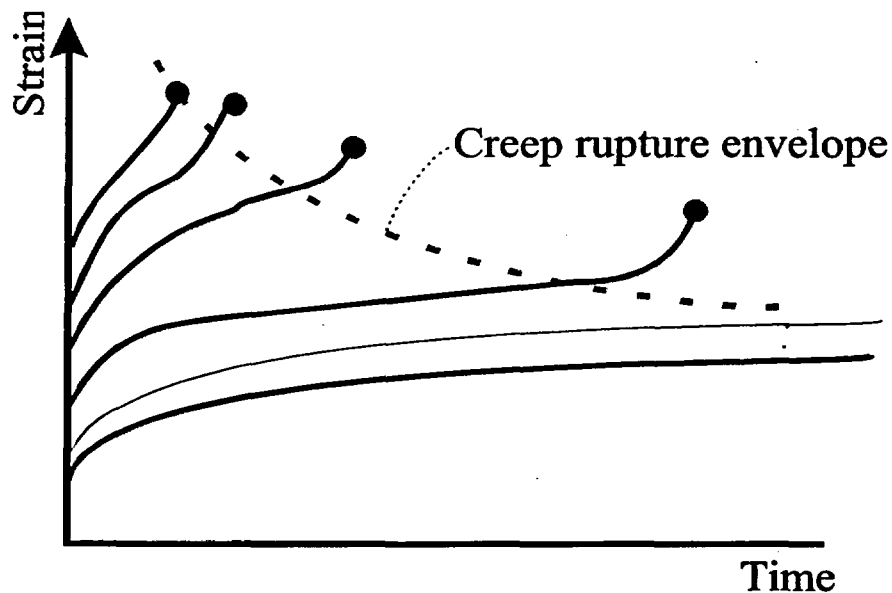


Figure 3: Creep Rupture Envelope (2)

3.1.6 Compressive creep

Beside tensile creep behavior, the compressive creep behavior should be evaluated. Effectively a landfill liner is submitted to a constant vertical load during a long period of time, causing geometric deformations and eventual damage leading to the liner's failure.

Montanelli and Rimoldi (6) evaluated the effect of long term hydraulic flow capacity of compressive and intrusion phenomena. One aspect of this test was the assessment of the compressive creep behavior of two drainage geocomposites (Tenax TNT 300 presenting a thickness of 7 mm, and Cleymax GCL 500 SP presenting a thickness of 5.2 mm). The specimens (100x100 mm) were placed between two rigid steel plates and loaded with specific pressures equal of 100 kPa and 200 kPa.

The test was performed for 10,000 hours and as expected a decrease in thickness was observed but no failures were recorded. The thickness decrease ranged from 3 to 6 percent of the original thickness.

Reddy and Daniel (7) evaluated the effects of compressive creep on landfill liners by testing the compressive creep behavior of a HDPE geonet. In the first part of this study specimens of different thickness (160, 220, and 300 mil) were tested in untreated and treated (by an agent inhibiting the development of excessive biological growth) leachate at a constant pressure of 110 psi. The percent strain, in the untreated leachate, ranged from 3.8% (160 mil) to 5.8% (220 mil). Values for the treated leachate were significantly lower than those for the untreated one, which implies that the more contaminated the leachate, the larger are the compressive creep effects. Nevertheless, no failures were observed for the time period of 120 days.

On the sides of a landfill, the liner is not only submitted to compression stress but also to shear stress due to the side slope. Some studies analyzing the effects of shear stress on the membranes have been realized. Cazzuffi (8) presented the procedures for combined normal and shear compressive creep testing. Similar to regular compressive creep testing, the specimens must be tested at a constant temperature of 20°C, and humidity of 65%; their shapes can either be rectangular or circular. The test is carried out in a compressive machine, the apparatus is composed of a fixed base plate and a top plate free in the vertical and horizontal directions. The inclination of the membrane should be adjustable. The test is conducted like a regular compressive test: the change in thickness is measured for a prescribed period of time, at least for 1,000 hours.

Fig. 4 presents typical compressive creep curves under three different pressures.

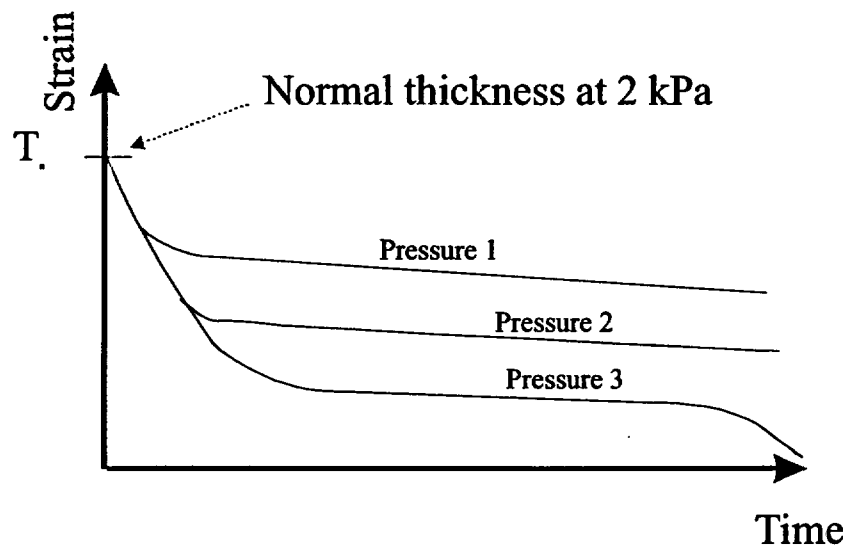


Figure 4: Typical compressive creep curves (8)

Methods are available to predict the life of a geomembrane based on creep failure. These methods are discussed in detail in the Chapter 5, devoted to life prediction of geomembranes.

3.1.7 References

1. Environment Protection Agency: "How to Meet Requirements for Hazardous Waste Landfill Design, Construction and Closure", Pollution Technology Review, 1990, No. 185, pp. 113.
2. ASTM D 2990-93a: "Standard Test Methods for Tensile, Compressive, and Flexural Creep and Creep-Rupture of Plastics", 1993.
3. Cazzuffi D., Ghinelli A.: "European Experimental Approach to the Tensile Creep Behavior of High-Strength Geosynthetics", Geosynthetics '97 Conference Proceedings, Long Beach, pp.253-266, 1997.
4. Bush, D.I., "Variation of Long-Term Design Strength of Geosynthetics in Temperature up to 40°C", Proc. IV Int. Conf. on Geotextiles, Geomembranes and Related Products, 1992, pp. 673-676, The Hague, The Netherlands, 1990.
5. Merry S.M., Bray J.D.: "Temperature Dependent Multi-Axial Creep Response of HDPE Geomembranes", Geosynthetics '97 Conference Proceedings, Long Beach, pp.163-177, 1997.
6. Montanelli F. and Rimoldi P.: "Long Term Performance of GCL and Drainage Composite Systems", Proceedings Sardina 95, Fifth International Landfill Symposium, pp.359-368, 1995.
7. Daniel E.H.: "The Effect of Compressive Creep on the Structural Integrity and Drainage Capacity of Landfill Lining Systems", Master of Science Thesis, Florida Atlantic University, Advisor: Reddy, D. V., December 1995.
8. Cazzuffi S. and Corbet S.: "Compressive Creep Test and Inclined Plane Friction Test for Geosynthetics in Landfills", Sardina, pp. 477-491, 1995.
9. Sing A., and Mitchell J.K.: "General Stress-Strain-Time Function for Soils", Journal of the Soil Mechanics and Foundation, ASCE, 94 (SM1), pp. 21-46, 1994.

3.2 Stress Cracking

3.2.1 Definition

Stress cracking (SC) is the brittle fracture (internal or external) of thermoplastic material under sustained tensile stress at a significantly lower stress than the material yield strength (1). Environmental stress cracking is the stress cracking of materials subjected to environmental conditions such as weather or chemical agents.

Many failures due to SC reported are restricted to uncovered liquid impoundment liner or liner caps; but no failures in landfill bottom liner have been presented (2). Even if no evidence was found to show that SC occurs in the covered liner, it is important to assess this phenomenon since it occurs in the uncovered liner, therefore chances are that it also occurs in the buried one. It may be only a question of time before buried liners damaged by SC will be reported.

SC not only occurs in polyethylene material but also in plain carbon steel, several stainless steels, metallic alloys, PET, and in plasticized and unplasticized PVC.

3.2.2 Different types of failure

Two different modes of SC may occur: rapid crack propagation (RCP) or slow crack growth (SCG). As the name indicates, RCP is associated with very high velocities (over 300 m/s), and may spread over hundred of meters in length. Failures of this type, also called shattering failures, occur in geomembranes exposed to extremely cold weather with temperatures lower than -20°C . The triggering is some kind of dynamic or impact type of failure (3).

SCG is associated with velocities less than 0.1 m/s and propagates at a specific (possibly varying) rate during the membrane service life. The rate of propagation is a function of the polymer material, applied stress, and temperature. This mode is really problematic since failures can appear with stresses as low as 20% of the material yield stress.

In a rapid crack failure, the rupture occurs in a brittle manner (rupture abrupt, without plastic deformation). In a slow crack failure, the geomembranes may fail either in a totally ductile (important plastic deformation) or totally brittle manner, or may start with a ductile behavior and change to a brittle mode. This depends mainly on the stress applied.

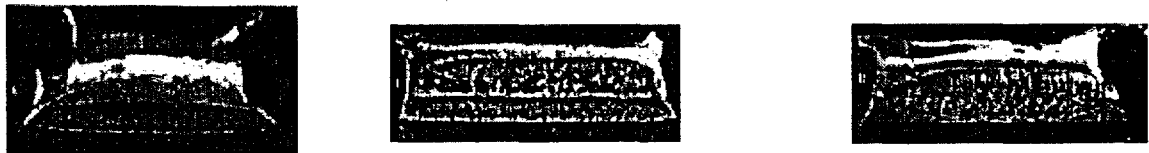


Figure 5: Different faces of the specimen. Left: Ductile, Center: Brittle, Right: Quasi Brittle

Fig. 5 presents the three different types of failure: ductile fractures usually occur at high temperatures with low load application velocity, while brittle fractures occur at low temperatures under high velocity loading.

3.2.3 Mechanism of Stress Cracking

A crack failure can be divided into three different phases: first a craze (a non-opening defect) appears at the notch, then it progresses to an open crack, and finally the crack propagates through the geomembrane thickness creating the failure (Fig. 6).

As soon as a crack is initiated, it is extremely difficult to predict the propagation rate, since it depends on a multitude of factors.

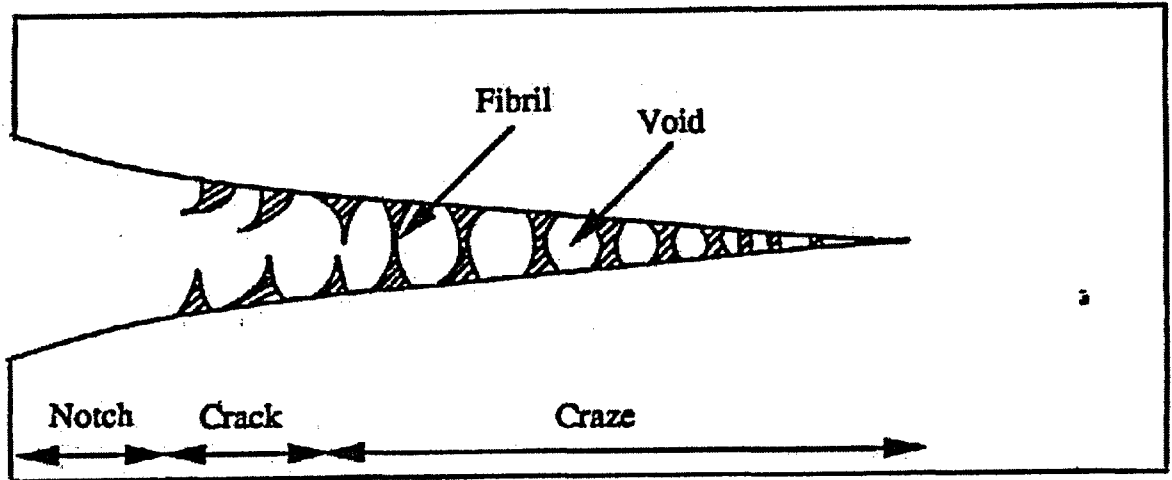


Figure 6: Crack and craze formation in HDPE geomembranes (3)

The crack propagates perpendicularly to the stress orientation through the membrane thickness due to the periodical rupture of the fibril. The rate of slow crack growth can be mathematically modeled by the following equation:

$$K = q \left(\frac{da}{dt} \right)^p \dots\dots\dots[3.2.1]$$

Where:

- K: Fracture Toughness (Mpa/m^{0.5})
- da/dt: Crack Growth Rate (m/s)
- p: Constant Dimensionless (ranging from 0.5 to 0.125 for PE Materials)
- q: Constant with Dimensions of [(Mpa/m^{0.5}) (m/s)^{-p}]

Table 9: Fracture Toughness (K) Values of Different Polymers (4)

Materials	Fracture Toughness (Mpa-m ^{1/2})
Polystyrene (PS)	0.7-1.1
Polycarbonate	2.2
Polyvinyl Chloride (PVC)	2.0-4.0
Polypropylene (PP)	3.0-4.5
Polyethylene (PE)	1.0-6.0
Polyamide (PA)	2.5-3.0
Polyester (PET)	5

3.2.4 Microscopic aspects of SC

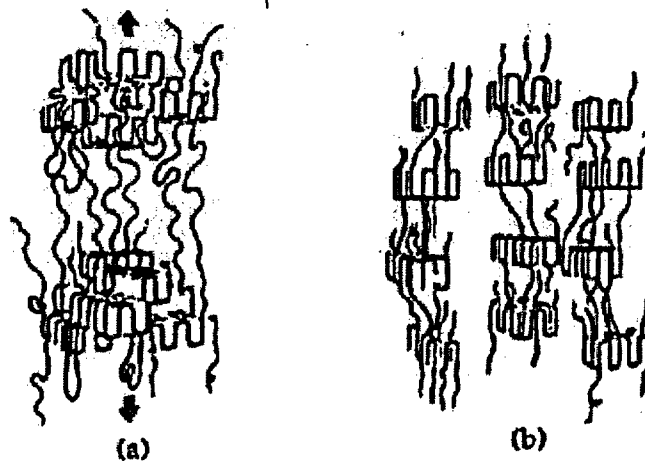
Polymers are composed of crystalline and amorphous regions. The crystalline region is made of long parallel molecule chains forming lamella, which form a spherulitic geometry. Other molecule chains, comprised of tie molecules crossing and joining the lamella without specific orientation, form the amorphous part of the polymer (5).

The tie molecules bind the lamellas and so provide the strength, when their numbers decrease the strength reduces (6). Their role is primordial since they tie or bond the crystalline region into a coherent structure unit, thus forcing ductile behavior rather than brittle behavior (3). The molecular arrangement affects the SC behavior of the material. The SC resistance will decrease with the increase in material density and crystallinity, since when the density increases the amount of amorphous material decreases, and consequently the number of tie molecules.

The co-monomer content tends to affect the entanglement of the tie molecules and the loose loops, it also tends to reduce the polyethylene crystallinity, thereby increasing the SC resistance. Nevertheless, molecular weight does not necessarily increase the SC resistance, since an increase of crystallinity does not always imply an increase of density.

The molecular mechanisms causing SC are chain scission, bond breaking, cross linking, or extraction of various components.

(a) Initial steps in the deformation of polyethylene



(b) Steps in the ductile deformation of polyethylene



(c) Final step in the slow crack growth of polyethylene

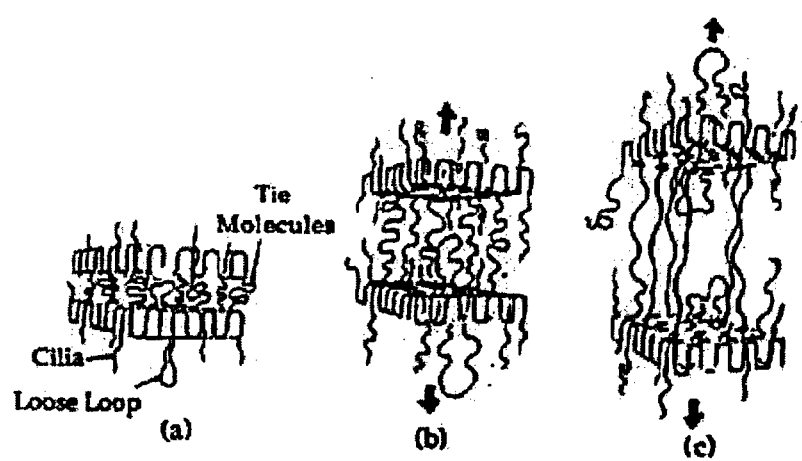


Figure 7: Conceptualization of ductile and brittle failure mechanisms in semi-crystalline polymer materials, after Lustigier and Rosenberg (4).

Fig. 7 shows the different steps for different modes of rupture at a molecular level. Fig. 7a presents the effect of a small deformation, Fig. 7b presents a ductile failure where the crystalline region is pulled apart in a cold drawing mode (plastic deformation of fractured face material, occurring parallel to the applied force), and Fig. 7c presents a brittle failure where the tie molecules are separated in an abrupt mode, while the crystalline region remains intact (3).

As an HDPE liner ages, the amount of crystallinity increases; the number of tie molecules decrease, thus decreasing the SC resistance of the membrane (7).

Even if the SC properties of a polyethylene membrane decrease when the amount of crystallinity and density increase, some medium density polyethylenes are more susceptible to stress cracking than HDPE.

The polyethylene microstructure characteristics and the manufacturing process are the primary influence in the behavior of the geomembrane vis-à-vis SC. Therefore, some geomembranes are better than others, and some seam geometries act better with a specific resins: the problem is to determine the optimum best performance combination of resin and seam geometry (8).

3.2.5 Reasons for SC

To initiate, a crack needs two triggers: a stress and a geometrical imperfection creating a stress concentration point. SC phenomenon is mainly linked to overstressed liners due to restrained thermal contraction during low temperature cycles (8). The stress may be initiated by contained fluid or landfill waste, subgrade settlement, thermal contraction due to geomembrane's shrinkage at low temperatures, or the manufacturing process. A polymer may present ductile behavior and withstand a particular SC agent in an unstressed state, but may fail in a brittle way while in a stressed state, even with low stress values (5). Crazes can be developed by membrane exposure to stress. These crazes are porous regions that absorb chemical fluids, which accelerate the relaxation of the polymer's yield point at the tip of the craze. Crazes may grow into cracks and lead to brittle fracture. The study of the stresses in a liner slope (8) shows that the highest thermal contraction stresses are on the top of the slope, where the material is clamped to the ground and stress relaxation is prevented. In contrast, at the center of the slope the material is free to relax.

The stress concentration factors can be three or more. Stress concentration points are created by surface scratches, extrusion die lines, grinding gouges, seaming machine gouges, re-entrant angles at the edges and on the surfaces of seams, water vapor voids within seams, lack of bonding at seam interfaces, and carbon black agglomerates (8). However, it appears that in most cases the stress concentration point is located at a seam. The problems appearing at seams are due to natural discontinuities of the overlap configurations used to seam geomembranes, and also possibly due to overheating of fusion seams and /or excessive grinding associated with extrusion flat or fillet seams (3).

Failures can also occur along folds or at surfaces. Especially, when different thermal contraction stresses occur on the inside or outside of the fold, the situation is aggravated by unfolding of the membrane during cold weather. Surface cracking can occur due to single bending of a panel exposed to solar radiation. For an uncovered geomembrane, special care must be taken to ensure that the material contains sufficient carbon black or that it is UV treated.

Residual stresses are created by the manufacturing and installation processes, particularly in high crystalline polymers; HDPE is a very sensitive material for the occurrence of residual stresses (9).

In order to determine the residual stress values, Koerner et al. (3) attempted to extrapolate the 'hole method' used in metals and composites to HDPE geomembranes.

This method tends to quantify the residual stress in a material by drilling a hole in the center of a rosette strain gage (see Fig. 8). The rosette is placed on the surface of the material, the indicator is set at zero. After the hole has been drilled the material releases its

residual stress, leading to an ovalization of the hole due to the strain relaxation. At this stage, the material changes from a stressed to an unstressed state; this change in strain is measured by the rosette gives the residual stress.

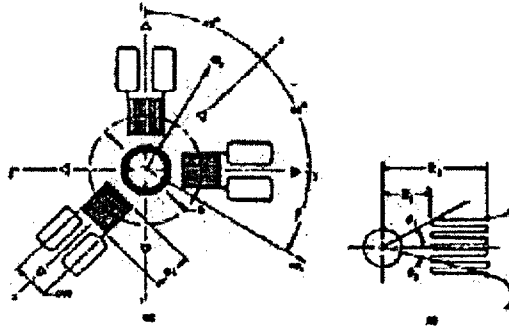


Figure 8: Strain gage rosette for hole drilling method (9)

The results of this first study show that HDPE membranes can have residual stresses as high as 10% of their yield stress. This method has been explained in detail by Lord et al. (9), along with the results on sheet and seam tests.

3.2.6 Different factors affecting the SC behavior of geomembranes

Several field investigations indicate that ultra-violet radiation is an important cause of stress cracking. While exposed to solar radiation, fine parallel cracks appear on the membrane's surface. UV provokes the loss of plasticizer, particularly in PVC material, stiffening the membrane, and enhancing its brittle behavior.

Temperature is also an important factor in the SC of geomembranes. Elevated temperatures promote the oxidation of stabilizer added to the HDPE to retard the liner's breakdown, also reducing its properties (7), while cold temperature causes brittle behavior, and shattering.

The temperature gradient plays an important role since a rapid change in temperature provokes thermal stresses in the material. During winter it is possible that the temperature can change from -20°C at night to 80°C in the day (8), which implies a gradient of 100°C ; in this case the amount of material compensation should be at least 2.5m.

Temperature influences the SC behavior by reducing the time of failure. Thus, by combining factors such as temperature, chemical agents, and stress it is possible to accelerate the failure of membranes in a very short time.

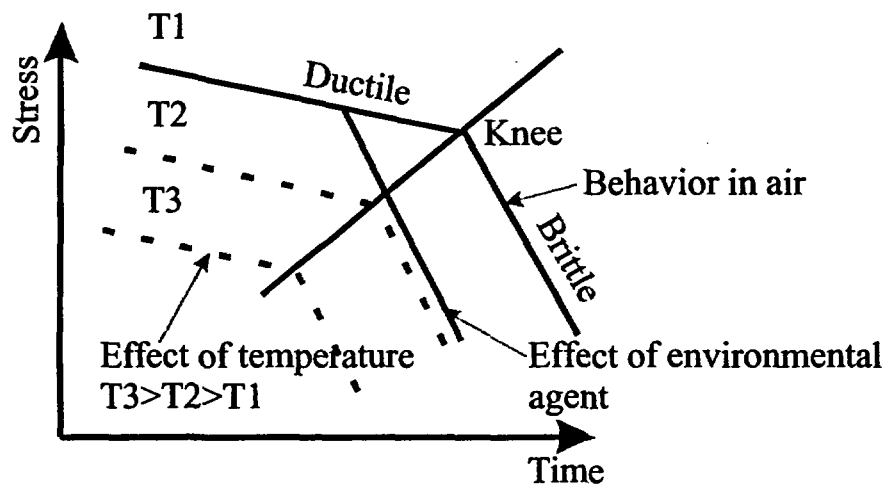


Figure 9: Effect of different factor on stress cracking behavior (5)

Fig. 9 shows the effects of different factors on stress cracking, the effect of temperature is obvious in this figure.

The most common chemical agent to accelerate SC of polyethylene is Igepal CO-630, which is a nonionic surfactant featuring a cloud point (temperature at which turbidity appears) of 52-56°C. The assessment of polymer time to failure with accelerated testing using chemical agents, such as Igepal at a temperature different from the cloud point are not accurate, or provide suspect data since a change of agent concentration will affect the time to failure (5).

Cyclic stress (fatigue) induces faster SC than constant stress (6), which implies that during the design of a liner special care must be taken to account for cyclic loading. However, fatigue may be used for accelerated testing. Unfortunately, no standard test has been developed as yet.

3.2.7 Repair of crack

In stainless steel, repairing a crack by welding can aggravate the crack growth due to the chosen repair process. This may also happen in HDPE geomembranes due to repair of a notch by welding (10).

The repairing of a crack cannot be effected by simply placing a bead of extruded material over the crack zone to close the opening, since more heat in an already stressed region may cause other cracks or increase the rate of propagation of existing crack.

3.2.8 Study of Geogrids

Jailloux and Anderson (1) tested the SC behavior of HDPE geogrids. Two types of specimens were evaluated at different stress values. Specimen Type 1 had a notch in the rib, while the Type 2 specimen had a notch in the transition zone. The notch depth was 30% of the geogrid thickness. The specimens were immersed in an 1% Igepal solution at temperatures equal to 50°C, 65°C, and 80°C. The results of this test showed that the stress

rupture properties were affected by temperature, and that the rib part of the geogrid is much stronger than the transition zone. The rupture for Type 1 was by brittle cracking, while Type 2 showed no evidence of brittle cracking. Moreover, plastic deformations occurred primarily due to creep and to cold drawing of the material from the adjacent node material (1). The temperature decreased the time to failure. The extrapolation from the resulting curve must be interpreted with caution since the curve is composed of 2 lines forming a knee. However, if the extrapolation is done only with the first part, the result will be extremely incorrect.

3.2.9 Field investigation

Koerner et al. (3) conducted a study to determine the occurrence of HDPE geomembranes SC in the field. Fifteen sites were analyzed and the reasons of failure determined. It appears that the ruptures at the seams are mostly associated with two extrusion types of seam, which are flat and fillet. Some failures were reported to occur in membranes in time periods as short as 3 months. The locations of failures were always in the exposed runout length or along the side of a slope; for the cases where cracks were in the bottom, the cracks initiated during construction. The causes of the stresses were mostly thermal, and the causes of crack initiation poorly constructed seams.

3.2.10 Brittle cracking

One particular type of stress cracking in geomembrane is the one associated with shattering failure, occurring mainly in polyethylene materials during cold weather with temperatures ranging from 5°C to -30°C. Many failures of this type have been reported on side slopes of uncovered liners.

Brittle cracks may vary from simple cracks (a few centimeter long) to sunburst cracks. Sunburst cracks are multi-branched shattering patterns covering areas reaching up to 70 x 15 meters (11). For all the reported failures, cracks initiated at the seams or spot tack welds, which implies that the seaming technique is the main cause for this problem, even though a small single crack is necessary to generate the shattering crack.

Peggs (11) presented the results of tests conducted to understand the shattering cracking phenomenon. The study of fracture faces with a microscope showed that the faces are very smooth showing no plastic deformation, and featuring chevron patterns pointing to the propagation point. The propagation points were found to be at seams where geometrical notch stress concentration points were located. It was also found that many propagation points were located at the intersections of seams and points resealed with a fillet bead.

Moreover, it is clear that excessive thermal energy input increases the possibility of brittle SC at seams; incorrect seams may reduce the SC resistance of geomembrane up to 50%. The crack growth rates were evaluated and different values found for different materials, implying that the different polyethylenes do not have the same mechanical durability (11). The thermal expansion factors were also assessed to understand the thermal SC caused by the cold weather. The curves are comprised of two parts: one below 50°C with a coefficient approximately equal to $1.2 \times 10^{-4} \text{ } ^\circ\text{C}^{-1}$ and the other above 50°C featuring a

coefficient of $7 \times 10^{-4} \text{ }^{\circ}\text{C}^{-1}$. Uniaxial tensile testing showed that the yield stress increases from 20.7 Mpa, with an elongation of 12%, to 35 Mpa, at 25°C, and an elongation of 6%, at temperature of -30°C. The break point stress also increases from 29 Mpa (850% elongation) to 35.2 Mpa (422% elongation), indicating that during cold weather the geomembrane possesses better properties with respects to stress but will break at lower elongations. This study showed that a stress (50% or less of the yield strength) must exist in the material to initiate the SC phenomenon. During seaming procedures, special care must be taken to prevent notches in the seams, particularly damage by overheating. A non-penetrating crack can be repaired without affecting the geomembrane, nevertheless while repairing wide shattering cracks, a compensation panel must be placed in the liner system to stabilize the effect of the temperature.

3.2.11 Review of the Stress Cracking Evaluation Test

The first test used the test standard ASTM D 1693 (12) “Bent Strip Test”. A surface notched (20% of the thickness) rectangular specimen is bent in a 180° arc and placed within the flanges of a small metal channel. Ten specimens are usually tested simultaneously in a surfactant agent and at an elevated temperature. The times to failure are monitored.

Although this test was used for many years, it was not included in material specifications for HDPE geomembranes (13). Effectively, this test is not aggressive enough toward modern resins since polyethylene can relax the applied stress, canceling the desirable stressing effects. This implies that whatever stress is applied, the material will relax and the stress will drop to nearly zero. Moreover, it takes an extremely long time to perform, more than 1,500 hours.

ASTM D 5397 (14) “Notched Constant Tensile Load Test, NCTL” is a much more severe test since the specimens cannot relax while under constant load. A dumbbell shaped specimen is notched, placed in a surfactant agent at a specific temperature, and constant stress is applied by a dead weight. The applied stress varies from 20% to 65% of the yield stress. Ten different stress values must be applied to test one specific material; moreover, to ensure the quality of the measure, three specimens must be tested for one applied stress, which means that thirty specimens must be tested to evaluate one material. The time to rupture is monitored and used to generate an applied stress versus failure time curve. Each different stress provides one point, which means that the curve is drawn by joining the ten different points.

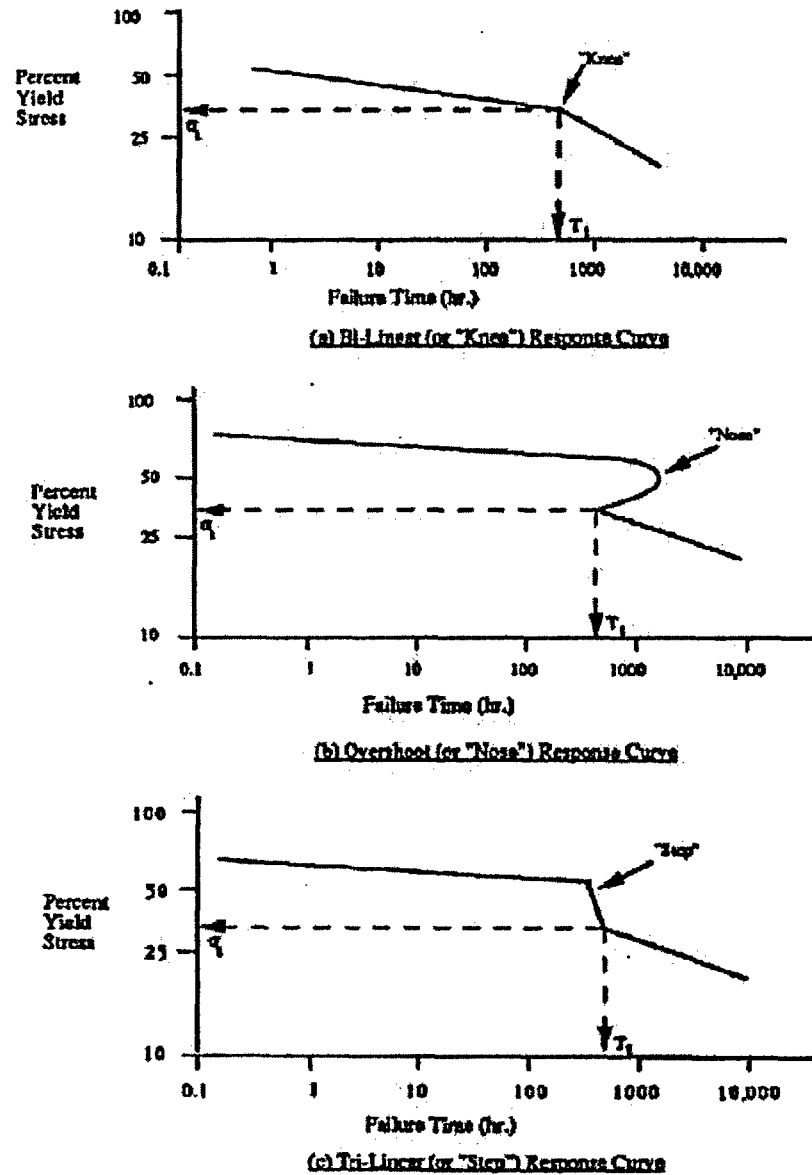


Figure 10: Behavior of HDPE Material in a NCTL Test (3)

Fig. 10 presents the different types of response curves for different HDPE materials. At least two distinct regions can be identified: for high stress level, the specimens respond in a ductile manner, while in the second region (lower stress level) they fail in a brittle manner. Depending upon the applied stress, a specimen can fail in a totally ductile or totally brittle manner. The transition time appears to be at 35% of the yield stress.

The problems associated with this test is that the time required sometimes over 1000

hours, for a sizable number of specimens. Moreover, if the statistical averages are not reasonable, some of the data points must be obtained by re-testing (3).

In order to modify the previous test, the "Single Point Notched Constant Load Test, SP-NCLT" (ASTM D 5397 Appendix) was developed. In this test only one notched specimen is tested at a constant stress equal to 30% of the yield stress (point slightly lower than the transition point). The minimum time a material must withstand is 200 hours. In order to obtain statistical correct values, five tests must be carried out. This test has proven to be the best tool (13). Since its results correlate with the field performance, it can be used with confidence.

However, some disadvantages have been encountered. This test cannot be performed on textured geomembranes since it is difficult to create an accurate notch on the rough surface of the material. Moreover, scattered results among different laboratories were found, increasing the difficulty to evaluate the SC of a geomembrane (13).

There are two reasons for the scattered results. Using an average 30% of the yield stress does not ensure accurate results since a yield stress for a specific material may vary from one roll to another, therefore the applied stress may range from 27.5 to 32.5 percent instead of the specific 30%. Another cause of scattered results comes from the notch; even if the razor blade is replaced every 20 notches, as specified in the ASTM standard, the size of the notch may vary from the first to the last notch. Nevertheless, a good method to prevent scattered results is to do five tests instead of one, and validate geomembranes for more than the 200 hours specified in the ASTM standard.

Some procedures have also been developed to test the SC behavior of seams. An adaptation of the SP-NCLT to seams, the "Seam Constant Tensile Load, SCLT", evaluates the quality of geomembrane seams. Therefore, comparisons between the seam test results and sheet test results can provide information on the effectiveness of the seaming technique. A notch is introduced in a seamed dumbbell specimen (see Fig. 11). The test conditions are similar to those for the SP-NCLT tests.

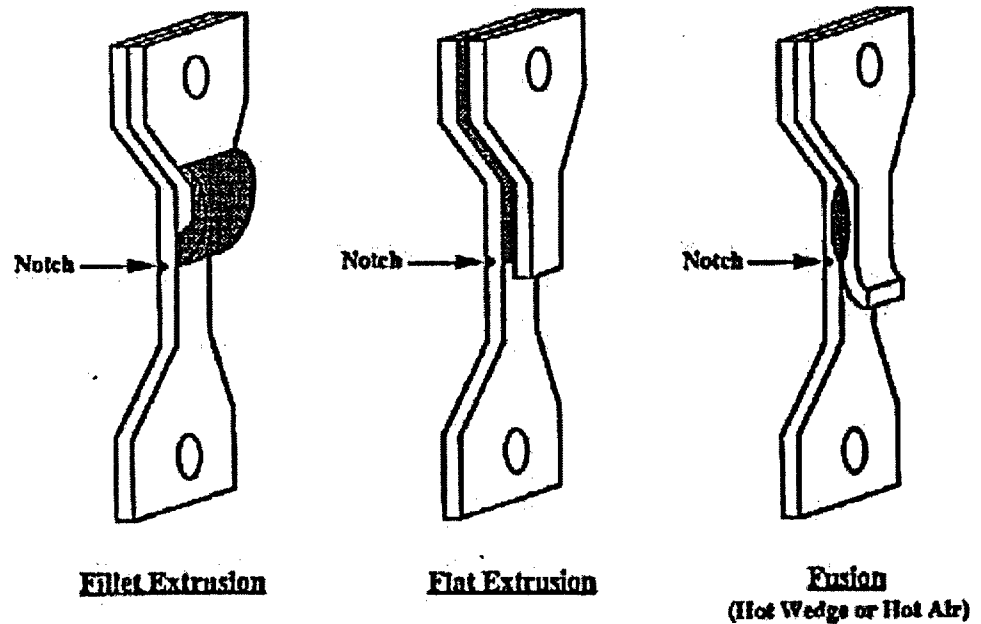


Figure 11: Seam test SCTL specimens (3)

3.2.12 How to prevent SC

It is of paramount importance to ensure that the membrane is installed with sufficient slackness and compensation for applications in cold weather. This creates an error margin, which guarantees non-failure in SC testing. HDPE compensation panels can be inserted allowing the elimination of the thermal stress. Uncovered geomembranes should feature a minimum slackness of 1% when exposed to UV; they must be covered by an insulating panel (10). Special care during seaming is required to minimize the risks of imperfections in the seams, which are stress concentration points that may lead to propagation. A properly selected resin and additive package together with proper manufacturing of the sheet, will ensure a stress crack resistant material (3).

3.2.13 Method of prediction

A method to predict the life of HDPE geomembranes based on SC has been developed by Kanninen (15), and is explained in the chapter devoted to life prediction.

3.2.14 References

1. Jailloux J.M.: "Testing Environmental Stress Cracking of High Density Polyethylene", Earth Reinforcement Practice, Ochlaï, Hayashi & Otani, Balkema, Rotterdam, pp. 91-94, 1992.
2. Peggs I.D. "Testing Program to Assure the Durability of Landfill Liner", Proceedings Sardinia 91, pp. 651-665, 1991.
3. Koerner R.M., Hsuan Y.G., and Lord, Jr. A.E.: Stress Cracking Behavior of HDPE Geomembranes and its Prediction, GRI Report #9, Drexel University, June 1993.
4. Lustigier A., Rosenberg J.: "Predicting the Service Life of Polyethylene in Engineering Applications. In: GRI-Seminar II, Durability and Aging of Geosynthetics", Ed. By Koerner R.M., Published by Elsevier Applied Science, pp. 212-229, 1988.
5. Bright D.G.: "The Environmental Stress Cracking of Polymers Used in Geosynthetic Products", Geosynthetics'93, Vancouver, Canada, pp. 925-933, 1993.
6. Peggs I.D., Carlson D.S.: "Brittle Fracture in Polyethylene Geomembrane", Geosynthetics Microstructure and Performance, ASTM STP 1076, Peggs I.D., American Society for Testing and Materials, Philadelphia, pp. 57-77, 1990.
7. Lowrance, S.K.: "Use of Construction Quality Assurance (CQA) Programs and Control of Stress Cracking in Flexible Membrane Liner Seams", EPA, July 1989.
8. Peggs I.D., Carlson D.S.: "Stress Cracking of Polyethylene Geomembranes: Field Experience", Durability and Aging of Geosynthetics, Koerner R.M., Elsevier Ed., London, UK, pp. 195-211, 1989.
9. Lord Jr. A.E., Koerner R.M., Wayne M.H.: "Residual Stress Measurements in Geomembrane Sheets and Seams", Geosynthetics' 91, Conference Proceedings, Atlanta, USA, pp. 333-349.
10. Peggs I.D., Kanninen M.F.: "HDPE Geosynthetics: Premature Failures and Their Prediction", Geosynthetics International, Vol. 2, No. 1, pp. 327-329, 1995.
11. Peggs I.D., Carlson D.S.: "Understanding and Preventing 'Shattering' Failure of Polyethylene Geomembranes", Fourth International Conference on Geotextiles, Geomembranes, and Related Products, Volume 2, The Hague, Netherlands, pp.549-553, May 1990.
12. ASTM D1693: "Test Method for Environmental Stress-Cracking of Ethylene Plastics".

13. Thomas R.: "Stress-Crack Test of HDPE: we Have the Tools, Now What do we do with them?", Geotechnical Fabrics Report, pp. 42-45, May 1996.
14. ASTM D 5397-93: "Standard Test Method for Evaluation of Stress Crack Resistance of Polyolefin Geomembranes Using Notched Constant Tensile Load Test"
15. Kanninen M.F., Peggs I.D., and Popelar C.H.: "A Methodology for Forecasting the Lifetimes of Geomembranes that Fail by Slow Crack Growth", Proceedings of Geosynthetics'93, IFAI, Vancouver, Canada, pp. 831-844.

3.3 Puncture/Installation Damage

3.3.1 Introduction

Installation damage is caused during the construction and installation of the liner; and decreases the strength of the liner. Puncture of the geomembrane or the geotextile is the most common and the worst type of damage to the liner.

One effect of puncture is the alteration of the liner's durability and impermeability. This is of serious concern, as after landfilling it is impossible to determine the state of the membrane, i.e. the puncture phenomena cannot be assessed. The designer cannot use test data to predict the geomembrane behavior.

During their life (installation included), landfill liners are submitted to short term as well as long-term puncture forces. Short-term forces occur during the installation of the drainage gravel, while long-term forces are caused by overburden loads of the waste (pressures of the order of 10,000 to 20,000 lb/ft³).

The puncture phenomenon can either be static or dynamic. Dynamic puncture is due to the fall of objects as stones, gravels or tools, and occurs mainly during installation. It is a function of the object weight and the fall height. It is a short-term effect. Static puncture is due to the contact of a stone or gravel with the geomembrane under static normal stress. It can either be a short-term (traffic) or long-term (fall of upper layer) phenomenon. Bursting, a sort of static puncture, occurs when static pressure pushes the geomembrane into a gap formed between two aggregates caused by local differential settlement.

Geotextiles are used with geomembranes because of their complementary properties. Geomembranes are impermeable and sensitive to puncture, while geotextiles are permeable and puncture resistant. Hence, to counter the problem of puncture sensitivity of geomembranes, it is common to install a geotextile layer over a geomembrane. Geotextiles possess different advantages when used with geomembranes: they provide a good puncture resistance layer as well as abrasion resistance, they also help welding by providing a clean surface (1).

3.3.2 Methods of prediction

The Solvay group developed a method (2) to ensuring no denting of the geomembrane, and, therefore, no change in durability, by determining the stress at failure and the admissible stress of the geomembrane.

The stress at failure is defined as the maximum static stress that can be applied without causing leakage. The geomembrane is tested with a hydraulic puncture pressure of 1,300 kPa, and the stress at failure is defined as follows:

$$\sigma_r = 1000 / (D_s \times D_c) \times [160 T_g - 0.12 + (1000 T_g - 0.3 M^{1.8})] \dots \dots \dots [3.3.1]$$

where

σ_r : stress at failure (Pa)

D_s : maximum diameter of crushed gravel in supporting layer (m)

D_c : maximal diameter of crushed gravel in protective layer (m)

T_g : thickness of the geomembrane (m)

M : total surface mass of both geotextiles above and under the geomembrane (kg/m^2)

These variables are presented in Fig. 12.

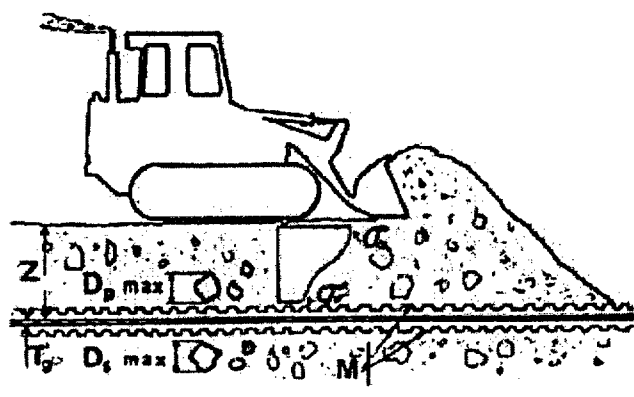


Figure 12: Mechanical puncture parameters (2)

From the stress at failure it is possible to determine the admissible stress, defined as the maximum stress for which no puncture marks will appear on the geomembrane. Using field experiments, the Solvay group determined that the admissible stress is approximately one-tenth the stress at failure. By using the Boussinesq model, the stress due to vehicular traffic at the geomembrane level can be determined with the plots in Fig.13.

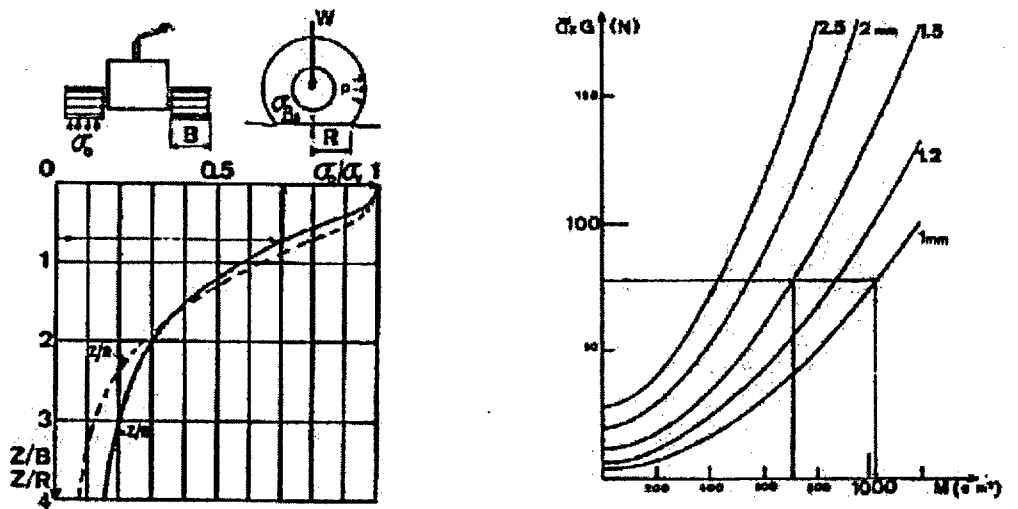
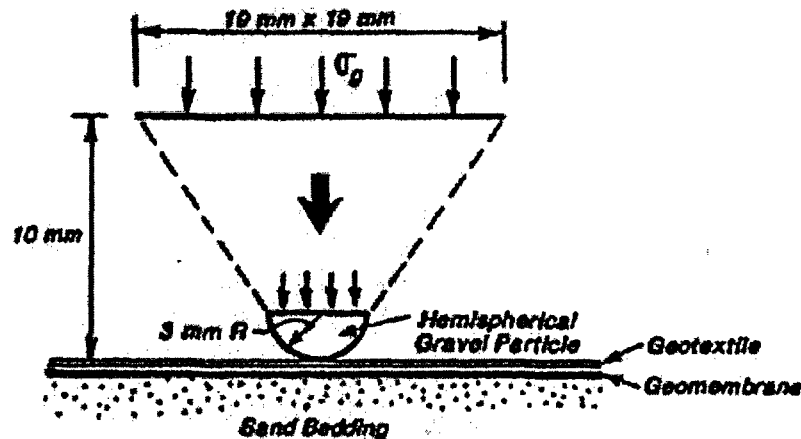


Figure 13: Graph providing the stress at the geomembrane level (left) and its thickness (right) (2)

Using this method it is possible to determine the state of the geomembrane and the thickness of the protecting liner. This method has been validated by many work site observations and can, therefore, be considered efficient.

Wong and Wijewickreme (3) developed a computer analysis method by using the FLAC (Fast Lagrangian Analysis of Continua) program to model the action of gravel on a geomembrane, Fig. 14. Several assumptions were made since the reality is extremely



complex.

Figure 14: Model of a gravel puncturing a geomembrane (3)

A hemispherical gravel particle was modeled, applying stress on the geomembrane, with the geomembrane placed over a sand bedding. A Mohr-Coulomb yield criterion was used to determine the “failure” of the geomembrane. An axisymmetric mesh was used as well as a postprocessor for determining the results. The results were close to the field data proving the efficiency of the program.

Giroud et al. (4) carried out a theoretical analysis of geomembrane puncture and established a relationship between the puncture by a probe, and by a uniform stone layer subjected to liquid pressure. The relationships between the geomembrane resistance to puncture by stone, under different conditions, was also established.

The first part of this study formulated an equation for theoretical puncture resistance of a geomembrane by a probe, based on the assumption that the contact area between the geomembrane and the object can be represented by a circle.

The equation was as follows:

$$F_p = \pi d_p \sigma_{\text{peak}} t_{\text{GM}} Z_{\epsilon \text{ peak}} \dots \dots \dots [3.3.2]$$

where F_p is the puncture resistance, d_p is the diameter of the probe, t_{GM} is the thickness of the geomembrane, σ_{peak} is the geomembrane stress at peak, and $Z_{\epsilon \text{ peak}}$ is the peak value of Z .

This equation was validated by comparing the theoretical results (from Equ. 3) with the test results based on NSF specifications for puncture resistance, tensile stress, and strain at yield of HDPE geomembranes. However, this equation can only be used for material yielding or rupturing at strains not greater than 57 %, since Z_e exists only in the range of 0 to 57 %. HDPE is one of the materials that allow prediction, since it yields at a strain of 10-15%.

In the second part of this study, the authors established a relationship between the puncture resistance of a geomembrane in a probe test and the resistance to puncture of the geomembrane (laid on a layer of stone) subjected to pressure applied by a liquid.

For the case of a stone, the equation becomes:

$$F_{ps} = \pi d_{cs} \sigma_{peak} t_{GM} Z_{e \text{ peak}} \dots \dots \dots [3.3.3]$$

where F_{ps} is the force exerted by a stone on the geomembrane, and d_{cs} is the diameter of the equivalent circular contact area between the stone and the geomembrane.

If the geomembrane is free to elongate, the probe and stone will have the same values of σ_{peak} and ϵ_{peak} causing puncture failure. But when the geomembrane is in contact with a solid material as a soil, in contact to stones it is not free to elongate. To counter this problem, the pressure is applied by a liquid, which allows it to elongate.

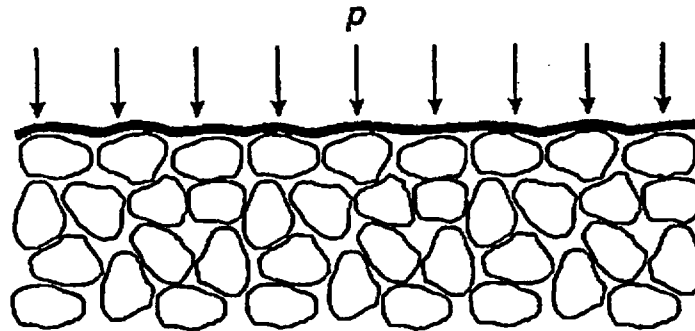


Figure 15: Configuration of a pressurized geomembrane placed on a uniform layer of stone (4)

The puncture force in this configuration is:

$$F_s = p A_{avg} - p \pi d_{cs}^2 / 4 \dots \dots \dots [3.3.4]$$

with p the pressure applied by the liquid, and A_{avg} the average surface area of the geomembrane associated with the stone.

$A_{avg} = \lambda d_s$ in the general case, with λ ranging from 0.87 to 1.

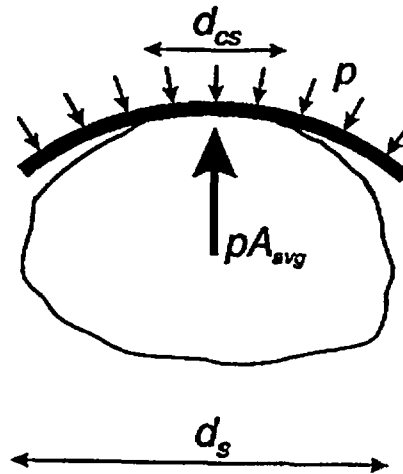


Figure 16: Stone contact on a geomembrane (4)

Since $d_s \gg d_{cs}$ the equation becomes:

$$F_s = \lambda d_s^2 p_p \dots \dots \dots [3.3.5]$$

with p_p being the pressure of the liquid.

For the case of round stone, Fig. 16, the puncture resistance is increased since the contact pressure is decreased due to the increased surface contact. But it is possible that the geomembrane will fail by bursting between the stones instead of failing by puncture. The authors established relations for geomembrane resistance to puncture by stone under different conditions. The relation that can be used for the design of field applications has to be based on laboratory probe puncture tests. This study also proved that the geomembrane puncture phenomenon is a function of the diameter of the contact area between the geomembrane and the puncturing object, the membrane thickness, and the tensile properties of the material.

3.3.3 Laboratory tests

Motan et al. (5) assessed the damage caused by overburden pressure (10,000 to 20,000 lb/ft³) on geomembranes. The first stage of the study was to expose the geomembrane (with or without geotextile) to gravel in a pressurized chamber, Fig. 17, pressures being set at 10,000, 15,000, and 17,000 lb/ft³. The second stage was multi-axial testing (according to the test method GRI-GM4). The air pressure was gradually increased, with monitoring of the central deflection of the geomembrane (only the specimens that did not suffer puncture during the first step were tested in the multi-axial chamber).

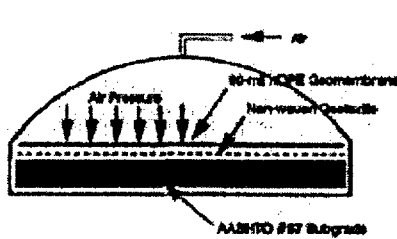


Figure 17: Setting of the pressure chamber used during the first part of this project (5)

Three configurations were studied to protect a smooth 60 mil HDPE geomembrane: a) a continuous-filament, polyester, non-woven, needle-punched geotextile, b) a continuous-filament, polypropylene, non-woven, needle-punched geotextile; and c) a staple, polypropylene, non-woven, needle-punched geotextile. The gravel (AASHTO #57) was chosen because of its angularity to induce damage.

To get important data, three different configurations were tested in the multi-axial test chamber: a) virgin specimens not exposed to pressure, b) specimens exposed to pressure but without geotextile protection, and c) specimens exposed to pressure with geotextile protection.

The results showed that for unprotected geomembranes, specimens failed during pressurization at $10,000 \text{ lb/ft}^3$. An interesting result is that when the geomembrane does not puncture during the first stage of the test (pressurization), it will yield the same results as a virgin geomembrane that is multi-axial tested. But it was not possible to classify the different geotextiles, since they showed the same protection properties. The breaking strains appear to decrease with the increase of pressure, and increase with the increase of the geotextile weight. Different failure modes occurred: loss of pressure, pinholes, large-scaled splits or tears.

Two test methods are commonly used to assess puncture properties: ASTM D5494 and GRI-GM3. Beside these methods, the Austrian standard ONORM S 2076 presents two interesting test methods to assess the long and short-term puncture effects on liners. The first test consists of a pressure plate to simulate the long-term effect, while a pyramid puncture test simulates the short-term effect. Werner and Puhlinger (6) used these two test methods to assess needle-punched PP continuous filament non-woven and needle-punched HDPE staple fiber non-woven geotextiles.

The pressure plate apparatus is composed of a plate embedded with steel balls to simulate gravel as well as obtaining an even distribution of defects. A plate is set in contact with the protecting geotextile, which is on the top of the geomembrane. Below the geomembrane, a soft metal sheet is placed (see Fig. 18), which will be deformed by balls; then laser scanning is used to evaluate the deformations (see Fig. 19). Two different temperatures are used to simulate the temperature inside the landfill; also, two loads are used: 589 kN/m^3 and 1104 kN/m^3 , which simulate waste heights of 50 and 90m respectively.

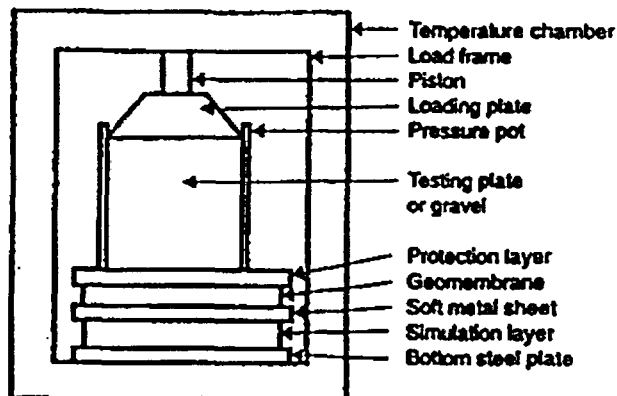


Figure 18: Pressure plate apparatus (6)

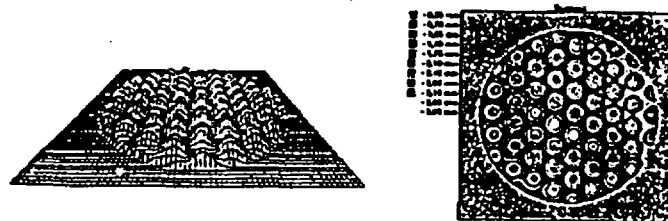


Figure 19: Profile of the sheet plate by laser scanning (6)

The pyramid test consists of a pyramid-ended rod pressing against the tested sample. An electrical current between the rod and the base plate indicates when the perforation occurs (see Fig. 20).

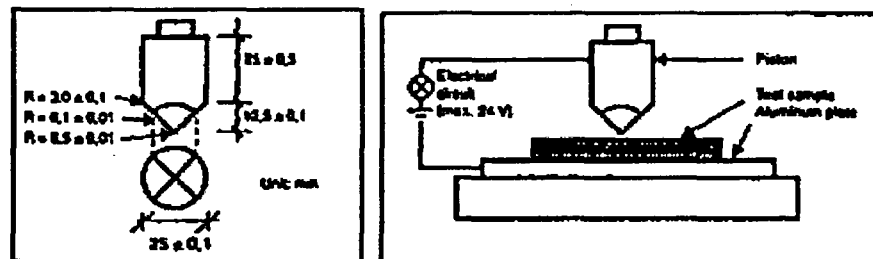


Figure 20: Pyramid piston apparatus (6)

The results of these tests showed that for both configurations the PP continuous filament non-woven geotextile has superior puncture resistance compared to the HDPE staple fiber non-woven geotextile.

It was also shown that the parameter-influencing punctures are as follows: overburden load, geomembrane type, geotextile type and mechanical properties, temperature, type and size of drainage gravel, and the evaluation method. The conventional scanning method used for the evaluation of the soft steel sheet deformation leads to misleading results since local deformation peaks are not detected. This problem emphasizes the efficiency of the laser scanning method.

Artieres and Delmas (7) presented different tests for the determination of liner puncture resistance on several liner materials. These tests were intended to characterize the behavior of the test specimens while exposed to dynamic and static puncture.

The puncture resistance system of a liner consists of a non-woven needle-punched geotextile protecting the geomembrane from the gravel of the drainage system. An efficient method to test material against puncture is to conduct larger scale performance tests that exactly reproduce the liner-layered structure. However, these tests are expensive, long, and cannot be repeated as wanted. To counter these problems, index tests have been developed which are inexpensive, rapid, and repeatable. Performance tests require the reproduction of the liner condition (same material, same scale), while for index tests some parameters are arbitrary fixed (usually the shape of the loading piston and the type of support) to facilitate laboratory tests and repeatability.

For dynamic testing, the stiffness of the matrix is an important parameter, which conditions the specimen deformations. A flexible geomembrane will have a lower puncture resistance than a stiffer product, even when a geomembrane protection layer is used. Protection against dynamic puncture has been shown to be very efficient, especially when using the combination of upper and lower geotextile protection layers (with good bearing capacity but small surface hardness). For static puncture, it has been shown that stiffer geomembranes possess better resistance than flexible ones. Moreover, the resistance is almost a linear function of the material thickness, indicating that thicker the geomembrane, more the resistance. Tests of geomembranes protected with geotextiles show that the resistance of the assembly is approximately equal to the sum of the puncture resistance of the different components calculated independently.

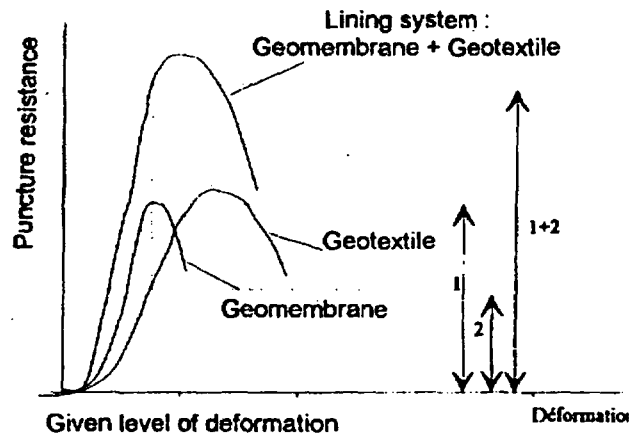


Figure 21: Puncture resistance summation of two different components of a liner (7)

Therefore, the designer can calculate the puncture resistance of a liner system by simply adding the puncture resistance of the different components (see Fig. 21). The index tests results are quite close to the field results, thus proving their effectiveness for preliminary design; the final design can be based on the analysis of the simulated real condition (7).

3.3.4 Full-scale tests

Wong and Wijewickreme (3) assessed the survivability of 40 mil HDPE and 30 mil VLDPE geomembranes submitted to puncture stress during installation with stress induced by vehicular traffic. This study modeled a cap preventing leakage. To protect the geomembrane a thick non-woven needle-punched geotextile blanket was placed above it.

A 300 mm thick layer of gravel was placed above the geotextile blanket that is placed above the geomembrane, which is installed above a bedding. For each geomembrane (30 mil VLDPE and 40 mil HDPE), three different bedding conditions were used: 1/3 of compacted sand and gravel, 1/3 with loose sand, and 1/3 with compacted sand. For each configuration, the blanket covered only 2/3 of the geomembrane surface to assess the geotextile efficiency. The loading consisted of a 51,477 lb truck which passed over the soil at 5 km/h. to simulate construction conditions; the truck stopped and started many times. After the application of stress, the geomembranes were exhumed and the density of the soil measured at different locations

The number of holes and deformations on the two geomembranes were determined, and then analyzed to evaluate the different parameters of the puncture effects. For sand bedding with a blanket, it was found that in both cases the geomembranes were capable of withstanding the load. It was also shown that disturbances in the sand due to footprints made during installation were not detrimental to the geomembrane survivability.

For the sand and gravel bedding with a blanket, the results showed the presence of many holes and pressure points, indicating that in these conditions this type of bedding is inappropriate and should not be used. Moreover, results from other studies confirmed the

same observations. In this configuration the gravel acts as a hard point, while the sand acts as a matrix compressing the gravel against the geomembrane, thus deteriorating it.

At locations where the geotextile did not cover the geomembranes, results showed that more holes and pressure points appeared, proving the efficiency and the necessity of the geotextile. The two geomembranes yielded the same results when well protected, but when gravel was used in the bedding, HDPE showed its superiority. Therefore, the 40mil HDPE is more adequate than the 30 mils VLDPE geomembrane in such conditions. It was proved that the most critical mode of loading is the stop/start action of the truck, which increases puncture stress at the geomembrane level, even with a geotextile blanket that decreases the puncture stress.

Darilek et al. (8) paper presented the effects of the installation of protection soil over a geomembrane during the construction of a landfill. This study is very interesting since liners are sensitive to the emplacement of a protection soil cover or gravel damaging the liner. The liner was composed of a 900 mm layer of compacted clay, 2mm HDPE geomembrane, 300 mm of gravel, a 2 mm HDPE geomembrane, a layer of geogrid and geotextile, another 300 mm of gravel, another geotextile, and finally a 300 mm layer of sandy clay.

To assess the damage caused by the installation of the gravel, an electrical leak location survey (composed of 12 leak locations) was carried out before and after the emplacement of the gravel on each geomembrane. The role of the gravel is to serve as a drainage medium to evacuate hypothetical leaks above the primary liner, and for a leak location system above the secondary liner.

The electrical leak detection system is based on the insulation properties of the liner materials and the conductivity of the water, thus when a leak exists the electrical current goes through the liner carried by the water conductivity. This method is accurate to locate leaks even as small as pinholes.

After the geomembrane is installed, an electrical leak survey is used to assess the leak in the geomembrane before the gravel installation. Several leaks were detected, most of them in the extrusion welds, but the largest ones were due to punctures and slits in the liner panels. These leaks were related to improper seaming and installation of the geomembrane.

Before the installation of the gravel, a test was carried out to assess the deterioration caused by a bulldozer on the geomembrane. This test took place outside the landfill with a geomembrane layer, covered by a thin layer (2.5") of gravel. A bulldozer drove over it and executed sharp pivot turns. No leaks were detected even though some marks appeared on the liner. However, it was indicated that a minimum layer of 12" of gravel should separate the geomembrane from the bulldozer.

Special care was used to place the gravel: a sacrificial sheet of liner was placed on the side slope to create an access ramp, a geofabric, plywood sheeting, and timber were also used to protect the geomembrane from installation damage. First, the slope was covered by gravel, and then two bulldozers scraped the gravel in the central section of the landfill by monitoring the minimum 12" of gravel layer. When the gravel was installed, one bulldozer

passed by the ramps, then the excessive amount of gravel in the ramp was taken out; finally, the last bulldozer was towed out on plywood in neutral gear.

After installation of the gravel nine leaks were detected electrically. These flaws, created during gravel installation, varied from pinhole size to 64 mm gage. Moreover, it was noticed that a concentration of these leaks happened to be near the emplacement of the temporary ramp. No leaks were detected on the primary liner; this is due to the utilization of geogrid and geofabric to protect the geomembrane, thus preventing damage. The study proved the efficiency and necessity of a protective layer, especially when heavy bulldozers are used to set the gravel. The efficiency of the electrical leak detection system was also proved. Finally, the quality and conscientiousness of the installation team was shown to be an important factor in the elimination of installation damage.

Reddy et al. (9) used various field testing procedures to evaluate the efficiency of different protective cover soils. Two kinds of gravel were used (fine and medium), with the same geomembrane (a 60 mil HDPE). The geotextile was a non-woven needle-punched polypropylene; two bulldozers (one light CAT D4 and one large CAT D7) were placed on the gravel. Before installation the geomembrane was inspected to detect hypothetical flaws. Then the entire liner was constructed in accordance with the real configurations. The construction procedure was identical to the real one (especially for the bulldozer work).

First, the different soils were tested before and after the construction of the liner, it was found that there were no significant differences between the "before" and "after" indicating that the properties of the soil were not modified by the liner construction.

Then, to assess the effect of the construction on the geomembrane, different tests were performed on the geomembrane before and after construction. The water vapor transmission test. (ASTM E 96) was used for permeability evaluation of the geomembranes. The larger the transmission values, the more the damage. The results showed no significant change between the virgin and the exhumed geomembranes for the different configurations, indicating that the geomembrane is marginally affected by the construction of the liner for the range of studied configurations.

Multiaxial tension tests (ASTM D 5617) were also carried out. It was shown that the average geomembrane tensile stresses from field specimens were approximately equal to the values for a virgin geomembrane.

Exhumed Geomembranes used without geotextiles showed slightly higher tensile stresses than the virgin geomembrane. The geomembrane with the geotextile showed a slightly lower tensile stress than the virgin geomembrane. However, the results of elongation at failure showed significant differences from one protection configuration to another. The elongation at failure decreased with increase of the soil particle size and use of a heavy bulldozer, but in the case of a protected geomembrane, the specimen elongation, at burst, increased significantly to a value larger than that for a virgin geomembrane, thus proving the efficiency of the protecting geotextile.

The last series of tests consisted of wide strip tensile testing (ASTM D 4885). It was shown that the geomembrane's yield stress under the different configurations is almost equal to that of the virgin specimen. Moreover, the specimen yield stress and strain were not affected by the configuration.

However, all the geomembranes failed at a lower value than the virgin geomembrane, with smaller difference for the protected geomembrane. It was also noticed that all unprotected geomembranes suffered scratches and dents, but no tears or holes were found. Finally, it was concluded that the use of a geotextile greatly increases the protection of the geomembrane.

Koerner et al. (10) assessed the installation damage of different geosynthetics products under two different backfills. The first backfill was made of angular, poorly graded gravel, while the second was composed of poorly graded sand. Six different geotextiles and one geogrid comprised the materials tested. Their properties were determined before and after installation. For each of the two sites, the specimens were placed and installed as part of the regular construction. After installation, the specimens were exhumed and tested. The results showed that the geosynthetics placed over the angular backfill suffered severe damage while those placed over the sand were not so affected.

The geogrid in the first case was less damaged than the other geosynthetics, while in the second case no visual damage was found on the geogrid. The heaviest geotextiles were the least affected in the first case, in the second case no holes were found on the geotextiles.

These results prove the influence of the backfill effects on the installation survivability of the geosynthetic products. The authors also defined a factor-of-safety expressed as the inverse of the percent strength remaining in the wide-width test (ASTM D 4595). These factors ranged from 1.4 for the geogrid to 4.3 for the thinnest geotextile.

Geotextiles can suffer damage during the different stages of their lives, but it is during the compaction that they are exposed to the maximum damage.

Billing et al. (11) assessed the installation damage of different materials (polypropylene P1, polypropylene P2, polyester, polyester strip, and polyethylene grid) for three different backfills (a well-graded crushed limestone, a uniformly graded quartzitic sand, and a silty sandy clay). The damage was caused by compaction of aggregate layers over the geosynthetics. Then, visual inspection and mechanical tests provided information on the behavior of the different materials versus the backfill type. The visual inspection indicated the damage caused by the aggregate. The rib is the most sensitive part of the geogrid, also different types of damage were seen on the geotextiles. The mechanical tests showed reduction in tensile strength for different materials, ranging from 7% for the polypropylene P1 to 36% for the polypropylene P2. Creep tests showed no change in the creep rate, even though the damage caused a reduction in the initial strain. This study agreed with expected behavior, and reinforced the findings of other studies, proving that the more angular the backfill, the more the damage.

3.3.5 Parameters influencing puncture resistance and installation damages

The different parameters that affect the puncture resistance of landfill liners are as follows:

- diameter of the contact area between the geomembrane and the puncturing object
- thickness and tensile properties of the geomembrane
- angularity and size of backfill particle
- weight and type of construction and compaction equipment
- type of material comprising the liner (weight, thickness and mechanical properties)
- overburden weight of waste
- quality and conscientiousness of the workers

3.3.6 Design and construction of the protecting layer

To protect the geomembrane liner, the protective liner should meet the following specifications:

- prevent the geomembrane damaging due to drainage installation and waste placement
- prevent the geomembrane from tearing, bursting, and puncture impact
- serve as a drainage system for the landfill leachate
- withstand landfill construction (i.e. waste placement, closure) without deformation.

In the United States, several problems exist concerning the protecting layer, as mentioned by Reddy et al. (9) and explained below:

- the type of soil that can be used is not explicitly defined, hence local material tends to be used, even if the properties do not match the specifications
- no specific rationale has been defined to determine the effective thickness of the protective liner
- no construction procedures exist

Ruetten et al. (12) presented a method for the designing of liner protective soil cover by using geotextile and soil layers.

A step by step explanation of the design is provided below:

- Identification of foundation conditions and physical properties of the geomembrane/geotextile, which comprise the liner.
- Determination of the availability of the material in a local region; the cost is an important factor during this phase. The drainage material may consist of either a single material, or composition of several materials or a geotextile layer.
- Determination of the material physical properties (grain size distribution, permeability, soundness, and shear strength), as well as chemical compatibility to the leachate.
- Determination of the possibility of waste migration to the granular material voids. The nature of the waste must be estimated.
- Analysis of constructibility and puncture resistance. A protection layer should be placed over the geomembrane to limit point pressure, support construction equipment, and limit rutting. To ensure and verify the proper design, a field trial is advised. During this trial, pressure is applied by the action of a bulldozer, then tests such as multi-axial burst, help to determine the geomembrane survivability. Based on the results of these tests, material must either be discarded or protected by a protective layer.
- Determination of the side slope stability of the protective cover.

The different materials that can be used in protective covers are as follows: geotextile, gravel, composite layer of different gravel, sand-filled geotextile, gravel-filled geotextile, geosynthetic clay liner, and concrete-filled geotextile.

The sequential steps for the installation of a protecting cover are listed here for the case of only one impermeable geomembrane:

- geomembrane liner is placed over compacted clay
- geotextile is placed over the geomembrane
- protecting cover soil is dumped on the geotextile; bulldozers spread the soil over the entire surface for a specific thickness.

The placement of the geomembrane liner should be effected between 40°F to 104°F. It should not be placed during precipitation, excessive moisture, or excessive wind.

The placement of the geomembrane should be done as follow (13):

- each panel should be rolled out and installed in such a way that all the seams run down the slope on the perimeter berms (perpendicular to top of slope)
- the geomembrane rolls should be placed using the correct spreader and rolling bars with cloth slings
- each panel should be inspected for damage or defect before seaming, defected panels should be automatically replaced
- the geomembrane sheet must not be dragged over the rough soil sub-bases
- the geomembrane should be anchored according to the manufacturer's recommendations
- workers should not smoke, wear damaging shoes, or act in a manner that can damage the material
- edge of the geomembrane should be loaded to prevent uplift due to wind
- no debris, tools, or unexpected objects should be kept on the geomembrane, the geomembrane should be neat in appearance
- vehicular traffic should not be permitted across the liner
- a scrap geomembrane sheet should be placed under each equipment necessary for the liner construction to prevent damaging the liner
- equipment should not remain on the liner overnight

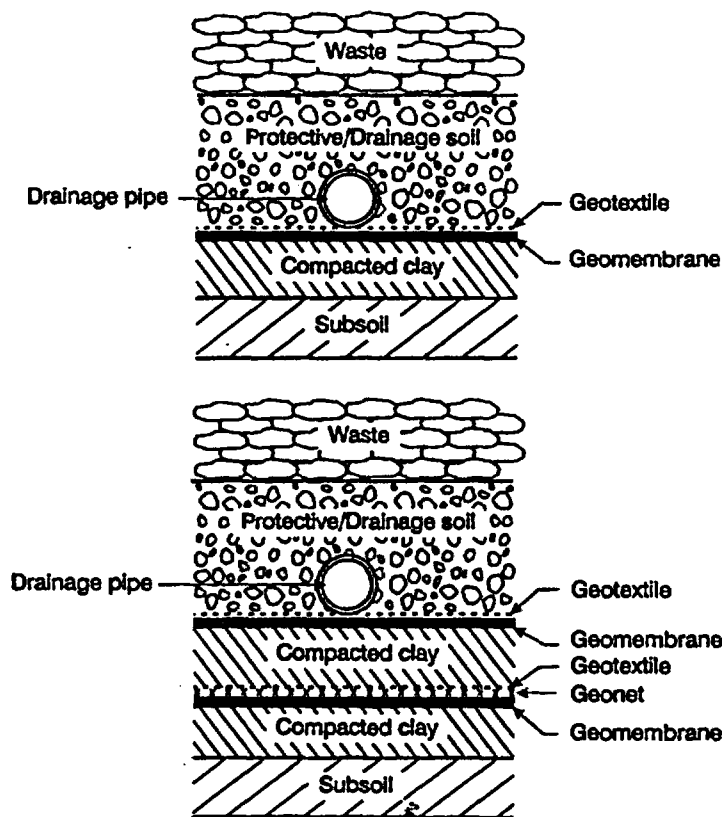


Figure 22: Cross section of single composite and double composite liners (9)

Fig. 22 presents the cross sections of typical single and double composite liners. During these steps, special care must be taken not to damage the geomembrane, especially due to the heavy equipment used to place the protecting cover soil. To minimize risks of damage, machines must not be driven directly over the geotextile, and a minimum thickness of the soil must always be maintained between the geotextile and the wheels.

Large aggregates are used as backfill material (14) to prevent clogging of the drainage system, which occurs when fine aggregates are used. However, the large aggregates increase damage to the geotextile and geomembrane used in the liner system.

3.3.7 Values of tests results

In his literature review, Allen (15) listed the survivability levels of different liner conditions (see Tables 10 and 13), he also gathered results from previous studies concerning installation damage on material properties (see Table 12) and indicated factors of safety (see Table 11).

Table 10: Survivability Levels for Slope and Wall Application (15)

Type of Compaction equipment	Backfill Characteristics	Initial Lift thickness (cm)		
		< 15	15 to 30	> 30
Tracked equipment	Fine to coarse, sub-rounded silty sand	Low	Low	Low
	Well-graded sub-rounded to sub-angular sandy gravel (75 mm minus)	Moderate	Low	Low
	Poorly graded angular gravel (75 mm minus)	Very High	High	Moderate
Full size steel roller or rubber tired equipment	Fine to coarse, sub-rounded silty sand	Moderate	Low	Low
	Well-graded sub-rounded to sub-angular sandy gravel (75 mm minus)	High	Moderate	Low
	Poorly graded angular gravel (75 mm minus)	Not Recommended	Very High	High

Table 11: Partial Factors of Safety to Account for Installation Damage (15)

Geosynthetic Polymer	Geosynthetic Type	Geosynthetic weight (g/m ²)	Range of Safety Factor	
			High Survivability	Low Survivability
PP and HDPE	Nonwoven	< 270	2.0	1.15
		> 270	1.8	1.05
	Woven	< 270	2.5	1.2
		> 270	1.4	1.1
	Grid	All weights	1.4	1.0
	Nonwoven	< 270	3.2	1.25
		>270	1.8	1.1
	Woven	< 270	?	?
		> 270	2.2	1.4
	Grid	All weights	?	?

Table 12: Effect of Installation Damage on Strength, Strain, and Modulus (15)

Study	Geosynthetic Type	Undamaged strength (Kn/m)	After Installation		
			Strength retained	Failure strain retained	5 % Secant modulus Retained
Allen (18)	PE geogrid	76.4	73 %	70 %	95 %
	PE geogrid	94.2	68 %	63 %	102 %
	PP slit film woven	31.0	60 %	64 %	97 %
	PP stitch/bond woven	62.0	77 %	83 %	101 %
	PP stitch bond/woven	92.3	88 %	75 %	122 %
	PETP multifil. woven	186.3	60 %	61 %	115 %
Watts and Brady (19)	PP woven	190.0	64 %	67 %	No change
	PP woven	46.1	46 %	55 %	
	PETP woven	187.9	35 %	50 %	
	PE geogrid	53.9	87 %	75 %	
Troost and Ploeg (20)	PETP multifil. Woven	150.0	46 %	Not reported	85 %
	PETP multifil. Woven	400.0	65 %		90 %
	PETP multifil. Woven	600.0	75 %		94 %
	coated PETP geogrid	55.0	82 %		103 %
Viezee et al. (21)	PETP multi. yarn	77.8	81 %	77 %	100 %
Elias (22)	PETP nonwoven needle	48	54 %	Not reported	67 %
	PETP nonwoven needle	17.7	21 %		33 %
	PETP nonwoven needle	9.8	25 %		33 %

	PP slit film woven	33.6	20 %		37 %
	PP woven monofil.	48.5	34 %		61 %
Leclercq et al. (1990)	PETP nonwoven needle	13.1	77 %	71 %	Not reported
	PETP nonwoven needle	41.9	92 %	75 %	
	PETP nonwoven needle w/PETP grid	28.4	80 %	72 %	
	PETP nonwoven bonded	5.3	95 %	84 %	
	PETP nonwoven bonded	12.4	92 %	85 %	
	PETP nonwoven bonded	17.7	88 %	87 %	
	PETP multifil. Woven	115.2	70 %	82 %	
	PETP multifil. Woven	158.7	65 %	83 %	
	PP slit film woven	21.4	87 %	101 %	
	PP slit film woven	37.8	88 %	81 %	
	PP slit film woven	40.8	85 %	90 %	
	PP slit film woven	96.3	91 %	99 %	
	PP monfil. woven	55.0	78 %	78 %	

Table 13: Survivability Level for Separation and Embankment Application (15)

Subgrade preparation conditions:	Low ground-pressure equipment (< 27 kPa), 15-30 cm initial lift	Medium ground-pressure equipment (>27 kPa, <55kPa), 15-30 cm initial lift	High ground-pressure equipment (> 55 kPa), 15-30 cm initial lift
Subgrade is smooth and level	Low	Moderate	High
Subgrade has been cleared of large obstacles	Moderate	High	Very High
Minimal site preparation is provided	High	Very High	Not Recommended
Type of cover Material		Medium ground pressure equipment (> 27 kPa, < 55 kPa), 30 cm initial lift	High ground pressure equipment (> 55 kPa), 30 cm initial lift
Fine sand to 2" minus gravel, rounded to subangular	N/A	Low	Moderate
Coarse angular aggregate with diameter up to one-half lift thickness, may be angular	N/A	Moderate	High
Some to most aggregate with diameter greater than one-half lift thickness, angular and sharp-edged, few fines	N/A	High	Very High

3.3.8 Conclusions

1) Through these studies it clearly appears that the use of a protecting layer (a single geotextile or a heterogeneous layer composed of layers of different materials), will significantly decrease the damage to the geomembrane during the construction of the liner, as well as during its service life.

2) Stiffer geomembranes possess better puncture resistance than flexible ones.

- 3) To obtain an approximate estimate of a liner system made up of liners of different materials, the puncture resistance of the different components should be added.
- 4) Most damage occurs during the compaction of the gravel, especially during the stop-and-start process of the heavy equipment.
- 5) The creep properties of geomembranes and geotextiles are not affected by installation damage.
- 6) The angularity and size of the backfill is of paramount importance for the puncture resistance of the layer, the more angular the backfill, the more the damage. However, if using round stone, the designer should be aware of the bursting possibility.
- 7) Thick and heavyweight geotextiles will provide a lot more protection than thin lightweight geotextiles.
- 8) The scanning method used by Werner and Puhlinger (6), as well as the electrical leak detection system used by Darilek et al. (8) are efficient and accurate.
- 9) The different failure modes associated with puncture and installation damages are marks, pinholes, large-scale splits, and tears.
- 10) Guglielmetti et al. (16) evaluated the installation and construction survivability of geomembranes used for landfill caps, and showed that truck loading caused more damage than low-ground pressure bulldozers.
- 11) The damage induced by construction affects the breaking strength properties, but not the yield properties (17), as yield properties are mostly functions of the resin densities, while the breaking strength properties are mostly functions of the flaws present in the materials.

3.3.9 References

1. Giroud J.P.: "Geomembrane Protection", Geotextiles and Related Materials, 1992, pp. 99-104.
2. Fayoux D. : "Durability of PVC Geomembranes and Resistance to Mechanical Puncturing", Plavina (Solvay Group), Oudenaarde, Belgium, Geotextiles, Geomembranes and Related Products, Den Hoedt ed. 1990, pp. 563, 564.
3. Wong C.L.Y., Wijewickreme D.: "HDPE and VLDPE Geomembrane Survivability", Geosynthetics '93, Vancouver, Canada, pp. 901-913.
4. Giroud J.P., Badu-Tweneboah K., and Soderman K.L.: "Theoretical Analysis of Geomembrane Puncture", Geosynthetics International, 1995, vol. 2, no.6, pp. 1019-1048.
5. Motan E.S., Reed L.S., Lundell C.M.: "Geomembrane Protection by Non-woven Geotextiles", Geosynthetics '93, Vancouver, Canada, pp. 887-899.
6. Werner G. and Puhlinger G.: "Tests for Evaluation of Synthetic Liner Protection", Proceedings Sardina 95, Fifth International Landfill Symposium, pp. 493-498.
7. Artieres G. and Delmas P.: "Puncture Resistance of Geotextile-Geomembrane Lining Systems", Proceedings Sardina 95, Fifth International Landfill Symposium, pp. 469-476.
8. Darileck G., Menzel R., and Johnson A.: "Minimizing Geomembrane Liner Damage While Emplacing Protective Soil", Geosynthetics '95, pp.669-676.
9. Reddy K.R., Bandi S.R., Rohr J.J., Finy M., and Siebken J.: "Field Evaluation of Protective Covers for Landfill Geomembrane Liners Under Construction Loading"" Geosynthetics International, 1996, vol. 3, no. 6, pp. 679-700.
10. Koerner G.R., Koerner R.M., and Elias V.: "Geosynthetic Installation Damage Under Two Different Backfill Conditions", Geosynthetic Soil Reinforcement Testing Procedures, ASTM STP 1190, S.C. Jonathan Cheng, Ed., American Society for Testing and Materials, Philadelphia, 1993, pp. 163-183.
11. Billing J.W., Greenwood J.H., and Small G.D.: "Chemical and Mechanical Durability of Geotextiles", Geotextiles, Geomembranes and Related Products, Den Hoedt (ed.), 1990 Balkema, Rotterdam, pp. 621-626.
12. Ruetten M.G., Bandi S.R., and Reddy K.R.: "Rational Design Approach for Landfill Liner Protective Soil Cover", 18th International Madison Waste Conference, 1995, pp. 302-307.

13. Solid Waste Authority: "High Density Polyethylene Geomembrane Liner", Section 02776, June 1995, pp. 1-45.
14. Richardson G.N.: "Field Evaluation of Geosynthetic Protection Cushions", Geotechnical Fabrics Report, March 1996, p. 20-25.
15. Allen T.M.: "Determination of Long-Term Tensile Strength of Geosynthetics: A State-of-the Art Review", Geosynthetics '91 Conference, Atlanta, USA, pp. 351-375.
16. Guglielmetti J.L., Sprague C.J., and Coyle M.J.: "Geomembrane Installation and Construction Survivability", Geosynthetics '97, Conference Proceedings, pp.235-251.
17. Thomas R.: "Puncture Protection for Geomembrane", Geotechnical Fabrics Report, June/July 1996, p. 6-8.
18. Allen T.M.: "Strength Losses Occurring Due to Installation Damage for Several Geosynthetics", WSDOT Report, 1989.
19. Watts G.R. and Brady K.C.: "Site Damage Trials on Geotextiles", Proceedings of the Fourth International Conference on Geotextiles, Geomembranes, and Related Products, The Hague, pp. 603-607, 1990.
20. Troots G.H. and Ploeg N.A.: "Influence of Weaving Structure and Coating on the Degree of Mechanical Damage of Reinforcing Mats and Woven Geogrids, Caused by Different Fills, During Installation", Proceedings of the Fourth International Conference on Geotextiles, Geomembranes, and Related Products, The Hague, pp. 609-614, 1990.
21. Viezee D.J., Voskamp W., den Hoedt G., Troost G.H., and Schmidt H.M.: "Designing Soil Reinforcement with woven Geotextiles – The Effect of Mechanical Damage and Chemical Aging on the Long-Term Performance of Polyester Fibres and Fabrics", Proceedings of the Fourth International Conference on Geotextiles, Geomembranes, and Related Products, The Hague, pp. 651-656, 1990.
22. Elias V.: Durability/Corrosion of Soil Reinforced Structures, FHWA/RD-89/186, 1990.
23. Leclercq B., Schaeffner M., Delmas P.H., Blivet J.C., and Matichard Y.: "Durability of Geotextiles: Pragmatic Approach in France", Proceedings of the Fourth International Conference on Geotextiles, Geomembranes, and Related Products, The Hague, pp. 679-684, 1990.

3.4 Seams

The purpose of seaming is to join the different geomembranes forming the liner to prevent leaks between sheets. Seaming consists of joining geomembrane sheets by reorganizing the surface of the polymer structure in a specific manner. The sheets are bonded either by chemical or thermal process; for certain processes such as extrusion seaming, an addition material is required (1).

Theoretically, the properties of the sheets and the seams should be identical with no loss of tensile strength. However, differences between the seam and the sheet properties have been noticed for almost every type of seam. These differences are due to stress concentrations resulting from seam geometry. The seam characteristics are functions of the seaming technique, seam geometry, geomembrane resin and residual stress in the seams.

3.4.1 Different seaming technologies

Currently, seven different techniques are used (1), they are categorized either as thermal or chemical processes. The seven techniques, presented in Fig. 23, are thermal extrusion: fillet and flat, thermal fusion: hot wedge and hot air, chemically fused: chemical and bodied chemical, and chemical adhesive.

- *Thermal extrusion (welding):*

This technique is only applicable to polyethylene material. A ribbon of molten polymer is extruded over the edge of, or in between, the two surfaces to bond. The hot extrudate brings the two sheets to the melting temperature, then the sheets join together while cooling. When the extrudate is placed over the leading edge of the seam, the technique is called extrusion fillet, and when the extrudate is placed between the two sheets, it is called extrusion flat. Extrusion fillet is the only technique allowing the seaming of polyethylene patches and seaming in poorly accessible areas such as sump bottoms and around pipes. Temperature is a very important factor in order to obtain a proper seam. Effectively, too much melting weakens the geomembranes, while too little results in an inadequate flow across the seam interface, and in poor seam strength. Pressure, seaming rate, and geomembrane resin are also very important factors.

To prepare sheets for extrusion fillet seams, it is necessary to grind the upper sheet to a 45° bevel, when the sheet is greater than 60 mil thick. While grinding, special care must be taken to insure that grinding is done in the direction perpendicular to the seam thus reducing the possibility of initiating cracks. Excessive grinding has been recognized as an important cause of geometry default causing stress cracking. The purpose of grinding is to remove the oxide layer and waxes from the surfaces and to roughen the sheets. The grinding depth should range from no less than 5% to no more than 10% of the sheet thickness. To avoid the recurrence of surface oxide, the grinding should be done less than 10 minutes before the seaming. After seaming, it is important to verify that no puckering (sign of excessive temperature or too slow rate of seaming) appears, and that the grinding marks do not exceed 0.25" beyond the extrudate.

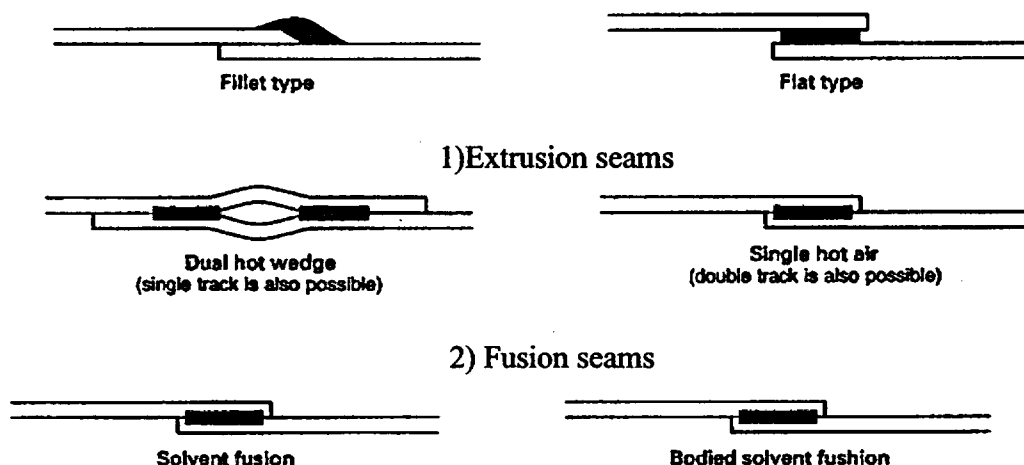
- **Thermal fusion:**

The techniques using thermal fusion involve the melting of a portion of the mating surfaces. The hot wedge or hot shoe method uses an electrical heater resistance, featuring a wedge shape, which moves between the sheets, thus seaming the two geomembranes. As the surfaces melt, shear flow occurs across the upper and lower surfaces of the wedge. A roller to form the final seam applies the pressure needed to create a strong bond. This technique allows the creation of either single uniform width or dual seams. A dual seam is constituted of two parallel seams with a uniform unbonded space between them. This space can be extremely useful to assess the seam quality; leaks can be detected by pressing this space. No grinding or brushing must be used, the sheets must not be tacked since the wedge moves between them.

The hot air method uses a heater, a blower, and a temperature controller, to blow hot air between the two sheets to melt the opposing surfaces. After the hot air is introduced, pressure bonds the surface. This technique allows the creation of single or dual seams. This method is used for a pre-seaming process, tacking the surfaces before the final seaming. For the extrusion welding, temperature, pressure, seaming rate, and material are of primary importance to create a proper fusion seam.

- **Chemical fusion:**

Chemical fusion is induced by applying a liquid chemical agent between the sheets. Then after a few seconds, pressure is applied bonding the two surfaces. Too much chemical will weaken the sheets, while too little will yield a poor seam. Bodied chemical fusion seams are identical to the chemical fusion seams with the exception that a small percentage, ranging from 1 to 100 %, of the geomembrane resin is dissolved and added to the chemical agent, thus increasing the working time as well as causing an increase of viscosity for slope work, preventing runoff of the chemical. The chemical adhesive process consists of applying a dissolved bonding agent, different from the geomembrane material, to both the mating surfaces; then a roller applies pressure to bond the assembly. Two distinct approaches exist: the solvent adhesive and the contact adhesive methods.



3) Chemical solvent seams



4) Chemical adhesive seams

Figure 23: Different techniques of seaming (16)

For each of the previous techniques, a minimum and maximum overlap of the sheet is required, which may vary from 3 to 6 inches after seaming. Prior to seaming, the overlapped surfaces must be clean (no scratches or flaws) and free of moisture. No seams must be made during rainy, snowy, frozen soil or hot temperature conditions. The sheet temperature during seaming must be above 40°F and below 104°F.

Table 14 presents the compatibility between seaming techniques and resins. It can be seen that certain techniques cannot be used with any type of resins, i.e. HDPE cannot be seamed using solvent fusion or adhesive techniques.

Table 14: Compatibility Between Seam Techniques and Resins (17)

Type of Seaming Method	Type of Geomembrane							
	HDPE	VLDPE	PVC	CSPE-R	EIA-R	LLDPE	PP	FCEA
Extrusion (fillet and flat)	A	A	N/A	N/A	N/A	A	A	N/A
Thermal fusion (hot wedge and hot air)	A	A	A	A	A	A	A	A
Solvent fusion (solvent and bodied solvent)	N/A	N/A	A	A	A	N/A	N/A	A
Adhesive (solvent and contact)	N/A	N/A	A	A	A	N/A	N/A	A

A=Available, N/A=Non-available

The hot wedge fusion seam method features more advantages since, unlike other techniques, it can be used to seam all thermoplastic geomembranes. Moreover the wedge temperature, nip roller pressure, and the seam's speed are adjustable, implying that depending on the seaming condition (weather, sheet temperature, time of the day, etc.) the operator has the possibility to adjust these features to obtain and maintain proper and identical seams. The different techniques have been described by Landreth (1).

The surfaces to be bonded must be clean; grinding can be used to clean-up the sheet, but special care must be taken since excessive grinding will create grind marks reducing the sheet thickness and possibly initiating cracks. In order to ease the fabrication of seams, surface preheating is recommended especially in cold weather. Hot air can be used to preheat the sheet to a temperature ranging from 90 to 110° C.

3.4.2 Tests of double track fusion seams and effect of wedge geometry and roller pressure

Thomas et al. (2) evaluated ten double track fusion seams made with two different types of wedges and drive wheels, and five different resins. Peel separation and strength, shear elongation at break and strength, optical microscopy, impact resistance, and stress cracking resistance were the tests performed. Peel and shear testing provided pass or fail information, while impact and stress cracking tests enabled the classification of geomembranes according to their seams quality.

Impact resistance testing was done by following the draft Canadian standard method CAN/CGSB 148.1-113 (modification of ASTM D 1709). A specific weight is dropped from a known height causing fracture of the specimen. The energy to cause rupture is determined by the height and weight, before testing the specimen, which has been frozen for 21 hours at -40°F. The stress cracking test is a regular NCTL test (see stress cracking chapter). Different geometries had different impact properties implying that the resin and welding processes affect the seam response at cold temperature.

No seams showed failure from the peel and shear tests. It appears, from the microscopic photographs, that the shapes of the welding zone are controlled by the shapes of the wedge and drive wheels, and are different for each type.

The stress cracking test showed that breaks were initiated at some types of crack initiation sites (corroborating the results of the chapter concerning stress cracking). The sites are at the edge of the seam near the root of the squeeze-out bead. The results of the stress-cracking tests were extremely scattered, distinguishing the good from poor stress cracking-resistant geomembranes; moreover, they showed the effects of resin and wedge geometry. First, for the same wedge geometry, the results varied from 3 to 283, proving the importance of the use of a proper resin; then for the same resin, values varied from 283 to more than 3300, identifying the importance of the wedge geometry. All the seams used with the second wedge were at least three times more resistant.

It was concluded from the different tests that the peel and shear tests are not suitable for seam evaluation, since the stress-cracking phenomenon is not considered. Wedge and roller geometries affect the quality of fusion seams. Impact and stress cracking tests are very useful to assess seam behavior.

3.4.3 Peel and shear tests

A liner is composed of different sheets (bonded together by seams) forming an entire system. In order to obtain a proper system (no leaks or failures), every single seam should transfer tensile forces without shearing and peeling. The peeling phenomenon has often been described as non-existent in liners, however, Peggs (3) proved that it may appear at edges of wrinkles, which often align along the more rigid seams due to different causes. Peeling occurs when a geomembrane is dragged on a soil subgrade, or when soil is spread

against the seam overlap (3). It also occurs when shear stresses occur as the seam rotates to align the two geomembranes (4).

The main seam tests are for peel, Fig. 24b, and shear strengths, Fig. 24a, however the elongations should also be evaluated. The reason of this is that the failure may occur outside the seam (FTB) due to improper welding either by excessive grinding or by overheating (3).

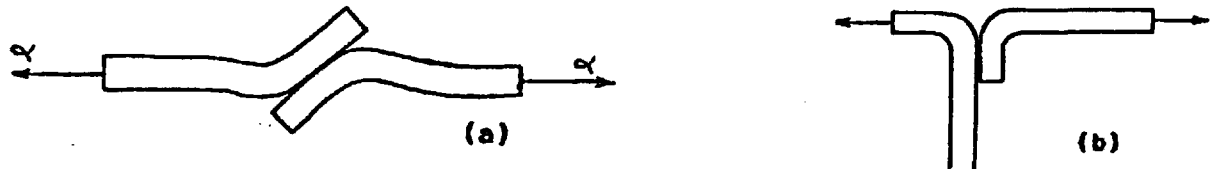


Figure 24: Shear (a) and peel (b) tests (4)

Overheating increases the probability of stress cracking adjacent to the membrane due to consumption of the protective antioxidant, and increase of oxidation and crystallinity. Overheating may cause stress concentration notch geometries.

While opening in a peel mode, crazes may occur in an incorrectly bonded geomembrane reducing the stress cracking resistance (up to 70%). In the shear strength test, failure ruptures will always occur in the adjacent sheet and not in the seam (3), since the seam bond is a lot stronger than the sheet (1000 ppi versus 2000 ppi). Therefore, it is not possible to get information on the seam strength.

If the seam is over-ground, it will fail with a low strength value and a low elongation value, while if overheated, failure will occur with a high strength and low elongation. Thus, only a low elongation identifies both conditions (3). This implies that only the shear elongation test should be used, or at least taken into consideration. Shear elongation should exceed 100% of the distance between the edge of the seam and the nearer grip.

The problem during the shear strength test also occurs in the peel strength; the rupture will always occur in the sheet since the bond is stronger, therefore, no information on the seam is obtained. The peel separation test is the most effective since it provides information on the minimum required criterion for bond strength (no separation), and the effect of welding on the adjacent geomembrane (no loss of ductility) (3). Therefore, while evaluating a geomembrane, only the peel test is sufficient to provide the required information.

For geomembranes made of materials different from HDPE, the peel resistance is about 1 to 3 kN/m, while for tensile strength the resistance is about 4 to 70 kN/m, and shear resistance is about 80% to 90% of the tensile value. This implies that the seam is the weakest point for the geomembrane. However, for HDPE geomembranes, resistance to

peel and shear is at least equal to the tensile value of the sheet, implying that the rupture will more probably occur in the sheet than in the seam.

Heavily reinforced geomembranes are more weakened by peel than unreinforced geomembranes (4); and to prevent this, the seam width should be greater for heavily reinforced geomembranes than for light reinforced one.

Carlson et al. (11) presented the results of more than 74,000 HDPE geomembrane seam tests. The seaming techniques used to bond the sheets were extrusion fillet, extrusion lap, single-track hot wedge, and double-track hot wedge. The common seam tests; shear and peel were used to assess the seam properties, and the notched stress rupture tests to evaluate the effects of seaming on geomembrane sheet properties. During peeling, crazes appeared at the unbonded surfaces; crazes are the precursors of cracks. Therefore, it is very important to consider peel while designing the liner. The peel test is extremely useful since it is the only means to evaluate the uniformity of adhesion between geomembranes.

The shear strength test does not provide information on the seam itself, since barely no seam failure occurs for HDPE material, but it provides the elongation in and adjacent to the seam. If the elongations in the seam and in the sheet are almost identical, the seam area has not been altered. Different values of elongation imply an alteration of the seam area, probably due to incorrect seaming procedures.

3.4.4 Impact resistance test

An interesting test procedure has been developed and described by Rollin et al. (5), to evaluate the impact properties of seams, which mainly depend on the sheet thickness and quality of the seam. This Canadian procedure is a modification of ASTM D 3029: "Standard Test Methods for Impact Resistance of Rigid Plastic Sheeting or Parts by Means of Tip (falling weight)". The impact resistance test provides information on the seam's brittleness, a predominant factor in the long term behavior of HDPE lined facilities (6).

Prior to doing impact testing, the authors first determined the two moduli characterizing a HDPE geomembrane: modulus of elasticity and secant modulus at different locations near the seams, by trimming and testing dumb-bell specimens which provided these values for the adjacent sheet. It was concluded that both moduli were higher near the seams enhancing the sheet rigidity. However, the results did not allow the identification of brittle seams. Thus, this test is not sensitive enough to evaluate brittle seams.

The impact test apparatus consists of a vertical steel pipe, a seam specimen holder, and a metallic mass. The weight of the mass and falling distance provide the impact energy. As defined by Rollin et al. (7), the impact resistance is the average energy, W_{50} , necessary to fail 50% of the tested specimens.

Two methods can be used: the Probit and the Bruceton Staircase methods. The first method consists of the grouping into many sets, an equal number of specimens (20 to 40) selected at random locations from the seam, and testing each set at a specific different energy level.

The Bruceton Staircase method consists of determining W_{50} (average rupture energy) of a randomly chosen specimen by increasing the mass of the falling weight. This procedure was used by the author to test more than 700 specimens. The seams were made by two different welding techniques: hot air (single and double seams) and wedge double seams. All seams were made at the same temperature: 23° C for the sheets and 400° C for air and wedge. However, in order to assess the effect of incorrect manufacturing (overheating, incorrect pressure), different welding speeds were used. Two other sets were made with high roller pressure (high pressures are expected to cause brittle seams).

Seams made with low speed had low impact energy, which was expected since low seam speed implies overheating, leading to poor performance. The seams made with high pressure also had lower impact energy, implying that high applied pressure causes brittle seams. A microscopic analysis showed that rupture is always initiated along the edge of the seams in the top sheet. The results proved that a highly brittle seam would break with low energy.

Hot air-produced seams were tested at different temperatures ranging from -10° C to 21° C; the seams become more brittle with a decrease of temperature, however, for temperatures higher than 10° C, the seam behavior was constant.

The thickness plays an important role since a 80 mils thick sample requires approximately two times more energy to fail than a 60 mils thick sample (95 Joules against 47 J). However, the rupture level is the same for single or double seams, proving that both types behave in an identical manner. The different results from the testing proved the importance of correct equipment calibrations, like welding speed, temperature, and roller pressure, and also the effects of sheet thickness.

The notched stress rupture test was used for seamed and unseamed sheets, to enable the comparison of the different values. The test procedure was identical to the test procedure used for the NTCL test (test described in the stress cracking chapter), except that the specimen was seamed, see Fig. 25.

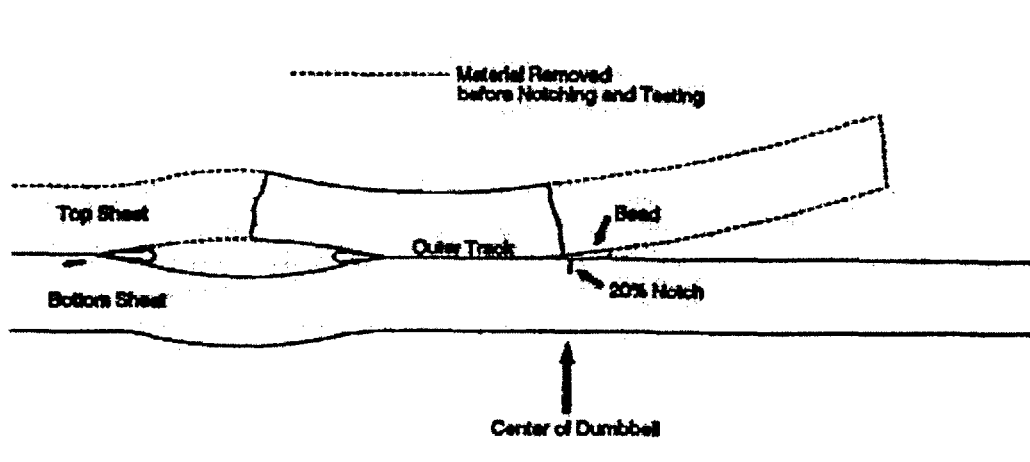


Figure 25: Notch location on a double track fusion seams for a notched stress rupture test (11)

The results of these tests did not show consistent differences between specimens with and without seams. This is probably due to the special care taken by the manufacturer to seam the sheets. Nevertheless, it was impossible to determine if the non-seam effect was due to the improper test method, or if there were really no differences. However, this test proved that HDPE seams could be used without altering the sheet properties, when processed with care. The rate of crack growth may be multiplied by two for the specimens; this is due to the differences in the resin and seaming techniques. It appears that single-track extrusion lap seams were the most susceptible to failure, while the double track fusion seam had the lower rate of failure.

3.4.5 Effect of temperature and freeze-thaw cycles

The effects of freeze-thaw cycles on geomembranes seams were evaluated by Lafleur (8). The results of his study showed no reduction in the seam shear strength. Comer et al. (9) also carried out freeze-thaw cycle experiments on geomembranes and seams. Different resins (PVC, HDPE, VLDPE, etc...) were seamed with different seaming techniques such as chemical, hot wedge, fillet extrusion, and dielectric. The study was divided into three parts in order to assess the effect of freeze-thaw cycling, cold temperature, tensile strains, and temperature-induced cyclic stress on the geomembranes.

In the first part, specimens were submitted to freeze-thaw cycles at -20°C for approximately 16 hours and tested at room temperature (20°C). In the second part, the specimens were cycled the same way but tested at a temperature of -20°C . In the third part, specimens were strained to 25% of their yield or break strength during the freeze-thaw cycling, and then tested at 20°C . To assess seam behavior, the 25mm strips were tested in the peel and shear modes.

The results of parts one and two showed that the 1.5mm HDPE-T seams, CSPE-R chemical seams, and EIA chemical seams showed strength increases of 10%, 35%, and 15%, respectively in the shear mode. Neither the peel mode nor the shear mode failures were encountered. In part 3, only the CSPE-R chemical seams showed an increase in strength. An explanation for this is the seam's aging. Seams failed during peel tests due to

ply delamination (between the membrane ply and the scrim), however, these failures were not attributed to freeze-thaw but to poorly fabricated seams.

It was shown that freeze-thaw cycles have no real influence on the seam behavior, only a few (3 or 4) specimens were affected. Colder temperatures had more effects since the shear and peel test values were higher at -20°C than at room temperature. Finally, the tensile straining seems to have had no significant effects, this could be due to the stress relaxation in the materials. This study was restricted to 50 cycles, which is a small number. Therefore, other tests must be carried out with freeze-thaw cycles of 200 and more to get definitive findings.

Hsuan et al. (18) assessed the effects of freeze-thaw cycling on 321 combinations of seams made with five different techniques: chemical, hot wedge, fillet extrusion, hot air, and dielectric seams.

The freeze-thaw cycling was carried out with temperature oscillation ranging from -20°C to $+30^{\circ}\text{C}$. Three sets of specimens were used: first unconstrained specimens were submitted to 200 cycles, then tested at $+20^{\circ}\text{C}$, a similar second set was cycled the same way but tested at -20°C , while for the third test the specimens were constrained and submitted to 500 cycles and then tested at $+20^{\circ}\text{C}$. The results of the shear and peel tests showed no significant changes between the different temperature tests. Also, the values were not affected by freeze-thaw cycles.

3.4.6 Residual stresses in geomembrane sheets and seams

Lord et al. (10) evaluated the residual stresses in geomembrane sheets, in and near the seams by the hole drilling method. Dual hot wedge, extrusion fillet, extrusion flat, and hot air seams were tested, the residual stresses were assessed at different locations: in the air channel for the dual seam, in the seam tracks, and at difference distances from the seam (12, 37, 62, 100mm). Values were monitored just after the hole was drilled as well as 30 min. later. Stresses were all compressive, except in the air channel where tensile stresses were applied. Values near the seam and in the sheet were approximately equal, which was particularly strange. The stress magnitude was approximately 10% of the sheet's tensile strength. After 30 min., the values decreased slightly due to the stress relaxation on the material. This test only allows the assessment of the surface residual stress (up to 0.75 mm deep), but does not provide information on the stress in the material's core.

3.4.7 Strain concentrations adjacent to the seams

Giroud et al. (12) carried out a complete study on the analysis of strain concentrations next to the geomembrane seams, compared different seaming techniques, and provided recommendations to minimize the strain concentration. To enable this study several assumptions had to be made; therefore, the geomembrane was only subjected to tension (in a direction perpendicular to the longitudinal direction of the seam). The geomembranes were homogeneous (reinforced geomembranes are not included) and the seams were free to translate and rotate.

Three different seaming techniques were studied: fusion seams (single and double), extrusion lap seams, and extrusion fillet seams. When a geomembrane is submitted to tensile strains due to the applied force, thermal contraction, or shrinkage, strain

concentrations occur adjacent to the seams. At the unstressed seam location, the two sheets are in different planes, but when tensile forces are applied they tend to align in the same plane; this alignment is only possible if the seam rotates (see Fig. 26).

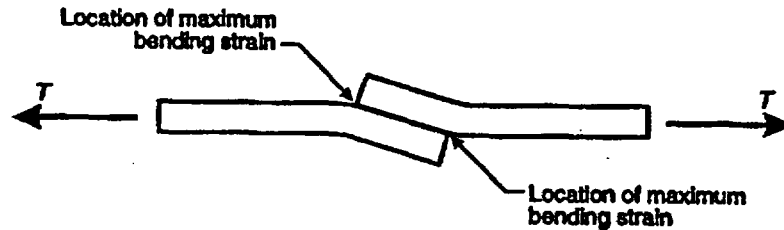


Figure 26: Sheet alignment due to tensile forces (12)

When the seam rotates, bending strains occur in the vicinity of the seam. The bending strains add to the already present tensile strains, and are amplified by the strain concentration factors. The maximum values of bending strain occur at the connection between the geomembrane and the seam. It was shown that for small angles, about 1 to 5°, the bending strain ranges from 0.75 to 1.5 times the tensile strain in the geomembrane, with a stress concentration approximately equal to 2.

This study proved that bending strains are higher in the lower sheet for the extrusion. This explains why failures often occur in the lower geomembranes for extrusion fillet seams, Fig. 28, but no reasons have yet been found to explain why it occurs in the case of the other techniques.

However, an explanation was found for cold weather, where thermal strains are not uniformly distributed throughout the geomembrane thickness. The thermal strains cause bending which causes strains that are always greater next to the seam at the upper surface of the lower geomembrane, Fig 27.

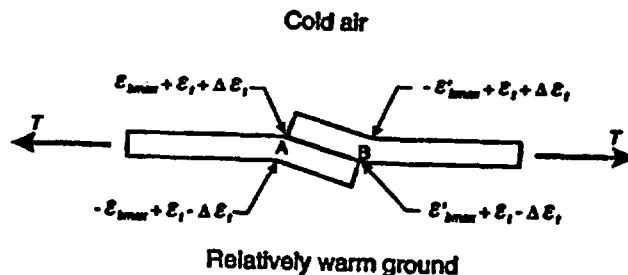


Figure 27: Strains in an air exposed geomembrane (12)

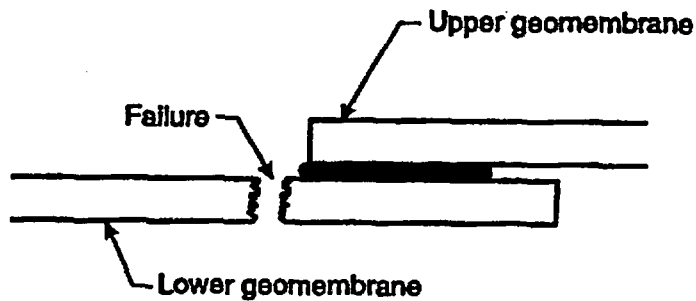


Figure 28: Failure occurs in the lower sheet (12)

Fusion seams cause low maximum bending values; for a 1 mm geomembrane seamed by fusion or extrusion fillet seams, the relation between bending strains and applied tensile strains is linear, unlike other configurations.

The thicker the geomembrane, the greater the bending strains. However, for wide seams thickness has poor influence on the bending strains. Bending strains are functions of the seam width. Therefore to minimize them, a 1 mm thick geomembrane should be used, with at least 40 mm fusion seams, 50 mm extrusion lap seams, and 25 mm extrusion fillets.

3.4.8 Stress cracking in the seams

Peggs et al. (13) assessed the different phenomena of stress cracking in polyethylene geomembranes sheets and seams, providing the field experience for real data.

It was found that many features may initiate cracks, such as extrusion die lines, grinding gouges, seaming machine gouges, re-entrant angles at the edges and on the surfaces of seams, water vapor voids within seams, or lack of bonding at seam interfaces. In the majority of cases involving extruded lap or fillet seams, cracks occurred along the edges of seams, even though they were observed to occur within the extruded bead, on the top and underside of the seams, and slightly removed from the edge of the seam.

Identical cracks may also occur in the fusion welded seams, but failures along the edge are less frequent. However, when this happens, cracks lengths are greater for fusion seams than for extrudate ones.

Cracks along the edges of extrudate fillets seams invariably occur in the bottom of the two geomembranes panel (confirming Giroud et al. (12) finding), this is due to the larger mass of extrudate located on this side of the seam and the higher energy input.

In other types of cracking, the initiating point can be located at other parts of the seams, such as the seam's surface or within the body of the seam, and not only on the lower sheet. This is especially true for cracking within the extruded fillets, hot air extrudate seams, and extrudate lap seams.

Overheating is an important cause of cracking in seams, cracks have been reported on the edges of a regular seam as well as at the seam's intersections, where the input thermal energy is greater than in the adjacent area causing stress concentration cracks.

3.4.9 Brittle fracture in seams

Peggs and Carlson (14) have studied brittle fracture in polyethylene seams emphasizing field results. They found that brittle cracks occurred along the edges of fused seams even in geomembranes considered acceptable by visually inspections and by peel/shear tests. For all the cases studied, failures appeared on the side of the seam of the overlapped geomembrane.

Seaming consists of melting the surfaces to rearrange their microstructure to form one piece. But problems will appear if the seam is overheated, if it cools rapidly or asymmetrically due to wind, if the melt indices of the parent material and the extrudate do not match, or if it is not heated uniformly.

Crazes that are the precursors of cracks have been seen to occur at the edges of hot wedge seams, at the edges of the top sheet in extrudate fillet seams, and at the edges of the extrudate bead in extrudate lap seams. For extrudate fillet seams, cracks often occur at the edges of the top sheet, due to crazes initiated in the weld deposit.

Residual stresses often appear in seams due to asymmetrical processing (temperature or pressure not uniform over the seam's width). This phenomenon may cause crazes to initiate, as it was found in hot wedge seams, where residual stresses at the root of the extruded bead initiated crazes, which propagated through the sheet and seam. They also occurred in extrudate fillet seams, where crazes were initiated by residual stresses at the intersection of the edges of the top sheet, the bottom sheet, and the extrudate bead. It was concluded that most of the brittle cracks that occurred in geomembranes were due to unexpected stresses acting at geometrical stress concentration points created by mechanical damage or seams overheating.

3.4.10 Seam inspection

Seams must be inspected by different means, such as shear and peel tests, visual inspection, microscopic analysis (cross section must be assessed during classification tests), and non-destructive testing (such as vacuum box and hot air pressure).

Richardson and Koerner (17) presented the different non-destructive seams tests. They are summarized in Table 15. The costs are those in 1987, date of publication.

Table 15: Nondestructive Geomembrane Seam Testing (17)

Test method	Cost of equipment	Speed of tests	Cost of tests	Type of result	Recording method	Operator Dependency
Air Lance	\$200	Fast	Nil	Yes-no	Manual	Very high
Mechanical point stress	Nil	Fast	Nil	Yes-no	Manual	Very high
Dual seam (positive pressure)	\$200	Fast	Moderate	Yes-no	Manual	Low
Vacuum chamber (negative pressure)	\$1000	Slow		Yes-no	Manual	High
Electric sparking	\$1000	Fast	Nil	Yes-no	Manual	Low
Electric wire	\$500	Fast	Nil	Yes-no	Manual	High
Electric field	\$20,000	Slow	High	Yes-no	Manual and automatic	Low
Ultrasonic pulse echo	\$5000	Moderate	High	Yes-no	Automatic	Moderate
Ultrasonic impedance	\$7000	Moderate	High	Qualitative	Automatic	Unknown
Ultrasonic shadow	\$5000	Moderate	High	Qualitative	Automatic	Moderate

3.4.11 Difficulties associated with seaming and the mode of failure

Defective seams must be repaired by placing capstrips (15) over flaws. Regrinding and re-welding are highly inadvisable, since they increase the possibility of stress cracking. Seaming must not be used at locations where testing is difficult due to the geometry, corner for instance. For these cases, factory-formed corners, or dumps must be placed.

The reasons why field seaming is difficult have been listed by Koerner (16) as follows:

- Horizontal (sloped) preparation surfaces
- Non-uniform preparation surfaces
- Nonconforming sheets to the subsurface (air pocket)
- Slippery liners made of low-friction materials
- Wind-blown dirt or bentonite in the area to be seamed
- Moisture and dampness in the subgrade beneath the seam
- Frost in the subgrade beneath the seam
- Moisture on the upper surface of the geomembrane
- Penetrations, connections, and appurtenances
- Wind fluttering the sheets out of position
- Ambient temperature variations during seaming

- Uncomfortably high (and sometimes low) temperatures for careful working
- Expansion and/or contraction of sheets during seaming

Efforts must be made to increase the role of nondestructive testing, in particular the ultrasonic shadow method. Nondestructive methods assess both the quality and the continuity of the seams.

Table 16 and 17 present the different modes of failure of dual wedge-weld seams and extrusion fillet-wedge seams, respectively.

Table 16: Different Possibilities of Failure for Dual Wedge-Weld Seams (19)


















Type of Break	Code	Break Description	Classification
	AD	Adhesion Failure. Complete separation on one or both sides of the air channel.	Non-FTB
	BRK	Break in Sheeting.	FTB
	SE-1	Break at outer edge of seam. Break can be either top or bottom sheet.	FTB
	SE-2	Break at inner edge of seam.	FTB
	AD-BRK	Break in first seam after some adhesion failure. Break can be either top or bottom sheet.	FTB

Table 17: Different Possibilities of Failure in an Extrusion Fillet-Wedge Seam (19)

Type of Break	Code	Break Description	Classification
	AD-1	Failure in adhesion. Specimens may also delaminate under the bead and break through the thin extruded material in the outer area.	Non-FTB
	AD-2	Failure in adhesion.	Non-FTB
	AD-WLD	Break through the fillet. Such breaks range from those that start at the edge of the top sheet to those that run through the fillet after some adhesion failure between the fillet and the bottom sheet.	FTB
			
			
	SE-1	Break at seam edge. Specimens may break anywhere from bead/outer area edge to the outer area/buffed area edge. (Applicable to shear only.)	FTB
	SE-2	Break at seam edge. Specimens may break anywhere from bead/outer area edge to the outer area/buffed area edge.	FTB
	SE-3	Break at seam edge. (Applicable to peel only.)	FTB
	BRK-1	Break in sheeting. A "B" in parenthesis after the code means the specimen broke in the buffed area. (Applicable to shear only.)	FTB
	BRK-2	Break in sheeting. A "B" in parenthesis after the code means the specimen broke in the buffed area.	FTB
	AD-BRK	Break in sheeting after some adhesion failure between the fillet and the bottom sheet. (Applicable to peel only.)	FTB
	HT	Break at the edge of the hot tack for specimens which could not be delaminated in the hot tack. (Applicable to shear tests only.)	FTB

3.4.12 References

- (1) Landreth R.E.: "Inspection Techniques for the Fabrication of Geomembrane Field Seams", Risk Reduction Engineering Laboratory, U.S. Environmental Protection Agency, Cincinnati, Landfill and Solid Waste Treatment Technology, pp. 238-243, 1990.
- (2) Thomas R., Kolbasuk G., and Mlynarek J.: "Assessing the Quality of HDPE Double Track Fusion Seams", Proceedings Sardinia 95, Fifth International Landfill Symposium, pp. 415-427.
- (3) Peggs I.D.: "We Need to Reassess HDPE Seam Specifications", Geotechnical Fabrics Report, June-July 1997, pp. 46, 47.
- (4) Giroud J.P.: "Analysis of Stresses and Elongations in Geomembranes", Proceedings of the International Conference on Geomembranes, Denver, Vol. 2, pp. 481-486, 1984.
- (5) Rollin A.L., Marcotte M., Lafleur J., and Mlynarek J.: "The Use of Impact Test Procedure to Assess Seam Brittleness", Geosynthetics' 93, Conference Proceedings, March 30-April 1, Vancouver, Canada, pp. 1559-1573.
- (6) Rollin A.L., Vidovic A., Denis R., and Marcotte M.: "Evaluation of HDPE Geomembrane Field Welding Techniques; Need to Improve Reliability of Quality Seams", Geosynthetics' 93, Conference Proceedings, San Diego, USA, pp. 443-455.
- (7) Rollin A.L., Lefebvre M., Lafleur J., and Marcotte M.: "Evaluation of Field Seams Quality with the Impact Test Procedure", Geosynthetics' 91, Conference Proceedings, Atlanta, USA.
- (8) Lafleur J., Akber S.Z., Hammamju Y., and Marcotte M.: "Tensile Strength of Bonded Geotextile-Geomembrane and Composites", Second Canadian Symposium on Geotextiles and Geomembranes, Canadian Geotechnical Soc., Edmonton, Canada, 99. 219-224, 1985.
- (9) Comer A.I., Sculli M.L., Hsuan Y.G.: "Effects of Freeze-Thaw cycling on Geomembrane Sheets and Their Seams", Geosynthetics' 95, Conference Proceedings, pp. 853-866.
- (10) Lord Jr. A.E., Koerner R.M., and Wayne M.H.: "Residual Stress Measurements in Geomembrane Sheets and Seams", Geosynthetics' 91, Conference Proceedings, Atlanta, USA, pp. 333-349.

- (11) Carlson D.S., Charron R.M., Winfree J.P., Giroud J.P., and McLearn M.E.: "Laboratory Evaluation of HDPE Geomembrane Seams", Geosynthetics '93, Conference Proceedings, Vancouver, Canada, pp. 1543-1557.
- (12) Giroud J.P., Tisseau B., Soderman K.L., and Beech J.F.: "Analysis of Strain Concentration Next to Geomembrane Seams", Geosynthetics International 1995, Vol. 2, No.6, pp. 1049-1097.
- (13) Peggs I., Carlson D.S.: "Stress Cracking of Polyethylene Geomembranes: Field Experience," Durability and Aging of Geosynthetics, Koerner R.M., Elsevier Ed., London, UK, pp. 195-211, 1989.
- (14) Peggs I., Carlson D.S.: "Brittle Fracture in Polyethylene Geomembranes," Geosynthetic Microstructure and Performance, ASTM STP 1076, I.D. Peggs Ed., American Society for Testing and Materials, Philadelphia, 1990, pp. 57-77.
- (15) Sylvia K. Lowrance, Office of Solid waste: "Use of Construction Quality Assurance (CQA) Programs and Control of Stress Cracking in Flexible Liner Seams," US EPA, Washington, D.C., 1989.
- (16) Koerner R.M.: Design with Geosynthetics, Third Edition, Prentice Hall, 1994, pp.578-593.
- (17) Richardson G.N., Koerner R.M.: "Geosynthetic Design Guidance for Hazardous Waste Landfill Cells and Surface Impoundments," Final Report U.S. EPA Contract No. 68-03-3338, 1987, GRI, Philadelphia, PA.
- (18) Hsuan Y.G., Sculli M.L., Guan Z.C., and Comer A.I.: "Effects of Freeze-Thaw Cycling on Geomembrane Sheets and Their Seams- Part II Cold Temperature Tensile Behavior and Thermal Induced Cyclic Stress," Geosynthetics '97, Conference Proceedings, pp. 201-216.
- (19) Haxo H.: "Lining of Waste Containment and Other Impoundment Facilities," EPA/600/2-88/052, 1988.

3.5 Seismic Response and Interface Strength

3.5.1 Introduction

The seismic response of a landfill may be important for the survivability of the installation. Different studies were carried out to present the possible damage that may be induced by an earthquake, to help designers and constructors to protect the landfill against this threat. The response of a landfill to seismic forces is closely linked to both the slope stability and the interface shear strength between the liner and the soil. Therefore, many tests were performed to assess the shear behavior of different interfaces under different types of excitation.

The landfill should be designed with the following regulations: US Code of Federal Regulation of Environment (1), which states that a landfill located within the seismic impact zone should be designed for a level of acceleration associated with 10% chance of exceedance in 250 years. USGS (2), published a map of the US indicating the different levels of acceleration to be considered for each region of the country.

Studies of different failures due to seismic excitation show that problems appear in the majority of the cases at the interfaces between the different components of a composite liner, since these interfaces are characterized by a very low shear strength (3).

Singh and Sun (3) investigated the response of clay liners to seismic excitations and outlined guidelines to be taken in consideration while designing a composite clay/geomembrane liner. One of the main conclusions of this paper is that the sliding surface (featuring a noncircular shape) will most probably pass through the clay-geomembrane interface, because of the low shear strength of the interface. This is further decreased by the presence of water, which accumulates in the vicinity of the interface (3).

To assess the shear behavior of interfaces different tests are available, some involve static loads, while others feature oscillating excitations.

3.5.2 Monotonic tests

Pasqualini et al. (4) carried out direct shear tests on different interfaces to determine their interface shear strength. The interfaces tested were LDPE geomembrane/geotextile, HDPE geomembrane/geotextile, LDPE geomembrane/geonet, geotextile/geonet, and LDPE geomembrane/compacted clay.

This study enabled the following important findings:

- Temperature has an important influence on the shear behavior of the geomembrane/geotextile interface; it was proved that at 30°C the interface possesses better shear resistance than at 26°C.
- The shear resistance of smooth geomembrane/clay interfaces is clearly affected by the wetting of the compacted clay.
- The geonet penetrates the geotextile, which increases the shear resistance of this interface; moreover water has very little influence on this configuration.

- In contradistinction to the geonet/geotextile interface, wet conditions decrease the shear resistance at most other interfaces.
- It is advisable to carry out tests leading to relatively large displacements in order to obtain correct values.

Vaid and Rinne (5) assessed the coefficients of interface friction between the geomembrane and sand by using a ring shear apparatus. The ring shear test (Fig. 29) is more convenient than a regular direct shear test, since it allows the determination of the true normal load on the plane of shear, thus providing a better definition of the peak interface friction, as well as the residual interface friction.

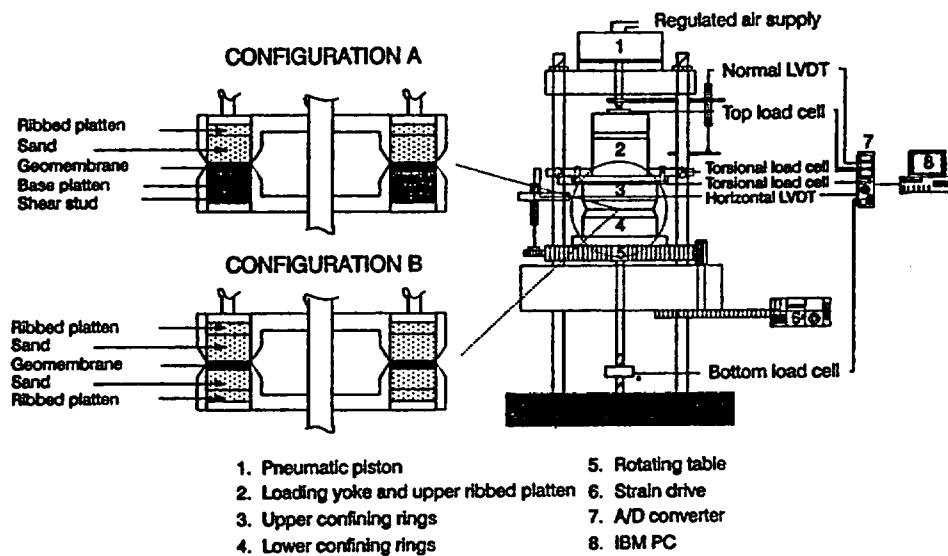


Figure 29: Ring shear test apparatus (5)

Two different sands were used, they had the same gradation but not the same grain shape, the Ottawa C-109 sand was comprised of round particles with a grain size equal to 0.4 mm, while the Target 20-30 sand is comprised of angular shapes with a grain size of 0.55 mm. The constant values of friction ($\phi_{cv} = 29^\circ$ for the Ottawa sand and $\phi_{cv} = 33^\circ$ for Target sand) are better values for friction than ϕ_{peak} , since they are constant and independent of the packing density, gradation, and normal stress.

PVC and HDPE geomembranes were tested. The PVC geomembrane was medium stiff, with one side rough and the other one smooth; for this study the geomembrane thicknesses were 20 and 30 mil. The HDPE geomembrane was stiff and hard, the smooth specimens were 20 and 100 mil thick, while the rough specimens were only 100 mil thick.

This study established the influence of the materials, their textures, the angularity of the sand, and the normal stress on the behavior of the geomembrane/sand interface.

The peak interface friction was found to be a function of the smooth HDPE resistance to shearing. The rough HDPE and the smooth PVC geomembranes had friction angles equal to the constant volume friction angle of the sand. The best configuration to obtain maximum shear strength is a rough geomembrane with Ottawa sand. The waviness component of roughness is not an influencing parameter for the interface friction. Smooth geomembranes present scraping grooves after testing, which is not the case for rough materials. The roughness of geomembranes is unaffected by the testing.

Table 18, from Vaid and Rinne (5), summarizes the results of different studies that provide friction angles for different types of soil and geomembrane.

Table 18: Summary of Tests Results (5)

Soil Type	Geomembrane Type				Type of Test	Reference
	HDPE		PVC			
	δ, δ_p (°)	σ' (kPa)	δ (°)	σ' (kPa)		
Concrete Sand	24	15-100	25 ¹	15-100	Direct Shear	Martin et al. (6)
Ottawa Sand	20	15-100	27 ²	15-100		
Concrete Sand	27	Up to	26	Up to	Direct Shear	Williams and Houlihan (7)
Ottawa Sand	19	100		100		
Sand	20-25	120	30-34 ³	120	Direct Shear	Akber et al. (8)
Sand		100-400	42		Direct Shear	Lam and Tape (9)
Concrete Sand	18-22,24-28	50-400			Ring Shear	Negussey et al. (10)
Ottawa Sand	15, 18	50				
Ottawa sand	21, 19	200			Direct shear	Saxena and Wong (11)
Sand			27-31	5-50	Direct shear	Weiss and Batereau (12)
Ottawa Sand	19	3-70	30	3-70	Direct shear	O'Rourke et al. (13)
Ottawa Sand			24.1	10-27	Direct Shear	Lauwers (14)

Where:

δ : friction angle (degree)

δ_p : peak friction angle (degree)

σ' : normal stress (kPa)

¹smooth

²rough

³PVC-2 = 17mm (67 mils) thick

⁴PVC-4 = 0.76mm (30mils) thick

Cazzuffi et al. (15) presented a European pre-standard method to assess the shear behavior of an inclined interface. The apparatus is quite similar to a regular shear box used for direct shear testing, but instead of being horizontal, it is inclined at a certain angle, Fig. 30.

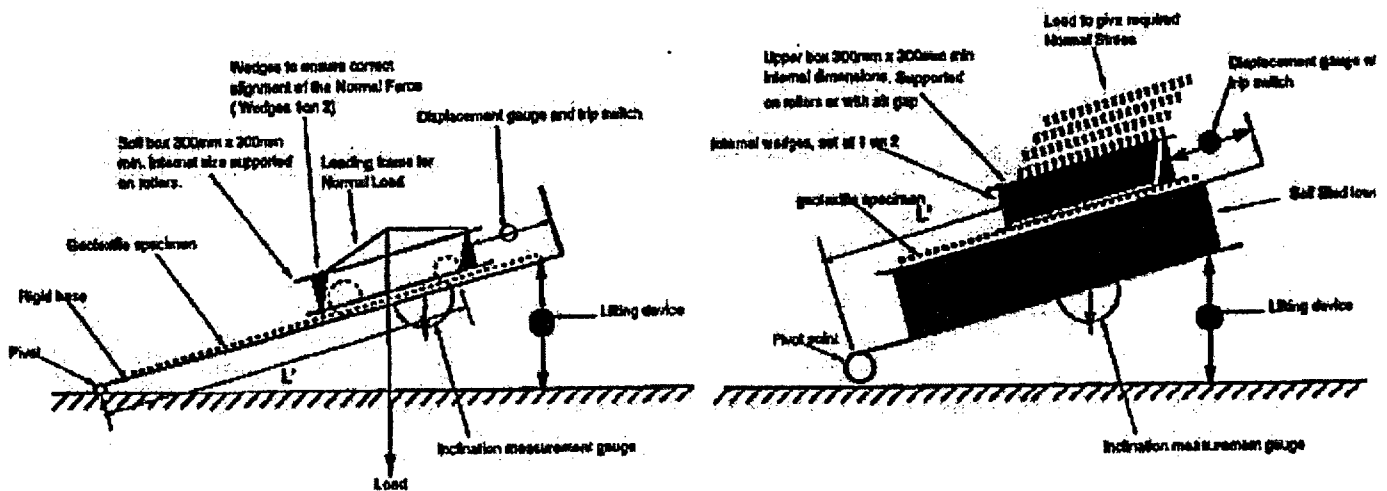


Figure 30: Inclined friction test apparatus (15)

This paper describes exhaustively the apparatus and the test procedures that allow the determination of the angle of friction and the shear strength. Only preliminary results are available (see Table 19), and even if some problems need to be resolved, it is thought that this test method would be an efficient tool in the characterization of the interface shear properties.

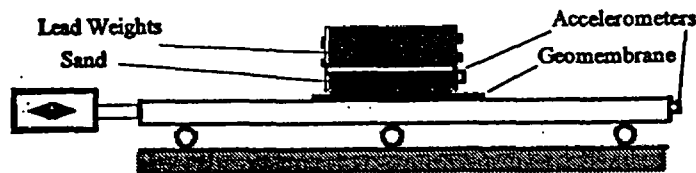
Table 19: Results of Inclined Friction Tests (15).

Geosynthetic	Support	Cover soil	Friction angle: ϕ_{sp} (°)
PET woven geotextile	Rigid plate	Sand	30.9
PET nonwoven needle-punched geotextile	Rigid plate	Sand	32.5
		Gravel	40.1
PVC geomembrane	Rigid plate	Sand	29.3
PET woven geogrid	Sand	Sand	30.1
	Rigid plate (with 2 layers PE film)	Sand	40.9
	Rigid plate	Gravel	41.9
HDPE extruded non-oriented geogrid	Rigid plate	Sand	32.4
		Gravel	37.0
	Rigid plate (with 2 layers PE film)	Sand	29.7
		Gravel	39.9

3.5.3 Seismic Response/dynamic shear tests

Yegian et al. (16) presented the results of tests to evaluate the dynamic response of geomembrane/geotextile and geomembrane/soil interfaces excited by seismic excitation.

For both interfaces, the materials were placed on a shaking table (see Fig. 31) and the accelerations and displacements (slip) of the lead blocks weights (12.4 kPa) and the table were recorded.



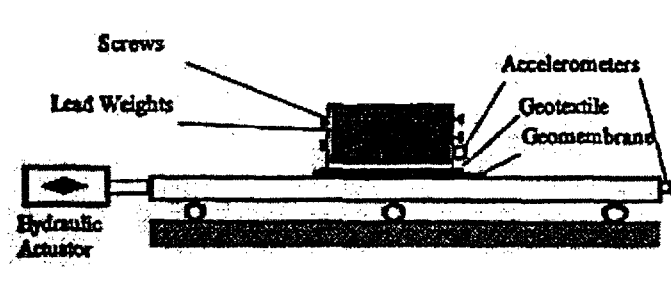


Figure 31: Test apparatus for dynamic shear properties (16)

The different materials used for the tests were a nonwoven, continuous filament, needle punched geotextile (Polyfelt TS 700), a smooth 60 mil HDPE geomembrane, and Ottawa sand.

The peak acceleration of the block a_b is function of the dynamic interface friction angle ϕ_d , and the gravity g , and is defined as:

$$a_b = g \tan \phi_d \dots \dots \dots [3.5.1]$$

For the first part of this study the excitations were steady state harmonic.

For the geomembrane/geotextile interface, it was shown that for accelerations less than 0.2g the table and the block move together, which indicated no relative displacement (slip), but for higher accelerations slip of 0.75" occurred.

Since the threshold limit between the slip and the no slip occurs at 0.2 g, it is possible to determine ϕ_d as follows:

$$\phi_d = \cotan (a_b/g) = 11.3^\circ \dots \dots \dots [3.5.2]$$

Only a limited shear stress can be transmitted through the interface; the value of the maximum shear stress is given by:

$$\tau = \sigma \tan \phi_d \dots \dots \dots [3.5.3]$$

where σ = normal stress and ϕ_d = dynamic interface friction angle, are both known.

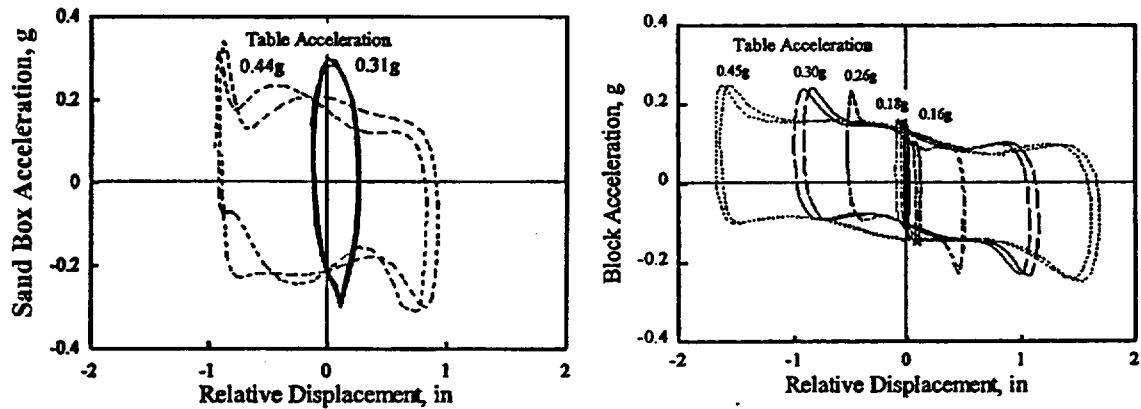


Figure 32: Dynamic response of geomembrane/sand interface (left) and geomembrane/geotextile interface (right) (16)

From Fig. 32, it is possible to determine the dynamic stiffness and damping characteristics of the interface, as well as the interface shear force. The stick-slip phenomenon occurs when the table motions are reversed. The dynamic interface shear property is non-linear. For the geomembrane/sand interface, slip occurred at a level of acceleration equal to 0.3g corresponding to $\phi_d = 16.7^\circ$.

The sand/geomembrane interface is able to transmit more shear stress between the two components than the geotextile/geomembrane interface, this explains why the slips were smaller in this case.

In the second part of this study, the dynamic response of the sand/geomembrane interface submitted to earthquake excitations was investigated. The excitations of the table were set to reproduce the earthquake in Spitak, Armenia in 1988, during which the maximum recorded acceleration was 0.4g. The response is more complex in the case of earthquake excitations than for steady state harmonic excitations. It was observed that the yield acceleration is not constant and is difficult to define. For a peak acceleration of 0.4g, the maximum slip was 1.2", while the permanent slip was 0.4", and the acceleration of the block 0.3g.

These tests showed that the stick-slip phenomenon occurs during the inversion of the table motion, which temporarily increases the shear force. Because of the complexity of the response under earthquake excitation, designers should be careful not to extrapolate results from the steady state harmonic excitations to earthquake application. The geotextile acts as a base isolator since the level of acceleration pulses of the ground motion is reduced by it and the wave energy is absorbed by the interface due to slip (17).

During, slip the different layers of the liner, including the geomembrane, may sustain plastic deformation, or tearing with consequent decrease of the impermeable properties of the liner. One of the main causes associated with landfill failure due to seismic excitation is

very low shear strength of the liner composed of different layers of geosynthetics, especially when a smooth geomembrane is utilized (18).

De and Zimmie (19) tested four different interfaces: geotextile/smooth geomembrane, smooth geomembrane/smooth geomembrane, smooth geomembrane/geonet (longitudinal), and smooth geomembrane/geonet (transverse).

First, the different interfaces were tested by monotonic and cyclic (frequency of 0.25 Hz) direct shear tests. Shear stress versus displacement curves were almost linear under monotonic loading, up to a maximum point (peak). Past this point, the curves dropped, even though some showed a residual stress larger than the peak value. An interesting finding was that the geonet transverse and longitudinal interfaces exhibit the same behavior indicating that orientation is not a factor in the shear strength at interface. Two sizes of specimens were tested and only small differences were noticed.

Under cyclic loading, the shear stresses tend to decrease with time. The ratio of the values of initial and terminal shear stresses is defined as the coefficient of dynamic friction for the studied cycle. The final stress is either larger or smaller than the initial value depending on the nature of the interface; moreover, the difference between initial and terminal values is a function of the normal stress applied. The decrease of shear stress associated with cyclic tests is explained by the wearing of the contact surfaces, which reduces the surface roughness (19).

The second part of this study addressed shake table tests, which allow the determination of the dynamic friction angle and therefore, the shear force. Small as well as large values of acceleration were used for the table excitation. In order to provide a high level of acceleration, up to 40 g, a 100 g-ton geotechnical centrifuge was used. For both small and large levels of acceleration, the dynamic friction angles were found to be similar, approximately 12.5° , implying that slip occurs at the same level of excitation (0.2g) for each interface. Moreover, results of the direct shear tests corresponded to the results found by the shake table.

3.5.4 Influence of material roughness

Dove et al. (20) assessed the relationship between the geomembrane roughness and the interface shear strength for geomembrane/soil interfaces using a newly developed optical technique OPM (Optical Profile Microscopy), which characterizes the roughness of a geomembrane.

The surface roughness parameter is defined as follows (se Fig. 33):

$$R_s = A_s/A_o, \text{ see Fig. 33} \dots \dots \dots [3.5.4]$$

But in practice, the stereology relation is defined as follows:

$$R_s = R_L \Psi \dots \dots \dots [3.5.5]$$

With R_L is the profile roughness parameter, and Ψ the profile structure factor.

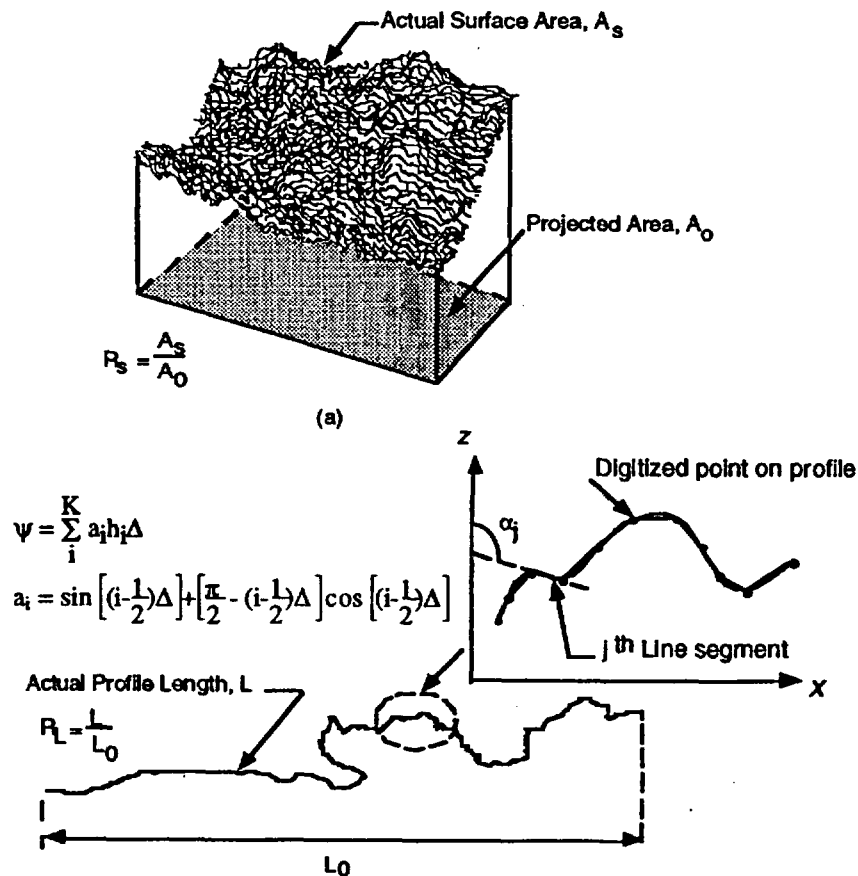


Figure 33: Definition of roughness parameter by Dove and Frost (21).

In this study, one smooth and three textured HDPE geomembranes were tested over two standard Ottawa sands, and a upper drain material from a landfill (the three soils possessed approximately the same properties).

Before testing, the shear strengths of the different interfaces in round and square direct shear boxes, and the geomembrane roughnesses were assessed with the OPM technique. These tests confirmed that roughness is a very important parameter in the shear resistance of the geomembrane/sand interface. The shear strength increases with an increase of the roughness up to a limit value of R_s approximately equal to 1.4; then beyond this value, the shear strength is less affected by the geomembrane roughness. Thus, to optimize the design of a liner, it is important to use a geomembrane possessing a roughness parameter equal to 1.4.

3.5.5 A theoretical evaluation of interface stability

Giroud et al. (22) developed a theoretical method to assess the stability of geosynthetics/soil interfaces on slopes. The slope instability of landfills is due to excess weight and low shear strength of the interfaces. Different methods of determining the factor of safety equation for slope liners have been presented by Giroud and Ah-Line (23), Martin and Koerner (24), Giroud and Beech (25), and Koerner and Hwu (26). All these methods are based on limit equilibrium making them simple to use (expression of the slope stability through a factor of safety), and their applicability has been proven through many years of utilization. But special care must be taken while evaluating a multi-layered liner, since the ultimate shear strength for each layer is not required at the same instant.

Different assumptions and calculations lead to equations defining the factor of safety.

For the case of uniform thickness:

$$FS = \frac{\tan \delta}{\tan \beta} + \frac{a}{\gamma t \sin \beta} + \frac{t}{h} \frac{\sin \phi}{\sin (2\beta) \cos (\beta + \phi)} + \frac{c}{\gamma h} \frac{\cos \phi}{\sin \beta \cos (\beta + \phi)} + \frac{T}{\gamma h t} \dots [3.5.6]$$

and for non-uniform thickness:

$$FS = \frac{\tan \delta}{\tan \beta} + \frac{a}{\gamma t_{avg} \sin \beta} + \frac{t_B^2}{h t_{avg}} \frac{\sin \phi}{\sin (2\beta) \cos (\beta + \phi)} + \frac{c}{\gamma h} \frac{t_B}{t_{avg}} \frac{\cos \phi}{\sin \beta \cos (\beta + \phi)} + \frac{T}{\gamma h t_{avg}} \dots [3.5.7]$$

with

FS: factor of safety

δ : interface friction angle along the slip surface ($^\circ$)

β : slope angle ($^\circ$)

a: interface adhesion along the slip surface (Pa)

γ : unit weight of the soil (N/m^3)

t: thickness of the soil layer for the case of a layer of uniform thickness (m)

h: height of the slope

ϕ : internal friction angle of the soil component of the layered system ($^\circ$)

c: cohesion of the soil component of the layered system (Pa)

T: tension in the geosynthetics above the slip surface (N/m)

t_a : thickness of the soil layer at the point A defined in Fig. 34

t_B : thickness of the soil layer at the point B defined in Fig. 34

t_{avg} : average thickness of the soil layer defined as $t_{avg} = \frac{t_a + t_b}{2}$ in the case of a tapered soil layer.

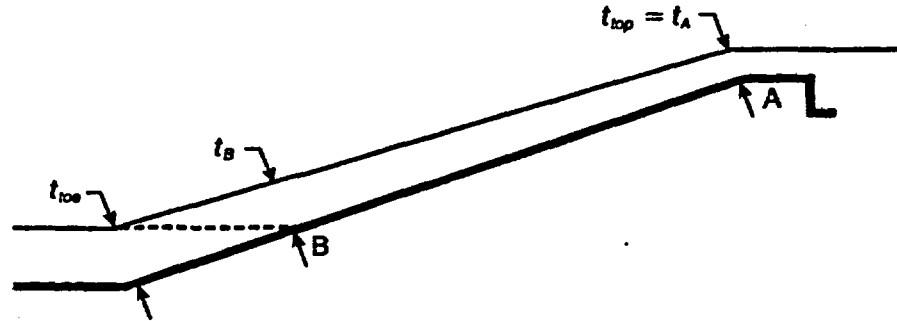


Figure 34: Definition of t_A , t_B , and t_{top} (22)

Design examples were presented for the method developed by Giroud et al. (22) to prove its efficiency. The method is very exhaustive, simpler than the previous ones, and features an accuracy totally acceptable. An important advantage is that equations defining the factor of safety are sums of five terms, which are the independent parameters, influencing the factor of safety (see Table 20).

Table 20: Explanation of Terms in the Factor of Safety by Giroud et al. (22)

Slope	Infinite Slope		Additional terms of finite slope		
Mechanism	Interface Shear		Toe buttressing		Geosynthetic
Parameter	Interface Friction	Interface Adhesion	Soil internal friction	Soil cohesion	Geosynthetic tension
Symbol	δ	a	ϕ	c	T
General equation	$\frac{\tan \delta}{\tan \beta} + \frac{a}{\gamma t \sin \beta} + \frac{t \sin \phi}{h \sin(2\beta) \cos(\beta + \phi)} + \frac{c \cos \phi}{\gamma h \sin \beta \cos(\beta + \phi)} + \frac{T}{\gamma h t}$				
ϕ (+)	\leftrightarrow	\leftrightarrow	(+)	(+)	\leftrightarrow
β (+)	(-)	(-)	(-)	(-)	\leftrightarrow
h (+)	\leftrightarrow	\leftrightarrow	(-)	(-)	(-)
γ (+)	\leftrightarrow	(-)	\leftrightarrow	(-)	(-)
t (+)	\leftrightarrow	(-)	(+)	\leftrightarrow	(-)

(+) corresponds to increase

(-) corresponds to decrease

This accounts for the factor of safety contribution to the interface friction angle, the interface adhesion, the internal friction angle, the cohesion of the soil component located above the slip surface, and the tensile strength of the geosynthetic located above the slip surface. Unfortunately, due to the assumptions made, this method cannot be used in cases where the slopes are submerged or if water is flowing along them.

3.5.6 Conclusions

It appears that the shear properties of liner interfaces are of paramount importance to prevent earthquake damage as well as to ensure a proper stability of the landfill. The materials composing the liner, their roughness, their stiffness, the normal load, as well as the temperature are factors influencing the interface shear strength.

However, review of the materials literature indicated that only very few articles present damage caused to geomembranes/geotextiles materials by slips and shear stresses due to seismic and steady-state harmonic excitation. Even if the slips are of small order, it should be interesting to evaluate their effects on the properties and durability of geotextile liners. Since it is possible that a landfill can survive an earthquake without collapsing, the liner may suffer excessive deformations or tears, which will allow leakage, or reduce the liner durability. This damage will be aggravated as other earthquakes occur.

3.5.7 References

1. U.S. Environmental Protection Agency, Title 40, Part 258: "Criteria for Municipal Solid Waste Landfills", Code of Federal Regulation, 1992, pp. 355-361.
2. U.S.G.S.: "Probabilistic Earthquake Acceleration and Velocity Maps of the United States and Puerto Rico", Map MF 2120, United State Geological Survey, 1991.
3. Singh S., and Sun J.I.: "Seismic Evaluation of Municipal Solid Waste Landfills", Geoenvironment 2000, Volume 2, pp. 1081-1096, 1995.
4. Pasqualini E., Roccato M., and Sani D.: "Shear Resistance at the Interfaces of Composite Liners", Proceedings Sardina 93, Cagliari, Italy, pp. 1457-1471.
5. Vaid Y.P., Rinne N.: "Geomembrane Coefficients of Interface Friction", Geosynthetics International, 1995, Vol.2, No. 1, pp. 309-325.
6. Martin J.P., Koerner R.M., Whitty J.E.: "Experimental Friction Evaluation of Slippage Between Geomembranes, Geotextiles and Soils", Proceedings of the International Conference on Geomembranes, Denver, Co, USA, 1984, pp. 191-196.
7. Williams, N.D. and Houlihan, M.F., 1987, "Evaluation of Interface Friction Properties Between Geosynthetics and Soils", Proceedings of Geosynthetics '87, IFAI, 1987, New Orleans, LA, USA, Vol. 2, pp. 616-627.
8. Akber, S.Z., Hammamji, Y. and Lafleur, J., 1985, "Frictional Characteristics of Geomembranes, Geotextiles, and Geomembrane/Geotextile Composites", Proceedings of the Second Canadian Symposium on Geotextiles and Geomembranes, Edmonton, Alberta, Canada, pp. 209-217.
9. Lam, D.J.S. and Tape, R.T., 1991, "Geomembrane Interface Strength Tests", Geosynthetics: Design and Performance, Sixth Annual Symposium, Vancouver Geotechnical Society, Vancouver, Canada, May 1991.
10. Negussey, D., Wijewickreme, W.K.D., and Vaid, Y.P., 1989, "Geomembrane Interface Friction", Canadian Geotechnical Journal, Vol. 26, No. 1, pp. 165-169.
11. Saxena, S.K. and Wong, Y.T., 1984, "Frictional Characteristics of a Geomembrane", Proceedings of the International Conference on Geomembranes, Denver, CO., USA, pp.187-190.
12. Weiss, W. and Batereau, C., 1987, "A Note on Plane Shear Between Geosynthetics and Construction Materials", Geotextiles and Geomembranes, Vol. 5, No. 1, pp. 63-67.

13. O'Rourke, T.D., Druschel, S.J. and Netravali, A.N., 1990, "Shear Strength Characteristics of Sand Polymer Interfaces", *Journal of Geotechnical Engineering*, ASCE, Vol. 116, No.3, pp. 451-469.
14. Lauwers, D.C., 1991, "PVC Geocomposite for Improved Friction and Performance Properties", *Proceedings of Geosynthetics '91, IFAT, 1991*, Vol. 1, Atlanta, GA, USA, February 1991, pp. 101-103.
15. Cazzuffi D., Corbet S., Montanelli F., and Rimoldi P.: "Compressive Creep Test and Inclined Plane Friction Test for Geosynthetics in Landfill", *Proceedings Sardinia 95*, Cagliari, Italy, pp. 477-491.
16. Yegian, M.K., Yee, Z.Y., and Harb, J.N.: "Seismic Response of Geosynthetic/Soil Systems", *Geoenvironment 2000*, Volume 2, pp. 1113-1125, 1995.
17. Yegian, M.K., Yee, Z.Y., and Harb, J.N.: "Response of Geosynthetics Under Earthquake Excitations", *Geosynthetics '95*, pp. 677-689.
18. Gunturi R., and De A.: "Seismic Analysis of Landfills", *Environmental Geotechnology with Geosynthetics*, 1996, pp. 266-274.
19. De A., and Zimmie T.F.: "Factors Influencing Dynamic Frictional Behavior of Geosynthetic Interface", *Geosynthetics '97*, Long Beach, CA, USA, pp.837-851.
20. Dove J.E., Frost J.D., Han J., and Bachus R.C.: "The Influence of Geomembrane Surface Roughness on Interface Strength", *Geosynthetics '97*, Long Beach, CA, USA, pp.863-876.
21. Dove J.E., Frost J.D.: "A Method for Estimating Geomembrane Surface Roughness", *Geosynthetics International*, 1996, Vol. 3, No. 3, pp. 369-392.
22. Giroud J.P., Williams N.D., Pelte T., and Beech J.F.: "Stability of Geosynthetic-Soil Layered Systems on Slopes", *Geosynthetics International*, 1995, Vol. 2, No. 6, pp. 1115-1148.
23. Giroud J.P., and Ah-Line C.: "Design of Earth and Concrete Covers for Geomembranes", *Proceedings of the International Conference on Geomembranes*, IFAI, vol. 2, Denver, CO, USA, June 1984, pp. 487-492.
24. Martin J.P., and Koerner R.M.: "Geotechnical Design Considerations for Geomembrane Lined Slopes: Slope Stability", *Geotextiles and Geomembranes*, Elsevier, 1985, Vol. 2, No. 4, pp. 299-321.

25. Giroud J.P., and Beech J.F.: "Stability of Soil Layers on Geosynthetics Lining Systems", Proceedings of Geosynthetics '89, Vol. 1, IFAI, San Diego, California, USA, February 1989, pp. 35-46.
26. Koerner R.M., and Hwu B.L.: "Stability and Tension Consideration Regarding Cover Soils in Geomembrane Lined Slopes", Geotextiles and Geomembranes, 1991, Elsevier, Vol. 10, No. 4, pp. 335-355.

3.6 Effect of Natural Parameters on Geosynthetic Aging

3.6.1 Introduction

Many investigations have addressed the aging of geosynthetics and geomembranes, since aging is one of the most important concerns for materials used for landfill liners. The environments in and around landfills are usually aggressive towards geosynthetics, i.e.: temperature, UV, oxidation, and chemical agents that deteriorate the liner. This chapter is restricted to the aging problem in landfill environments.

Haxo et al. (1) studied the factors in the durability of polymeric membrane liners and classified the different modes of failure of a membrane as follows: a) softening and loss of physical properties due to depolymerization and molecular scission, b) stiffening and embrittlement due to loss of plasticizers and additives, c) reduction of mechanical properties and increase of permeability, d) failure of membrane seams.

3.6.2 Conditions at the liner level

Landereth (2) summarized the conditions encountered in a landfill: temperature between 40 to 70°F, constant flow of leachate, no light, aerobic or anaerobic conditions, bacteria, acidity, gas, etc. In a hazardous waste landfill, microbes will be more active if the waste does not kill them, also less gas will be produced.

Typical chemicals found in a landfill environment are listed in Table 21:

Table 21: Typical Chemicals in a Landfill Environment

a) Typical Chemical in Landfill Gas (18):

Typical constituent in gas		Typical concentration of trace compounds	
Component	Percent	Component	Mean concentration (pbV, parts per billion by volume)
Methane	40-60	Toluene	34,907
Carbon Dioxide	40-60	Dichloromethane	25,694
Nitrogen	2-5	Ethyl Benzene	7,334
Oxygen	0.1-1.0	Acetone	6,838
Ammonia	0.1-1.0	Vinyl Acetate	5,663
Sulfides, Disulfides, Mercaptans	0-0.2	Tetrachloroethylene	5,244
Hydrogen	0-0.2	Vinyl Chloride	3,508
Carbon Monoxide	0-0.2	Methyl Ethyl Ketone	3,092
Trace Constituents	0.01-0.6	Xylenes	2,651

b) Typical chemical in Landfill Leachate (19):

Elements	Concentration (mg/kg)
Sulfates	< 328 000
Copper	< 295
Zinc	< 534
Arsenic	< 385
Benzo-a-pyrene	< 1300
Oils	< 9 000
pH	> 1.2

Typical conditions in MSW landfills are as follows:

- absence of oxygen and ultraviolet light
- humid to wet
- cool and uniform temperature (10-20°C)
- moderate acidity and dissolved organic constituents
- high overburden pressure, with moderate hydraulic head pressure

In MSW landfills, polymeric materials have proven to have acceptable resistance to aging even if depolymerization, and loss of strength occur.

Typical conditions in hazardous waste facilities are as follows:

- vast range of waste directly or not in contact with the material
- exposure to weathering: sunlight, rain, ozone
- wave action of the fluid in the pond
- significant temperature gradient
- ground settlement and movement

The environment in hazardous waste facilities is more aggressive towards the membrane than in MSW landfills

3.6.3 Different stresses to which the liner is subjected

Haxo and Haxo (3) described the different parameters influencing the durability and aging of geosynthetic products in landfill environments. Those parameters can be classified into three groups: chemical, mechanical, and biological stresses, possibly acting simultaneously, and causing different types of aggressiveness to the liner material.

Chemical stresses, which are affected by temperature, are induced by exposure to waste liquid, ultraviolet and infrared radiation, rain water, oxygen and ozone; these have different effects ranging from structure breakdown, cross-linking and gelling, swelling and dissolution of the polymer, volatilization or extraction of plasticizers, and increase of crystallinity.

Mechanical stresses are induced by penetration, overburden weight, hydraulic head, rain, hail, snow, and wind, stresses on slopes, and settlement. Their effects are tearing, cracking, breaking, and creep.

Biological stresses result from biodegradation by microorganisms and attack by rodents, birds, and insects creating clogging of the material.

3.6.4 Environmental effects during construction

During fabrication and through liner construction, geosynthetic products are exposed to different environmental factors, possibly aggressive. Many liner flaws are caused by defects created before or during liner construction, therefore, great care must be taken during this phase of life of the material.

The change in temperature may cause damage since the material is not yet buried. Temperature affects seaming, embrittlement (low temperature), shrinkage, and softening (high temperature).

Humidity, UV, and oxygen may be really harmful to uncovered material. Products that do not include carbon black are even more affected by UV light exposure. Careless placement of geosynthetics, as well as gravel, may result in stretching, tensioning, creep, scratch, tearing, and puncture. This can be prevented by skilled workers.

3.6.5 Environmental effect during service life

Multiaxial stresses are usually present at any location of any geosynthetic liner; uniaxial stresses are very rare in real situations. Anaerobic conditions are present in most landfills at the location of the liner, which reduce and eliminate the existence of microorganisms, and therefore, reduce the risk of biodegradation.

Absence of light and, therefore, UV reduces considerably the risk of degradation but leachate is almost always present at the level of liner. The leachate increases the possibility of loss of the material's compounds, and decreases the geomembrane properties. Temperature may vary from 40 to 70°F, and even higher in certain cases.

Overburden pressure may approach 100 psi, which, in the case for rough soil in contact with the membrane may deform, puncture, or even tear the material. The decomposition of waste creates gases such as carbon-dioxide and methane, which may cause mineralization of the soil, and clog the liner. The presence of ions may also cause clogging.

For hazardous waste landfills, aerobic conditions increase the possibility of bacteria and microorganisms, which can lead to fungal growth that would eventually clog the liner.

3.6.6 Degradation processes

- **Temperature:**

Schneider (4) characterized and summarized the effect of temperature and intensity of radiation on geosynthetic products. Degradation can be caused by weathering factors such as oxygen, radiation, humidity or heat.

Arrhenius developed a governing equation for chemical degradation, Equ. 3.6.1:

$$K_p = A \cdot e^{(-E_a/RT)} \dots\dots\dots [3.6.1]$$

where:

A = rate constant, $\frac{eKT}{h} \cdot e^{s/R}$ but under certain conditions, $A = 10^{-13}$ at 25 °C.

Ea: activation energy

R: gas constant

T: absolute temperature

Furthermore, many weathering tests were conducted on PP continuous fiber geomembranes under mechanical loads. It was observed that there was significant remaining strength (specimens are tested after exposition) when the temperature varied and the intensity of radiation was constant.

The temperature may be influenced by different factors and can differ for the surrounding material, geosynthetic surface and its core (difference of 20 °C between surrounding material and geotextile may exist). When temperatures over 100 °C are reached, water produced by condensation may cause hydrolytic degradation; however, proper storage will solve this problem.

Not only does the temperature act as an accelerator, but it may also affect the fiber's structure by stabilizing it as well as decreasing the inner stress. Another consequence of temperature is the increase of material's crystallinity associated with an increase of density. Thus, temperature is an important parameter in the aging process due to its capability to influence the reaction rate, mechanical (strength and elongation), and abrasion properties. Temperature in the sample may be significantly higher than in the surrounding environment, this is due to the material's thickness and opacity.

The results of the tests carried out by Fayoux (16) on the durability of PVC geomembranes show that temperature causes the evaporation of plasticizers, which at 40°C is about 0.7 to 3.5 g/m²/year.

Pierson et al. (5) assessed the thermal behavior of geomembranes exposed to solar radiation, which induces problems (such as wrinkles) and, even flaws at the construction stage, when the geomembrane is still uncovered by waste.

Temperatures may reach 80 °C in black exposed geomembranes, such temperatures acting on material with high coefficients of thermal expansion cause wrinkles over the entire exposed surface of the geomembrane.

Pierson et al. developed analytical expressions for the coefficient of thermal expansion (CTE), the coefficient of absorption (α), and the expected temperature in the membrane. They validated these expressions by tests and indicated values of CTE and α .

The coefficient of thermal expansion, CTE (m/(m.°C)), is defined in Equ. 3.6.2.

$$\Delta l/l_0 = \text{CTE} \times \Delta T \dots \dots \dots [3.6.2]$$

where $\Delta l/l_0$ (m/m) is the strain and ΔT (°C) is the variation in temperature.

Tests were carried out to assess the values of CTE for different materials, and show that HDPE is the material with the higher CTE, also the variation of CTE with the directionality of testing and the maximum width of the sheet, Table 22 gathers the results.

Table 22: Coefficient of Thermal Expansion of HDPE and PVC (5)

Material	HDPE 1		HDPE 2		PVC	
Direction	width	length	Width	length	width	Length
Irreversible variations after 3 tests (per thousand)	2.2	- 1.7	< ± 1	< ± 1	13	- 13
CTE (m/(m.°C))	2.6 E-4	1.7 E-4	2.9 E-4	3.1 E-4	1.4 E-4	1.2 E-4

The coefficient of absorption α was evaluated for different materials and colors using the heating plate test. Equ. 3.6.3 and 3.6.4 express α in geomembranes resting on ground:

$$\alpha \cdot G = h_H \cdot (T_m(t) - T_{cl}) + \Phi(x=0,t) \dots \dots \dots [3.6.3]$$

where: α : coefficient of absorption

G: solar radiation (W/m²)

h_H : constant=25±1 (W.m⁻².°C⁻¹)

$T_m(t)$: mean membrane temperature at x=0 and time t (°C)

T_{cl} : temperature of the boundary layer (°C)

$\Phi(x=0,t)$: conduction heat flux

The temperature in the membrane can be approximated by Equ. 3.6.4:

$$T_m(t) = T_a + 1/h_H \cdot \left\{ \alpha \cdot G + \frac{3\lambda[(T_i - T_a) - \alpha \cdot G/h_H]}{\delta(t) + 3\lambda/h_H} \right\} \dots \dots \dots [3.6.4]$$

where: T_a : air temperature ($^{\circ}\text{C}$)
 $\delta(t)$: value of x so that $\Phi(x=0,t)$
 λ : soil thermal conductivity

These equations were validated by tests proving their accuracy.

It was proven that a white coating applied on the surface of the membrane reduces considerably the overheating of the material (see Fig. 35). The use of a geotextile over a black geomembrane only delays the overheating, so this is not an appropriate means to eliminate long-term overheating.

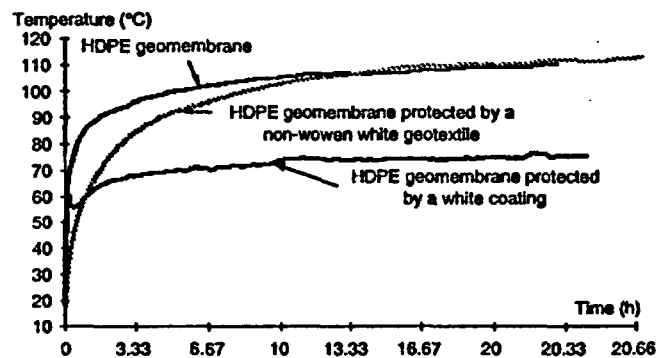


Figure 35: Influence of geomembrane coating on thermal properties (5)

From site tests and observations, the wrinkle phenomena can be outlined as follows:

- large wrinkles propagate along the sheet's length and weld
- small wrinkles propagate perpendicular to the large ones
- due to undulation, the contact between the soil and the membrane is not continuous
- temperatures in the wrinkles are higher than those in the non-wrinkled parts of the sheet
- spacing between two wrinkles does not change, if the temperature and height of the wrinkle increases.

*** UV light:**

UV is the worst factor affecting exposed PVC materials (16). A solution to prevent the effect of UV is to include carbon black. Its concentration is limited by the burning phenomena occurring during seaming. Another solution is the combination of light pigments, which by their presence decrease the temperature in the membrane and therefore, the aging, deformation, creep, etc. The study carried out by Fayoux (16) shows that the loss of plasticizers was in the order of $12 \text{ g/m}^2/\text{year}$.

Koerner and Koerner (6) analyzed the behavior of field-deployed HDPE geomembranes. Exposed to light, a geomembrane is subjected to three physical phenomena: radiation,

conduction, and convection. Radiation is a phenomenon in which the energy is carried by electromagnetic waves (solar radiation ranges between 0.1 to 4 mm). The transference of heat caused by a temperature gradient is the conduction phenomenon. Convection is the transfer of heat by molecular movement.

The first part of the study addressed the testing of black, white, textured and smooth geomembranes, exposed to field conditions throughout the year.

Table 23: Average Temperature in Black and White Geomembrane (6)

Season of Year	Max. Ambient Temperature	Black Geomembrane		White Geomembrane	
		Max. Temp.	Diff. Amb.	Max. Temp.	Diff. Amb.
Winter	5	13	8	2	-3
Spring	22	46	24	38	16
Summer	30	70	40	57	27
Fall	19	35	17	28	10

Table 23 presents the test results, from which it can be concluded that the temperatures in white geomembranes are always lower than those in black ones; only a small difference between the smooth and textured geomembranes exists in the advantage of the textured one in which lower temperature was found.

The second part concerns the analysis of wave occurrence due to light exposure in a 1.5 mm smooth black HDPE geomembrane. The weather conditions (sun, cloud, and wind) are important parameters in the development of waves. Sun and no wind will increase the temperatures in the membranes and the material will expand creating waves. Covering the geomembranes with a geotextile or gravel significantly reduces the temperatures and so the waves formation. The topography of waves was also monitored and is shown in Fig. 36.

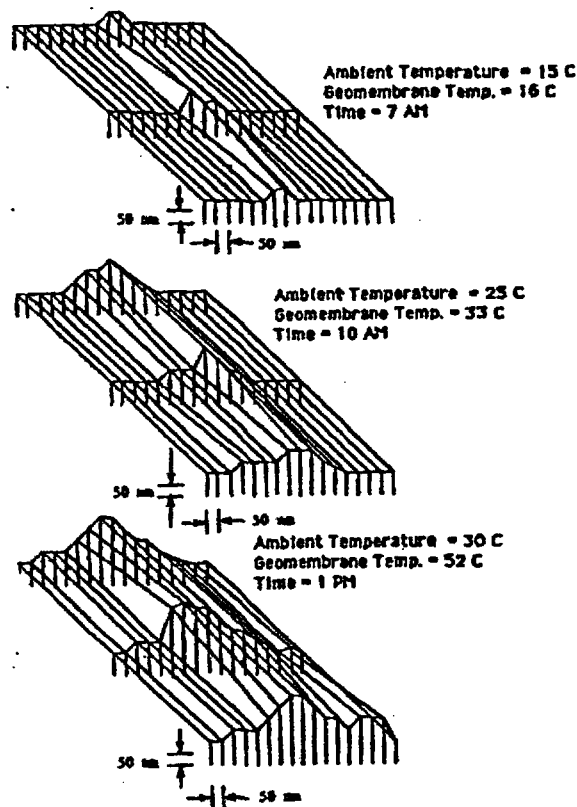


Figure 36: Topography of waves induced by UV radiation (6)

Cazzuffi et al. (7) provided a very detailed analysis of the reason for the degradation in polymeric material due to UV light: photodegradation breaks down the chemical bonds due to UV exposure leading to cracking, chalking, color changes, or loss of physical and mechanical properties. They also compared results of laboratory and outdoor exposure tests of seven different geosynthetics. The laboratory high temperature accelerated tests were performed for periods of 1,000, 2,000, and 3,000 hours, while the outdoor tests were performed for 1,080, 2,060, and up to 17,280 hours.

Geotextiles, geogrids, and geomembranes, made of PET, PP, PE, PVC, and HDPE, were tested for UV exposure effects. For geotextiles, outdoors and laboratory tests results correlated for strength: an exposure of 1,000 hours in the laboratory corresponds to one-year outdoors. Such correlations are also true for geogrids and geomembranes, proving good correlation for any type of material. It was also shown that one of the main parameters for UV resistance is the thickness of the material: the thicker the material, greater the resistance.

Geotextiles were subjected to embrittlement (increase of modulus up to 370%), while geogrids and geomembranes suffered a lot less to an acceptable degree. Moreover, for

geogrids and geomembranes, aging is not proportional to the exposure time, and the change occurs only superficially and not in the material core.

Ultraviolet radiation affects uncovered materials and can be dangerous during the installation of the liner and before the placement of the waste. Only the ultraviolet part of the light is harmful to the geosynthetic materials, moreover, each material is sensitive to a particular wavelength (i.e. polyethylene = 300 nm, polyester = 325 nm, and polypropylene = 370 nm).

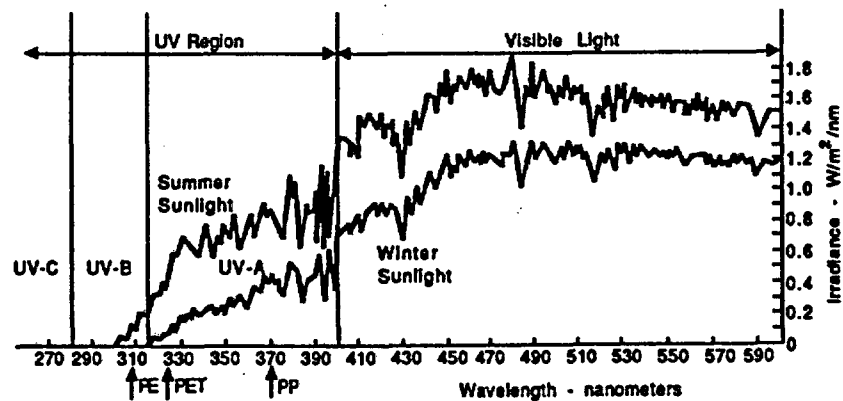


Figure 37: Wavelength Spectrum of UV radiation (12)

The degradation mechanism is due to molecular bond scission (in the primary polymer's backbone) created by the sensitive wavelength within the molecular structure.

Ultraviolet light causes material embrittlement and may induce cracks depending on the intensity of the radiation.

The best solution to prevent ultraviolet damage is to keep a minimum layer (15 cm) of soil, waste, or gravel over the liner so that light cannot penetrate the material. In the case of uncovered geotextiles, carbon black and chemical stabilization must be used. Carbon black is a powder that prevents the light from entering the material microstructure and also absorbs a part of the light energy. Chemical stabilization with (Hindered Amine Light Stabilizers, HALS), in which the free radical is liberated by scission due to the light, stops further degradation.

* Chemical:

Chemical stresses are characterized by cross-linking or scission of the polymer chain due to the reaction of oxygen with polymer (2). Organic absorption may cause the material to swell or soften.

An important concern is the crystallinity increase causing the embrittlement of the material that reduces its resistance to cracking. Leachate may extract some compounding ingredients from the geosynthetic.

Artieres et al. (8) analyzed the durability of different geomembranes under chemical stresses induced by the leachate over a period of 6 months. All the materials tested showed no significant modifications in microstructure, or mechanical stress, proving that the leachate has no effect on geomembrane material in a time period of 16 months. However, longer tests should be made since modifications of properties are expected due to the long-term exposure to chemical agent. Moreover, it was proved that bituminous geomembranes should not be used as liners, since they are porous under small deformations.

Billing et al. (9) assessed the chemical and mechanical durability of geotextiles. These synthetic materials are used in landfill as soil-reinforcement materials and can be exposed to chemically aggressive leachate environment.

Certain metal ions such as Fe, Cu, and Mn induce and accelerate the hydrolysis of polyester material. To prevent this problem, ion deactivators were embedded in the material during its processing. The samples were immersed in an extremely acid (sulfuric) solution of pH 3, and in an highly alkaline (calcium oxide) solution of pH 12. The results of this study showed that the different geotextiles (polypropylene, polyester, and polyethylene) were only slightly affected by the pH of the solution, in which they were immersed. Polypropylene showed a slight weight increase at high pH, and a significant tensile strength reduction after immersion in H_2SO_4 (pH 3). Polyester showed a weight loss accompanied by crystal growth, and also a reduction in tensile strength after immersion in pH 12 solution. Polyethylene materials were not affected by the immersion.

Overmann et al. (10) tested the chemical resistance of geomembranes and geotextiles to leachate. Their tests were based on the US EPA method 9091, but the time and temperature of immersion of the samples were increased. The materials tested were as follows: HDPE and Reinforced CSPE for the geomembranes (with seam samples being also tested because of their low resistance to chemical aggression); polyester, polypropylene and high-density polyethylene for the geotextile. The leachate was taken from existing landfills and had a pH of 8.8. The immersion temperatures were higher than those indicated in the EPA Method (25, 45, and 70°C), and the time of immersion varied from 1 to 24 months.

Non-exposed and exposed specimens were physically and mechanically tested and the results compared to assess the chemical effect on the specimens. The results showed that for HDPE geomembranes, there are only small differences between exposed and non-exposed specimens. The thicker the membrane, the better was the resistance against chemical aggression. The R-CSPE specimens performed quite poorly and showed significant increase of volatile content, thickness and mass, as well as tensile and shear strength.

Both geotextile materials performed well at low temperatures, but at 70°C the polyester showed a decrease in properties; polyethylene material seemed to have better properties than polypropylene.

Lord et al. (11) presented an interesting and complete review of the different degradation processes that decrease the durability of a geomembrane. The geomembrane may dissolve in the surrounding liquid, if the solubility parameter matches with those of the compounds of the liquid. This problem is easily avoided by conducting the tests in the appropriate liquid.

HDPE materials are not affected by alcohol or detergents, however, they are moderately affected by hexane, toluene, and carbon tetrachloride provoking stress relaxation. HDPE is severely affected (show high stress relaxation) in halogenated hydrocarbon perchlene. It should be noted that the moderate effect in most hydrocarbons and the severe effects in halogenated hydrocarbon perchlene will cause more or less stress relaxation in HDPE materials coupled with creep.

This paper reviews a study done by the Hoecht group on the chemical resistance of polymer in contact with four different liquids: a) aqueous solutions of strongly oxidizing substances, b) aqueous solutions of non-oxidizing inorganic substances, c) aqueous solutions of wetting agent, and d) organic materials. It was shown that the wetting agent may have the tendency to decrease the material's lifetime. This tendency may even be more accentuated in swelling agent testing.

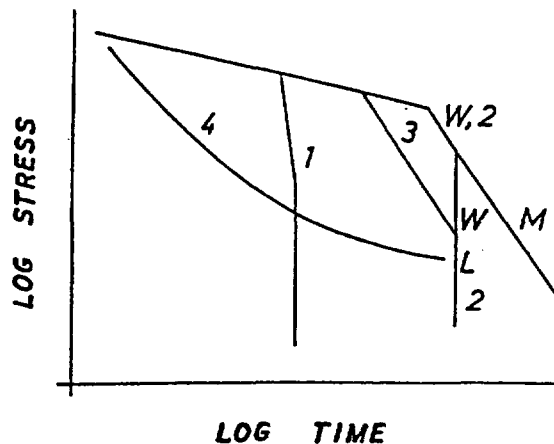


Figure 38: Burst test in presence of different chemicals (11)

Chemical degradation is one of the main phenomena affecting geomembranes (12), since in most of the liners the geomembrane or geosynthetic materials are in contact with the leachate, which is very often aggressive to the polymer. Many studies have been performed using the EPA test method 9090, by comparing exposed and non-exposed samples with physical and mechanical tests. The exposure was in different solutions, duration, and temperatures.

Three degrees of degradation are possible:

If no degradation occurs, the material has been proven to resist the test condition (temperature, leachate, duration, etc.) but not other conditions.

Swelling may occur, which is not a real problem if the phenomenon is monitored with care, since swelling is often the earlier sign of further degradation.

If the physical and/or mechanical tests show degradation, the material is not sufficiently resistant to the test conditions.

Oxidation degradation is the creation of free radicals that may activate chain scission. The reaction between carbon and oxygen atoms creates an hydroperoxy radical, which is passed around the molecular structure and can lead to chain scission.

The chemical reactions are given by:



with $R \cdot$ = free radical
 $ROO \cdot$ = hydroperoxy free radical
 RH = polymer chain
 $ROOH$ = oxidized polymer chain

In order to prevent this problem, anti-oxidants are embedded within the material, they stop the chemical reaction; another procedure is to eliminate oxygen from the material and then cover the geomembrane.

** Biological:*

Micro-organisms are potentially harmful when only moisture, temperature, and organic matter (5) are present simultaneously, which is not the common case in most current landfills. However, to prevent damage biocides and fungicides may be added to the PVC membrane.

Biological stresses are a little less compromising for geosynthetics, since biological organisms are unlikely to damage the material, however they can clog the drainage system and deteriorate the whole landfill (2). To prevent the material from clogging, special care must be taken by using low surface energy compounds, biocides by either incorporating them in the material, or by coating them, or by flushing the drainage system.

Biological degradation is the formation of bio-organisms (bacteria, actinomycetes, fungi, and algae) that can alter the properties of liner material (12). Polymer degradation is generally unlikely due to the high molecular weight of the resin, however plasticizers or additives may be attacked. Also, small mammals may cause physical damage.

*** Mechanical stress:**

Mechanical stresses are also very harmful to the material: scratch, seaming imperfections, and fabrication flaws may cause crack failures or decrease the creep properties of the material.

*** Swelling:**

The swelling degradation is function of the liquid in which the membrane is exposed. When plasticizers are extracted, the material tends to shrink. Swelling is limited in membranes embedded with high percentage of plasticizers since only the polymeric compound swells. Moreover, swelling is limited by crosslinking phenomena (1).

Degradation by swelling, as seen previously is not a very harmful problem and is not automatically associated with chain scission. But swelling is a good means to judge the material durability: the more the swelling, the less the material is susceptible to liquid absorption (12).

*** Radiation:**

Radiation degradation is due to γ and β rays penetrating and damaging the polymer material. β rays penetrate only the surface (about one millimeter), while the γ rays may penetrate the total thickness (12).

These radiations are only harmful to polymers at high intensities above 10^6 to 10^7 rads, compared to maximum levels of radiation acceptable for human beings, which is only 100 to 200 rads. Thus, except in radioactive environments, the geomembranes should not suffer damage from radiation. However, even at low radiation levels, small degradations may occur especially at the material surface. This degradation may cause loss of strength and stress-cracking.

*** Aging properties of membranes immersed in leachate:**

Surmann et al. (13) carried out two aging tests and studied the effect of irradiation on HDPE geomembranes. The immersion in leachate, combined with a light tensile strength as well as the multifunctional cell test, did not show important differences between virgin and aged geomembranes; even the leachate had no influence on the material tested. However, the test period was only 2 years; an increase of this time up to 5 years may give different results. Comparing the results of virgin and γ irradiated geomembranes, the effects of irradiation are clearly apparent: breaking and branching of the molecular chains results in the loss of the material's thermoplastic characteristics, as well as a change in the atomic arrangement.

Duquennoi et al. (14) tested a wide variety of liner materials to assess their aging properties. After 50 months of immersion in two different leachates and distilled water at 20°C and 27 months at 50 °C, the materials were tested using uniaxial and biaxial tensile tests to determine the macroscopic effect of leachate. They were also tested using Fourier Transform Spectroscopy, which enables evaluation at the molecular level. Sliced samples were analyzed under infrared light providing distribution profiles of the compounds.

However, opaque materials such as EPDM and bituminous geomembranes, cannot be tested by this method. So photoacoustic spectroscopy was used.

EPDM geomembrane made from an elastomer terpolymer of Ethylene-Propylene-Diene-Monomer, loaded with additives for protection against oxidation, showed increase in rigidity but no important differences in tensile properties. No chemical changes were noticed, even if water was absorbed at the surface of the specimen. It also appeared that absorption increases with immersion time. Physical modification of material, as cross-linking, may explain the water absorption and the increase in rigidity of the geomembrane.

SBS/bituminous membranes made of a polyester nonwoven geotextile, impregnated with bituminous and a Styrene-Butadiene-Styrene Copolymer, showed no difference in mechanical properties. Chemical evolution and water absorption were noticed in the leachate and water immersion cases.

PVC membranes with DOP additives are characterized by a material softening in each direction tested (uniaxial and biaxial tests showed identical results). This softening phenomenon may be due to the lubricant effect of absorbed water in the material. Plasticizers were observed varying differently depending on the immersion leachate. However, it was not possible to determine the effect of plasticizers on the mechanical properties. PVC with EVA plasticizer showed an oxidation of the plasticizer of a lower order than PVC loaded with DOP.

HDPE specimens did not exhibit changes in tensile or chemical properties. Nevertheless, at 50°C a small amount of ester-type antioxidant was lost probably indicating possible accelerated aging with high temperature. For PP geomembranes, neither mechanical nor chemical changes were observed.

This study proved the almost identical effect of leachate and distilled water on geomembrane aging, phenomena associated with very low concentration of organisms in the leachate. Accelerated aging occurred at 50°C, but not at 20°C. No chemical evolution occurred in the polymer matrix, but plasticizers were extracted.

Acidic, or basic diluted solutions and salts did not degrade the PVC. To prevent possible effect of hydrocarbons, specific plasticizers need to be used. Since a thicker membrane incorporates more plasticizers than a thin one, the degradation will be spread over a longer time.

** Extraction:*

The effect of water in the plasticizer loss process may be negligible, if the correct formula is used; in this study a rate of 0.8 g/m²/year was observed.

Extraction may occur long term by the loss of certain components of the compound; the materials affected by extraction are mainly those incorporating plasticizers or fillers (12). Extraction is associated with material embrittlement, which is characterized by an increase of modulus and strength, as well as a decrease of elongation at failure.

** Combined effects:*

Combined stresses are very harmful to the material, since chemical exposure can change the material composition, the mechanical properties will also change (2). One of the most serious concerns of combined stress is the stress-cracking caused by a change of chemical composition, acting simultaneously with a mechanical stress (see stress-cracking chapter).

All the degradation phenomena can act simultaneously, and become a lot more aggressive to the liner material. Synergetic effects increase the degradation of the material due to elevated temperatures when mechanical stresses are applied and during long exposure (ultraviolet, radiation, chemical agent), (12). Obviously the more simultaneous aggressive parameters, the more the geomembrane is attacked, and the less will be its resistance.

3.6.7 Assessment of long term aging through tests

Cassidy and Bright (15) evaluated the durability of geosynthetic materials after 9 years of natural weathering. PP, HDPE, and HMW uncovered membranes were exposed to field conditions in the Atlanta region. The results show that chain scission occurs in PP material, and cross-linking in HDPE. The changes are a function of the quantity of additives included in the product; generally the more additives, the more resistant the membrane. It was also shown that a concentration of 5 % of additives in the total weight will prevent a large amount of deterioration in tensile strength for the long-term exposure. Carbon black is a very effective means for preventing damage from UV light, a minimum of 2% by weight will be sufficient.

Fayoux et al. (16) assessed a PVC geomembrane after 10 years of utilization in a collective waste disposal site. Samples were taken at different locations of the liner, some samples were exposed to the leachate, some to UV light, and others to contact with stones. It was noticed that after 10 years the elongation and stress at failure are not affected and their values correspond to those at initiation of exposure.

At the bottom of the pond, the material was affected by a slight increase in modulus. The critical zone was located at the water table, where the geomembrane was subjected to simultaneous action of light, wave, and leachate. The loss of plasticizer was about 0.35 % per year in and outside the water, a value which is not dangerous for the integrity of the material. The minimum effect of the liquid on the material is explained by the very low concentration of solvent in the leachate, making the leachate not so aggressive to the liner.

Rollin et al. (17) investigated a seven-year old geomembrane placed in a landfill. After seven years of activity, the geomembrane was excavated and tested to assess the effect of aging. Samples from different locations were taken and tested for comparison of mechanical properties (tensile strength, tensile and peel resistance of seam, brittleness of sheet and seams, and microanalysis of cracks) with those of the initial liner.

Differences between the initial and the used membranes properties indicate that aging is more important at the bottom of the liner than at the slope and cover. The aging is

characterized by an increase of yield strength, decrease in the tensile resistance at rupture, and a reduction in the elongation at break.

Seams did not suffer much, since they were only subjected to a decrease of strength of the order of 5 to 20 percent. Also, no seams were debonded and only 2 cracks were observed.

3.6.8 Summary

Haxo et al. (1) summarized the effect of membrane exposure to weathering and waste in Table 24.

Table 24: Effect of Geomembrane Exposure to Weathering and Waste (1)

Process	Effect on membranes
<i>Weather exposure:</i>	
- oxidation	- stiffen and lose tensile strength, elongate, tear
- elevated temperature	- reduction of mechanical strength and degradation, generally stiffen, but sometimes softens
- ozone	- cracks at points of strain
- UV light	- stiffen and crack
- Loss of volatile plasticizer	- stiffen and can become brittle
- High humidity	- water absorption, leaching of anti-degradant resulting in greater susceptibility to oxidation and UV
<i>Waste exposure:</i>	
- Swelling	- soften accompanied by loss of properties, including increase in permeability
- dissolving	- hole or general loss of barrier function
- extraction of plasticizer	- may stiffen and lose elongation
- extraction of anti-degradant	- make more susceptible to degradation
- stress	- creep of liner, cracking, and breaking
<i>Combination of waste and weather exposure:</i>	combination of weather and waste exposure, often more severe than either alone
<i>Biodegradation if oxygen is present:</i>	plasticizers, oils and monomeric organic molecules can be degraded

Haxo et al. (1) summarized the factors affecting durability as follows:

Compatibility factors with waste liquids:

- chemical

- physical

Weathering factors – geographic location:

- solar radiation
- temperature
 - elevated
 - depressed
 - cycles and fluctuations
- water: solid, liquid and vapor
- normal air constituents: oxygen and ozone

Stress factors:

- stress, sustained, and periodic
- stress, random:
 - physical action of rain, hail, sleet, and snow
 - physical action of wind
 - movement due to other factors: settlement
 - discontinuity at penetration

Use and operational factors:

- design of system, groundwork and installation
- operational practice

Biological factors

3.6.9 References

1. Haxo H., and Nelson N: "Factors in the Durability of Polymeric Membrane Liners", International Conference on Geomembranes Denver, USA, 1984, pp. 287-292.
2. Landreth R.: "Durability of Geosynthetics in Waste Management Facilities: Needed Research", Durability and Aging of Geosynthetics, Edited by Koerner R.M., 1989, pp 6-12.
3. Haxo H. and Haxo P.: "Environmental Conditions Encountered by Geosynthetics in Waste Containment Applications", Durability and Aging of Geosynthetics, Edited by Koerner R.M., 1989, pp. 28-47.
4. Schneider H.: "Durability Testing and Prediction of Geotextiles and Related Products", Geotextiles, Geomembranes and Related Products, Den Hoedth ed., 1990, ISBN 90 6191 1192, pp. 723-726.
5. Pierson P., Pelte T., and Gourc J.P.: "Behavior of Geomembranes Exposed to Solar Radiation", Proceedings Sardinia 93, pp. 349-356.
6. Koerner G.R., and Koerner R.M.: "Temperature Behavior of Field Deployed HDPE Geomembranes" Geosynthetics '95, pp. 921-937.
7. Cazzuffi D., Fede L., Villa C., Montanelli F., and Rimoldi P.: "The Assessment of the Effects of Natural and Lab Weathering Exposure of Geosynthetics", Proceedings Sardinia 95, pp. 387-396.
8. Artieres O., Gousse F, and Prigent E.: "Laboratory-Aging of Geomembranes in Municipal Landfill leachates", Proceedings Sardinia 91, Italy, pp.587-603.
9. Billing J.W., Greenwood J. H., and Small G.D.: "Chemical and Mechanical Durability of Geotextiles", Geotextiles, Geomembranes, and Related Products, Den Hoedt (ed.), 1990, pp. 621-626.
10. Overmann L.K., Cowland J.W., Mattravers N.K., Shung W.K., Lee B.S., and Wan C.H.: "Chemical Resistance Testing of Liner Materials for Hong Kong Landfills", Proceedings Sardinia 93, Fourth International Landfill Symposium, pp. 333-347.
11. Lord A, and Halse Jr.: "Polymer Durability – The Materials Aspects", Proceedings Sardinia 95, pp. 387-396.
12. Koerner R.M., Halse Y.H., and Arthur E.L.: Long Term Durability and Aging of Geomembranes, Waste Containment Systems: Construction, Regulation, and Performance, Edited by Rudolph Bonaparte, 1992.

13. Surmann R., Pierson P., Cottour P.: "Geomembrane Liner Performance and Long Term Durability", Proceedings Sardina 95, Fifth International Landfill Symposium, Italy, 1995, pp. 405-414.
14. Duquennoi C., Bernhard C., Gaumet S.: "Laboratory Aging of Geomembranes in Landfill Leachates", Proceedings Sardina 95, Fifth International Landfill Symposium, Italy, 1995, pp. 397-404.
15. Cassidy L., Bright D.G.: "Durability of Geosynthetics exposed to Nine Years of Natural Weathering", Geosynthetics '95, pp. 841-851.
16. Fayoux D., Gousse F., and Rummens F.: "Assessment on a PVC Geomembrane in a Landfill After Ten Years", Proceedings Sardina 93, pp. 369-378.
17. Rollin A.L., Mlynnarek J., Lafleur J., and Zanesco A.: "The Investigation of a Seven Year Old HDPE Geomembrane Used in a Landfill", Proceedings Sardina 91, pp. 667-677.
18. Tchobanoglous G., Theisen H., and Vigil S.: Integrated Solid Waste Management, Engineering Principles, and Management Issues, McGraw-Hill, New York, 1993.
19. Zanesco A, and Demers L.: "L'emploi des ?Materiaux Geosynthetiques dans la Cellule a Securite Maximale de LaSalle-coke", Proceedings Colloque sur les Geosynthetiques, 43e Conference Canadienne des Geotechniques, 1990, Quebec.

3.7 Other Problems Affecting Geomembranes Life

The previous sections of this report presented the main problems associated with liners. This section deals with other important problems that have not been very well addressed in the literature.

3.7.1 Contaminated lifespan and stochastic analysis

Rowe and Fraser (1) assessed the long-term behavior of engineered barrier systems and developed a stochastic analysis for service life. The lifespan of a contaminated landfill corresponds to the period during which the environmental hazardous contaminants are produced by the landfill. It is obvious that to ensure the integrity of the landfill, the material used, especially the liner and any other material used to contain leachate, must have a service life longer than the contaminated landfill lifespan.

The contaminating lifespan is a direct function of the landfill rate of infiltration through the cover. Hence, large landfills with low infiltration rates may have lifespans as long as 600 years, while large landfills with high infiltration rates may have lifespans of the order of 200 years. Stochastic analysis provides information on the effect of leachate concentration on uncertain service life, by using Monte Carlo simulation.

3.7.2 Residual stresses

Lord et al. (2) carried out an interesting and complete study of residual stresses in geomembrane sheets and seams. Residual stresses are a very likely in geomembranes; they are induced by the fabrication and placement of the membrane. Those stresses are more likely to occur in high crystalline polymers, which are often more brittle.

The authors measured residual strains with the drilled hole technique. The results showed reasonable residual stresses with compressive stresses of about 5 to 10 percent of the yield value.

3.7.3 Geomembrane uplift by wind

Giroud et al. (3) published a very detailed paper on the effect of wind on geomembranes. As in airplane wings, a geomembrane is uplifted either by suction or wind flow between the soil and the membrane, see Fig. 39 for actual geomembrane uplift. Most of the time, an uplifted membrane will not be damaged but will be either torn, pulled out off its anchor trench, or ripped off a rigid structure.

Fig. 40 and 41 show the pressure distributions on a geomembrane due to wind for two different cases.

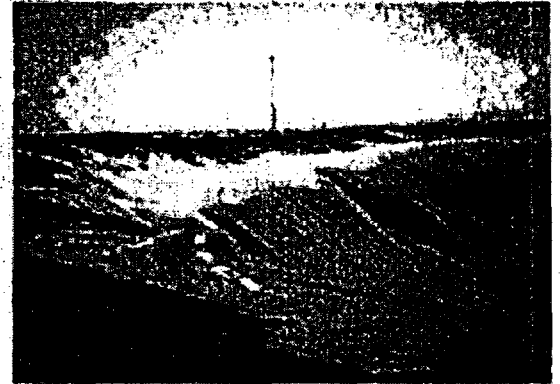


Figure 39: Geomembrane uplift (3)

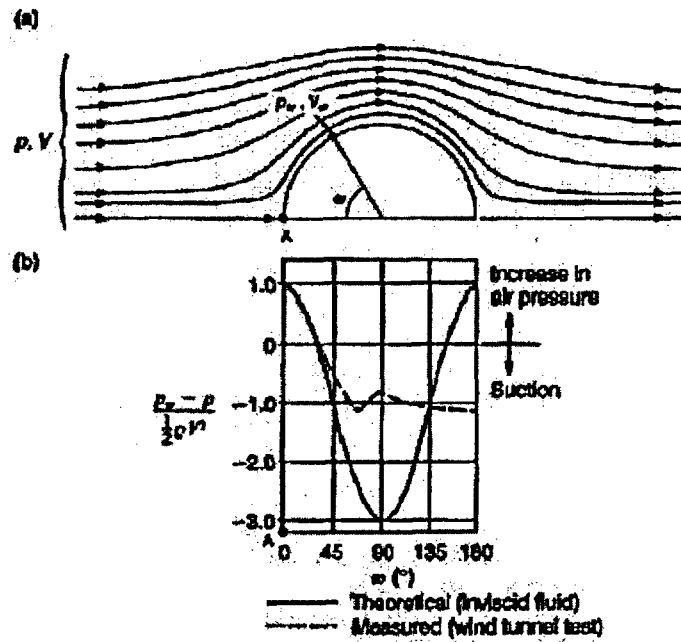


Figure 40: Pressure distribution on the surface of a cylinder (3)

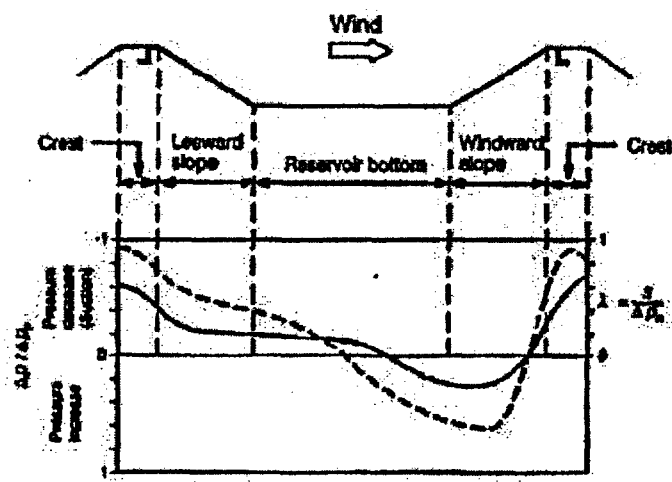


Figure 41: Wind blowing over an empty reservoir (3)

The authors presented equations validated by experimental data, relating the maximum available wind velocity to the required thickness, and strain induced in the geomembrane. Factors affecting geomembrane uplift are the wind velocity, altitude above sea level, and location of the membrane in the facility (the crest of a dike is a more sensitive location than the bottom). The membrane unit weight is also a very important parameter in the case of slow or medium speed wind: the heavier the geomembrane the less sensitive it is to wind effects.

High modulus material will deform less than the low modulus one, but will be affected by a larger tension. At low temperatures, the geomembrane will deform less but the internal forces will be greater. The authors also presented different means to prevent geomembrane uplift. The most effective procedure is to place a protective cover over the membrane (soil, rock, concrete slab or bituminous revetment). Sandbags spread over the liners are efficient only for low speed wind.

3.7.4 Rate of leakage through membranes

The EPA (4) provides a complete report on geomembrane liner leakage, that was based on studies made by Giroud and Bonaparte (11), Brown et al. (12), and Fukuoka (13, 14). The report lists the different methods of leakage through membranes, as well as the equations associated with leakage phenomena.

- Vapor diffusion through intact geomembrane is due to the liquid or vapor pressure difference on each side of the membrane. This transport takes place only at the molecular level, since the voids between the molecular chains of the polymer are very small. Darcy and Fick laws are used to establish the geomembrane leakage rate.
- Leakage through holes in geomembranes is due to the presence of flaws resulting from pinholes (generally polymerization deficiencies), seaming errors, abrasion and puncture. The rate of leakage of the leachate depends on the nature of contact between the geomembrane and the surrounding soil, the worst case corresponds to

free flow in the case of very poor contact, the better case corresponds to a perfect contact which decreases the leakage rate.

The following equations were derived:

For free flow:

$$q_{L1}(k)_i = K_g(k) \frac{h_g(k)_i T_g(k)}{T_g(k)} \dots\dots\dots[3.7.1]$$

where:

$q_{L1}(k)_i$ = geomembrane leakage rate by diffusion during time step i.

$K_g(k)$ = equivalent saturated hydraulic conductivity of geomembrane in subprofile k, (inches/day)

$h_g(k)_i$ = average hydraulic head on geomembrane liner in subprofile k during time step I, (inches)

$T_g(k)$ = thickness of geomembrane in subprofile k, (inches)

Free flow through geomembrane defects:

$$q_{L3}(k)_i = \frac{86,400 C_B n_3(k) a_3 \sqrt{2 g h_g(k)_i}}{4046.9} \dots\dots\dots[3.7.2]$$

where:

$q_{L3}(k)_i$ = leachate rate through defects in subprofile k during time step I (inches/day)

C_B = head loss coefficient for sharp edged orifices, 0.6

$n_3(k)$ = installation defect density for subprofile k, #/acre

a_3 = defect area, 0.0001 m²

$h_g(k)_i$ = average hydraulic head on geomembrane liner in subprofile k during time step I, (inches)

For pinholes in geomembrane with perfect contact:

$$q_{L2}(k)_i = \frac{\pi n_2(k) K_s(k) h_g(k)_i 0.04}{6,272,640}$$

.....[3.7.3]

where:

$q_{L2}(k)_i$ = leachate rate through pinholes in subprofile k during time step I, (in/day)

$N_2(k)$ = pinhole density for subprofile k, #/acre

$K_s(k)$ = saturated hydraulic conductivity of soil layer at the base of subprofile k, (in/day)

a_3 = defect area, 0.0001 m²

$h_g(k)_i$ = average hydraulic head on geomembrane liner in subprofile k during time step I, (in)

0.04 = diameter of a pinhole, 0.04 in

6,272,640 = units of conversion, 6,272,640 in² per acre

Leakage can occur vertically through the membrane or flow horizontally in-between layers of geomembranes and soil, causing soil erosion, Fig. 43.

Shivashankar et al. (6) reported experimental determination of flow patterns in geonets and presented new design formulation. The work was based on previous study by Giroud (7,8,9,10) who formulated an expression for the rate of leachate through liners. The experiments were done using a box mounted on a tilt-table, a constant flow was ensured by a system of tanks, Fig. 42. This study presents a new methodology for prediction of more accurate values of wetted areas in the geonet due to top liner leak, and also provides information on the probability of zero leakage into the ground. Finally, the authors developed modifications for the Giroud equations.

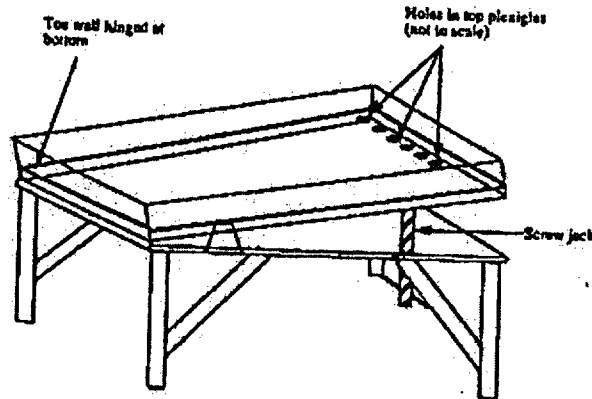


Figure 42: Schematic of a tilt-table (6)

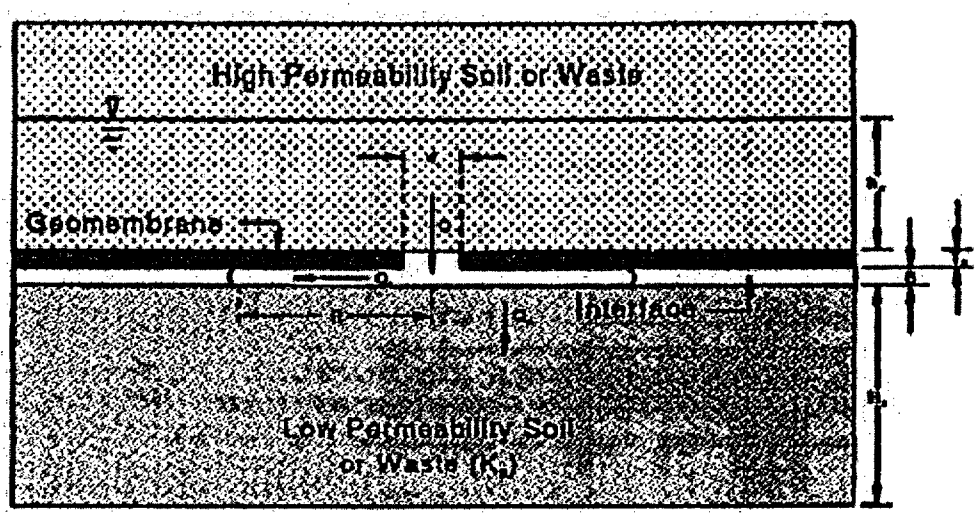


Figure 43: Horizontal flow between the soil and the geomembrane (4)

To conclude this section, reference must be made to the paper "Geomembrane Liners: Accidents and Preventive Measures" by Giroud (5), which summarizes all the problems that a geomembrane liner may encounter. The geomembrane deficiencies are listed for the different stages of the membrane life: manufacturing, fabrication, transportation, storage, placement, seaming, and placement of the material on geomembrane. The causes of the defects are listed for each stage.

Then the characteristics of the aging process are listed as follows: blistering, delaminating, cracking, increase of stiffness, shrinkage. The causes for induced distributed and concentrated stresses are as follows: uplift by wind, earth slides on slopes, erosion of

ground supporting the liner, punctures, abrasion, and tear. Finally the measures to solve the problems are outlined.

3.7.5 References

1. Rowe R.K., and Fraser M.J.: "Long-Term Behavior of Engineered Barrier Systems", Proceedings Sardina 93, pp.397-406.
2. Lord Jr A.E., Koerner R.M., and Wayne M.H.: "Residual Stress Measurements in Geomembrane Sheets and Seams", Geosynthetics 91, pp. 333-349.
3. Giroud J.P., Pelte T., and Bathurst: "Uplift of Geomembranes by Wind", Geosynthetics International, Vol. 2, No. 6, 1995, pp. 897-952.
4. Schroeder P.R.: "The Hydrologic Evaluation of Landfill Performance (HELP)" Ohio: Risk Reduction Engineering Laboratory, Office of Research and Development, U.S. Environmental Protection Agency, 1994, pp. 74-92.
5. Giroud J.P.: "Geomembrane Liners: Accidents and Preventive Measures", Proceedings of the International R.I.L.E.M. Symposium on Plastic and Rubber Waterproofing in Civil Engineering, 1987, pp. 1-6.
6. Shivashankar M., Fluet J.E., and Reddy D.V.: "Geonet Leakage Detection System Flow Patterns for Zero Leakage Estimation of Landfill Double Liner Systems", Proceedings, Geosynthetics Conference, Long Beach, Ca., 1997.
7. Giroud J.P., Gross B.A., and Durasse J.: "Flow in Leachate Collection Layers", in Design and Performance of Geosynthetic Lining Systems for Waste Containment, IFAI Publishers, St. Paul, MN, 1993.
8. Giroud J.P., and Bonaparte R.: "Leakage Through Liners Constructed with Geomembranes, Part I: Geomembrane Liners", Geotextiles and Geomembranes, Vol. 8, No.1, 1989, pp. 27-67.
9. Giroud J.P., and Bonaparte R.: "Leakage Through Liners Constructed with Geomembranes, Part II: Geomembrane Liners", Geotextiles and Geomembranes, Vol. 8, No.2, 1989, pp. 71-111.
10. Giroud J.P., Khatami A., and Badu-Twenaboah K.: "Evaluation of the Rate of Leakage Through Composite Liners", Geotextiles and Geomembranes, Vol. 8, No. 4, 1989, pp. 337-340.
11. Bonaparte R., Giroud J.P., and Gross B.A.: "Rate of Leachate Through Landfill Liners", Proceedings of Geosynthetics 1989 Conference, GeoServices Inc., San Diego Ca.
12. Brown K.W., Thomas J.C., Lytton L.L., Jayawikrama P., and Bahrt S.C.: "Quantification of Leak Rates Through Holes in Landfill Liners", 1987, Tyechnical Resource Document EPA/600/S2-87-062, US Environmental Protection Agency.

13. Fukuoka M.: "Outline of Large Scale Model Test on Waterproof Membrane"
Unpublished Report, 1985, Japan.
14. Fukuoka M.: "Large Scale Permeability Tests for Geomembrane Subgrade System"
Proceedings of the Third International Conference on Geotextiles, Volume 3, 1986,
Balkema Publishers.

4 Design, Construction, and Quality Program

4.1 Design

Koerner (1), devotes a complete section of his book to the design of landfill liners with geomembranes. The design consists of the following steps: site selection, geometric layout, geotechnical considerations, cross-section determination, geomembrane material selection, thickness determination, side-slope and cover soil details, anchor trench details, seam type decision, seam testing strategy, design of connections and appurtenances, leak scenarios and corrective measures, proper MQC (Manufacturing Quality Control) and CQC (Construction Quality Control), and finally proper MQA (Manufacturing Quality Assurance) and CQA (Construction Quality Assurance). The author provides detailed information on the different aspects of the liner design, and also summarizes the different problems to consider during design.

Richardson and Koerner (2) summarized the problems associated with the design of liners, Table 25.

Table 25: Problems Associated with Liner Design (2)

Problem	Liner Stress	Required Properties		Typical Factor of Safety
		Geomembrane	Landfill	
Liner self weight	tensile	$G, t, \sigma_{allow}, \delta_L$	β, H	10 to 100
Weight of filling	tensile	$t, \sigma_{allow}, \delta_L, \delta_u$	β, h, H, γ	0.5 to 10
Impact during construction	impact	I	D, W	0.1 to 5
Weight of landfill	Compression	σ_{allow}	γ, H	10 to 50
Puncture	puncture	σ_P	γ, H, P, A_p	0.5 to 10
Anchorage	tensile	$t, \sigma_{allow}, \delta_L, \delta_u$	β, γ, ϕ	0.7 to 5
Settlement of landfill	shear	τ, δ_u	β, γ, H	10 to 100
Subsidence under landfill	tensile	$t, \sigma_{allow}, \delta_L, \delta_u, \chi$	α, γ, H	0.3 to 10

where:

Geomembrane properties:

G = specific gravity

T = thickness

σ_{allow} = allowable strength

τ = shear strength

I = impact resistance

σ_P = puncture strength

δ_u = friction with material above

Landfill properties:

β = slope angle

H = landfill height

γ = unit weight

h = lift height

α = subsidence angle

ϕ = friction angle

d = drop height

δ_L = friction with material below
 χ = mobilization distance

W = weight
P = puncture force
 A_p = puncture area

Giroud et al. (3) described a design method based on strain calculations. Geomembranes are usually not structural elements, so it is more convenient to base the design on strain than stress. The first step is the determination of the maximum allowable strain ϵ_{max} . ϵ_{max} separates the safe part from the failure part of the membrane behavior. For HDPE, ϵ_{max} corresponds to the yield strain. This value may be determined using a biaxial test. In order to obtain a correct factor of safety, it is necessary to obtain an accurate ϵ_{max} .

The second step is the determination of the effective strain accounting for the stress concentration factor. Strains are induced by deformation of the membrane due to thermal contraction, differential settlement, etc.

Finally, the factor of safety was obtained by calculating the ratio of the maximum allowable strain to effective strain. Obviously, to ensure proper use of the membrane, the factor of safety must be larger than the one selected by the designer.

4.2 Safety Analysis

Heibrock and Jessberger (4) presented a safety analysis for a composite liner system, explaining the different properties that a safe liner should feature. These properties are listed in Table 26:

Table 26: Requirement of a Safe Liner System (4)

Requirements	Properties that need to be checked	Site specific influences
<p>Imperviousness</p> <p>Pollutant migration through the liner system should be comparable to that for a definable standard size</p>	<p>a) Permeability of the liner system hydraulic conductivity, diffusion coefficient, retention capacity</p> <p>b) Sensitivity of the system to imperfections</p>	<ul style="list-style-type: none"> hydraulic gradient kind of pollution amount of soluble pollutant concentration of pollutant in solution temperature <p>If a composite liner is considered:</p> <ul style="list-style-type: none"> kind of clay zone of higher permeability deformation or desiccation overburden loads
<p>Stability</p> <p>The liner system should be stable with respect to the mechanical influences</p>	<p>Shear resistance Cohesion (residual/non residual values)</p>	<p>Mechanical influences:</p> <ul style="list-style-type: none"> forces resulting from deformation forces resulting from overburden loads and

without significant change in its leachate behavior		inclination <ul style="list-style-type: none"> forces resulting from construction procedures
Resistance If proved that the lining system being exposed to the site specific influences is still stable and sufficiently impermeable.	Resistance to leachate Resistance to gas Resistance to temperatures	Chemical influences: <ul style="list-style-type: none"> kind of composition of leachate duration of exposure Thermal influences: <ul style="list-style-type: none"> low/high temperature duration of exposure
Combination of influences should be considered	Hydraulic resistance Resistance to exposure	hydraulic influences: <ul style="list-style-type: none"> forces resulting from water movements climate, hydrogeology of the site

The authors also presented the different criteria listed below to ensure the safety of the liner.

- **Description of the liner system:**
 Design of liner system, description of the materials and function of elements.
 Definition of requirements for the liner system and its elements.
- **Description of the basic landfill concept:**
 Type, amount, and geotechnical parameters of the waste, geometry of the waste disposal facility, hydrogeology and climate of the site, basic description of the operation phase (biological treatment, duration of waste placement, time of placement of the capping system, etc.), maintenance.
- **Assessment of the controlling factors:**
 Quantification of the controlling mechanical, thermal, chemical, biological, and hydraulic factors with respect to construction, operation, and the post-operation phase. Simplifying and idealizing assumptions may be necessary.
- **Description of the time-dependent development of the properties of the liner system**
- **Proof of the stability of the liner system**
- **Analysis of material properties after construction**
 Interpretation of test fields, description of varying properties

- Analysis of the leakage behavior of the liner system
Description of contaminant migration with respect to the assessed influences and the material properties after construction.
- Description of a monitoring program
Documentation of the operation phase, measurements to check the assumptions concerning the controlling factors.

As an example, the safety of a composite liner system made of HDPE geomembrane layer associated with a clay layer was studied. By analyzing the properties of the geomembrane and clay, before and after construction, and the assessment of the leakage behavior of the system it was concluded that this type of lining system (composite HDPE and clay) was very safe.

The estimated safe life of this lining system is approximately 80 to 100 years for the geomembrane, if no mechanical stress is induced by different mechanisms such as movement at the interface of the waste/geomembrane.

4.3 Construction/Installation

Voskamp et al. (5) listed the problems occurring during the installation of a liner. Those problems can be attributed to two separate causes: improper design and/or improper execution.

Problems due to improper design:

- The soil supporting the liner may cause a certain number of problems, depending on the degree of compaction, geometrical shape, or the presence or absence of a crust layer.
- The geomembrane is placed as a safety feature in an already designed system; the design of this system does not include the membrane, which can lead to a component that is exposed to a load larger than its capacity.
- Wrong installation can be extremely harmful; for example leaving a membrane exposed to sun radiation will damage its structure.
- Wrong requirement of the condition of the fill over the membrane may induce damage, since excessive compaction will increase the stress inside the material possibly leading to rupture.

Problems due to improper installation:

- The use of prefabricated sheets seems efficient as it requires less seams, but a major drawback is the difficulty to handle the roll which can weigh as much as 1500 kg.
- Exposed membranes will be damaged by weathering action, so they should always be protected from exposure.
- Installation not in accordance with the specifications, such as uncontrolled dumping of stone on membrane should not be allowed.
- It is possible that a different geomembrane from the specified one is installed which can lead to catastrophic consequences since the properties may differ totally. To prevent this problem the whole membrane roll should be marked.
- Damage during installation may result from equipment driven directly on the membrane, use of improper equipment (too heavy), improper handling of the membrane, or uncontrolled dumping of fill.

The book "Geotextiles and Geomembranes in Civil Engineering" (6) treats the design of geomembranes. The problems to be taken care of during the design are explained, and equations provided to determine the bearing capacity of the geomembrane submitted to normal, tensile, and shear forces. Also listed are the different failure mechanisms affecting the membrane's life, which can be avoided by proper design. These failure parameters (chemical attack, micro-organisms, UV radiation, etc.) have been addressed in chapter dedicated to geomembrane aging.

The authors also present some specific aspects for geomembrane installation: as indicated many times, the process of member fabrication and installation must be carried out with the greatest care to minimize the damage that may be induced. The ground on which the membrane is laid down must be stable, uniform, and free from sharp objects. The soil should also be uniformly compacted, using a Proctor test to verify the soil density. The installation site must be clean and free for easy access of the workers and equipment.

During the laying of the prefabricated sheet, special care must be taken to ensure that it is the correct side of the sheeting that faces up, also the sheet must be placed without tension or folds, and anchored properly. The sheet should be at least 5 m wide to minimize the seam areas. The seaming must be done carefully to decrease the possibility of flaws (the chapter dedicated to seams provides more detailed information).

The membrane interface conditions should ensure that no stress concentration is induced (since settlement differences induce stress concentrations). A good solution to prevent this problem is to use a flexible membrane, which can absorb the differences in settlement. Damaged geomembranes or seams can be repaired with a patch large enough to cover the flaws.

Fig. 44 to 46 give examples of some details that must be considered during design and construction. Fig. 44 presents the details of pipe penetration emphasizing the manner with which the liner covers the pipe and is attached to both the soil and pipe. Fig. 45 shows the

set-up of a roll spread bar that should be used when lining the geomembrane. Finally, Fig. 46 presents a U anchor trench of 15' deep x 2'.

Fabrication details:

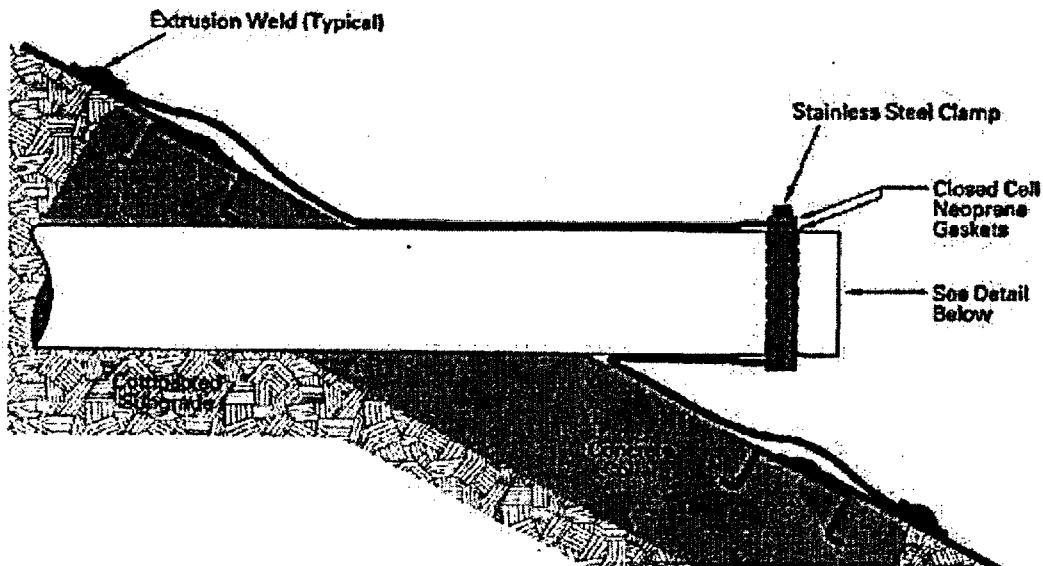


Figure 44: Pipe penetration (13)

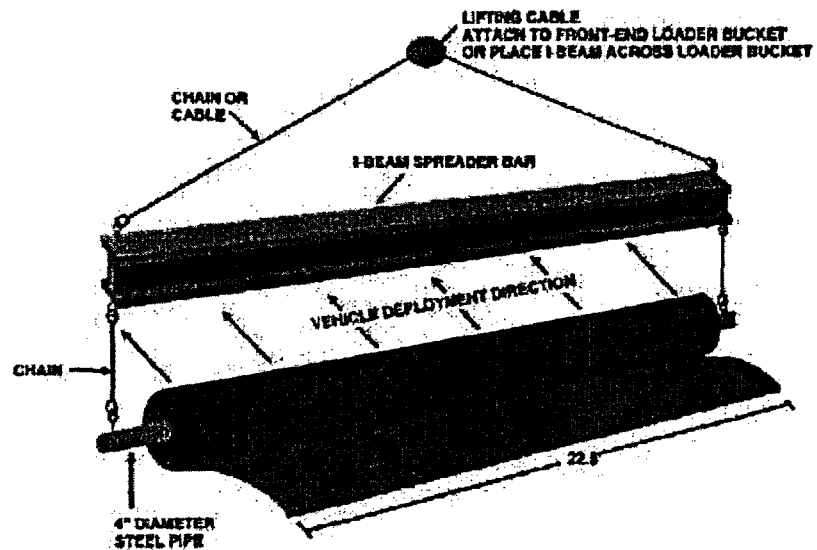


Figure 45: Roll spreader bar (13)

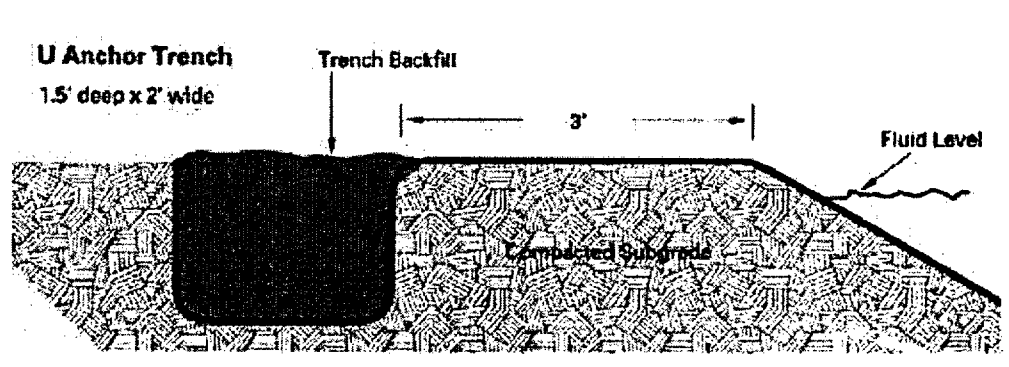


Figure 46: Anchor trench (13)

4.4 Quality Control

Inspections of the correct installation and functioning of the liner must be based on quality control (QC) and quality assurance (QA) criteria. Koerner (1) has defined the differences between the tools used for quality control:

- Manufacturing Quality Control (MQC) is a planned system of inspection specifically used for the control and monitoring of a product fabrication, usually followed by the geomembrane manufacturer.
- Manufacturing Quality Assurance (MQA) is a planned system of activities assuring the proper manufacturing of product vis-a-vis the specification document. This includes fabrication facility inspection, verifications, audits and inspections of the raw material. This is also the responsibility of the manufacturer.
- Construction Quality Control (CQC) is a planned system of inspection used to control and monitor the quality of a construction project by the geomembrane installer.
- Construction Quality Assurance (CQA) is a planned system of activity assuring that the facility is constructed according to the design.

In order to optimize quality control it is necessary to associate MQC/CQC and MQA/CQA., since MQA/CQA will allow the detection of flaws occurring during the MQC/CQC phase.

Fig. 47 presents the structural organization of MQC/CQC and MQA/CQA.

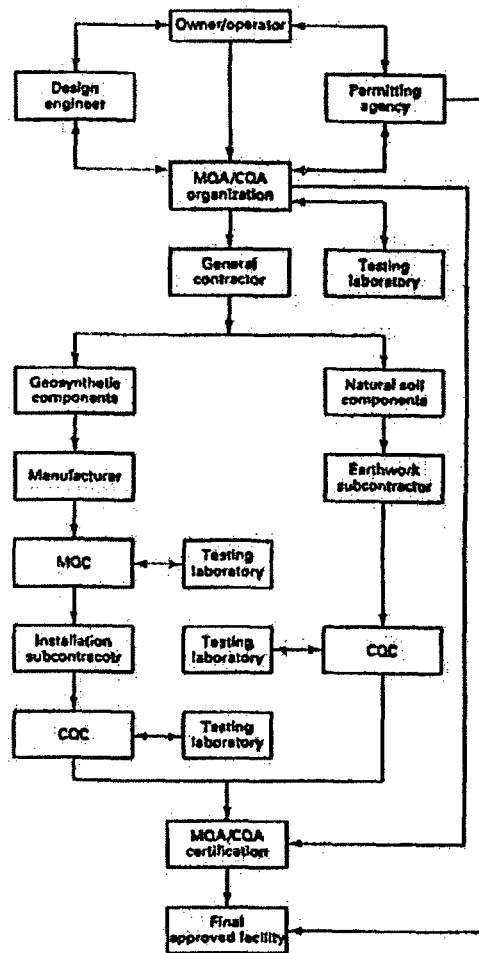


Figure 47: Structural organization of MQC/MQA and CQC/CQA (14)

The three basic components of a proper CQA program have been described by Giroud and Peggs (7) as follows:

- Conformance verification which ensures that the delivered geomembrane meets the specifications.
- Integrity verification, which ensures that the geomembrane is, installed to conform to the design and installation specifications.
- Survivability verifications, which ensure that the membrane will fulfill its functions in the expected time period.

Before shipping the geomembrane rolls to the installation site, a CQA plan must be adopted, and the following actions must be implemented:

- Visual inspection of the rolls.

- Carry out tests following the QC plan and sign the QC report to indicate the material conformity
- Remove and submit samples to the testing laboratory
- Monitor the loading of the roll for transport, only approved rolls should leave the plant.

Peggs (8) suggested the additional procedures to complete a CQA plan for the installation of HDPE. Those will reduce the stress cracking phenomena that mainly affect HDPE material:

- The slackness criterion must be incorporated into the design and construction of the liner, the amount of folds, and wrinkles must be minimized to a number close to zero.
- Damaged or improper seams must be repaired by extrusion seams, since it has been shown that re-seaming does not reduce the stress cracking resistance of the member.
- During the grinding operation, no defect larger than 10% of the sheet thickness must be left.
- Peel tests must be carried out on double hot wedge seams.

To ensure the proper design, installation, and functioning of a geomembrane, the following procedures must be carried out:

At the design stage:

- Select the two best geomembranes based on stress cracking and seam properties
- Select the best two based on chemical compatibility
- Chemical resistance evaluation must include both thermal and chemical structural analyses.

At the pre-construction stage:

- Monitor production and QC testing in the plant
- Perform testing before the rolls leave the plant

At the construction stage:

- Conduct destructive testing of the seams, and assess the shear and peel resistance of the seams
- Carried out non-destructive tests on seams: vacuum box, air pressure, ultrasonic, or electrical survey methods

At the post-construction stage:

- Conduct an electrical survey to detect holes in the geomembrane under drainage/ protective soil cover

A report by the Solid Waste Authority (9) lists all the factors that need to be taken into account in the fabrication and installation of a liner with minimum flaws.

Geomembrane quality control documentation:

- A meeting should be convened before the commencement of the work with the following participants involved in the installation of the liner:
 - owner's representative
 - field installation manager
 - installation manager
 - master seamer
 - contractor's representative
 - engineer's field representative
 - quality control laboratory representative
 - quality control technician
- The following documentation should be kept on site during the project duration:
 - start-up
 - liner pre-delivery
 - liner delivery
 - daily checklist
 - geomembrane panel placement
 - onsite geomembrane welding report
 - damage and failure report
 - post installation check list
 - daily field log
- Qualifications of the personnel:
 - The manufacturer must have proved his/her ability for the production of the liner: 5 years of continuous experience and fabrication of a minimum of 50 million square feet. The company should be certified and registered by NSF standard 54.
 - The installer should be the manufacturer or an approved installer.
- Packaging and shipping must be carried out with great care to prevent damage to the geomembrane.
- The rolls should be stored properly to protect them from puncture, dirt, yarn, water, moisture, mechanical abrasion, and excessive heat.
- The manufacturer should warranty the material against manufacturing defects for an exposed period of 20 years.
- The contractor should provide a two-year warranty against installation or workmanship defects.
- The material should be made of new prime first quality product. No pinholes, holes, blisters, or flaws must be present in the material. The rolls should be at least 22.65 feet seamless wide and labeled.

- Extrudate welding rods must be of the same compounds as that of the raw material.
- The quality control documentation should comprise the following:
 - origin identification and production of the resin
 - copies of quality control certificates issued by the resin supplier
 - Manufacturer's certification verifying that the quality of the resin used for the fabrication meets the specifications.
 - Identification of information for each roll: manufacturer name, product identification, thickness, roll number, and dimensions.
 - Quality control certificates featuring identification number, sampling procedure, frequency, and test results.
- Conformance testing (thickness, density, tensile properties, tear resistance, carbon black content and dispersion) must be carried out by an independent quality assurance laboratory.
- The surface sub-base must be smooth and uniform, without depression or protrusions larger than one inch, free from rocks, stones, or debris. No water must be present during installation and seaming.
- The installation of membranes should be done in the temperature range of 40 °F and 104 °F, and no installation should be done during precipitation, excessive moisture, or excessive wind.
- The panels must be rolled out and installed in accordance with the approval shop drawings, ensuring that the seams are perpendicular to the top of the slope. The engineer's field representative should inspect each panel, after placement and prior to seaming, for damage or defects. The sheets must not be dragged on a rough sub-base. The geomembrane must be anchored according to the drawings. The personnel working on the liner should not smoke, wear damaging shoes, or induce any damage.
- The edge of the membrane sheet must be bonded with weights to prevent uplift by wind. No vehicular traffic on the geomembrane should be permitted. All equipment must be placed on a protective layer, and must not remain on the geomembrane overnight.
- Seaming must be done in the temperature range of 40 °F and 104 °F.
- The field quality control consists of a start-up test to assess the seam quality and tune-up of the seaming equipment. Then non-destructive seam tests must be carried out on each seam using vacuum or air pressure tests. Finally, destructive seam testing must be carried out: one test sample per 500 feet of seam length; the location should be chosen by the engineer's field representative.

- Any flaw in the liner must be repaired as required by the engineer. The repair procedures include patching, spot welding or seaming, capping or replacement of seam with a strip of material welded in place.
- Any large wrinkles resulting from temperature expansion must be removed. To do this, the lower down-slope edge of the wrinkle should be cut, overlapped, and repaired.

Giroud and Peggs (10) presented an overview of the construction quality of geomembrane liner and summarized it in three steps:

- Verification and documentation by conforming tests that the geomembrane meets the specifications
- Verification and documentation by a number of monitoring operations, that the geomembrane is installed in conformance with the design and installation, and verification and documentation that the adjacent materials next to the geomembrane are placed according to the specifications.

The paper describes in detail the different steps and actions required to follow a correct quality assurance plan. The CQA operations are documented and compiled in a final report including, data, in situ reports, observations and records taken during the construction of the liner. An important part of this paper is dedicated to the seams, the mechanisms associated with seam failures, how to prevent those failures, and the different tests that establish the characteristics of the well being of a seam.

A CQA plan may vary from five to twenty percent of the cost of the material and construction of the geomembrane. However, this additional cost is justified by the increase of geomembrane and installation quality that decreases the material defects by a factor 30. The CQA plan allows a safer installation vis-a-vis the environment, which is probably the most important advantage of the plan even at relatively high cost.

Landreth (11) presented in detail the different type of seams, their uses, properties and applications to provide the required information for a proper QA/QC program (see Chapter "Seam" for more details). The EPA developed a quality manual to be followed for the proper design and installation of geomembranes. It has been proven, effectively, that the use of a QA/QC program during installation will significantly decrease the amount of leachate leakage in the landfill.

4.5 Cost of Quality Control

The cost of CQA and the different liner components have been summarized by Shepherd et al. (12) and are presented in Table 27:

Table 27: Typical Range of Quality Costs (12)

ITEM	TYPICAL RANGE OF COSTS
<i>Independent CQA:</i>	
single composite liner	\$31 000 - \$74 000/ha
double composite liner	\$52 000 - \$121 000/ha
1.5 mm HDPE liner	\$42 000 - \$62 000/ha
GCL	\$52 000 - \$74 000/ha
Extra Sump Liners	\$1 000 - \$5 000
Detection System, Sumps	\$15 000 - \$30 000
Extra Liner Under Pipes	\$25 000 - \$49 000/ha
30 cm Compacted Clay	\$12 000 - \$62 000/ha

Ha: Hectare

4.6 References

1. Koerner R.M.: Design with Geosynthetics, Prentice-Hill Inc., 1994, pp. 522-556.
2. Richardson G.N., and Koerner R.M.: "Geosynthetic Design Guidance for Hazardous Waste Landfill Cells and Surface Impoundments", EPA, Contract No. 68-03-3338, 1987.
3. Giroud J.P., Soderman K.L., and Monroe M.: "Mechanical Design of Geomembrane Applications", *Geosynthetics* 93, pp. 1455-1465.
4. Heibrock G., and Jessberger H.L.: "Safety Analysis of a Composite Liner System", *Proceedings Sardina* 95, pp. 169-183.
5. Voskamp W., Wichern H.A.M., and van Wijk W.: "Installation Problems with Geotextiles, an Overview of Producer's Experience with Designers and Contractors" *Geotextiles, Geomembranes and Related Products*, Den Hoedt (ed.), 1990, pp. 627-630.
6. Geotextiles and Geomembranes in Civil Engineering, Edited by Gerard Van Santvoort, 1994, pp. 516-575.
7. Giroud J.P., and Peggs I.D.: "Geomembrane Construction Quality Assurance", *Waste Containment Systems: Construction, Regulation and Performance*, *Geotechnical Special Publication No. 26*, ASCE, 1990, pp. 190-225.
8. Peggs I.D.: "Testing Program to Assure the Durability of Landfill Liners", *Proceedings Sardina* 91, pp. 651-665.
9. Camp, Dran, and McKee: "Contract forms and Specifications for Class I Landfill", prepared for Solid Waste Authority, BID #: SWA 77-202/JMD, August 1996.
10. Giroud J.P., and Peggs I.D.: Geomembrane Construction Quality Assurance, Waste Containment Systems: Construction, Regulation, and Performance, Edited by Rudolph Bonaparte, 1990.
11. Landreth R.E.: "Inspection Techniques for the Fabrication of Geomembrane Field Seams", EPA, Cincinnati, *Landfill and Solid Waste Treatment Technology* pp. 238-243.
12. Shepherd J.A., Rivette C.A., and Nava R.C.: "Landfill Liner CQA: A Summary of Real Costs and A Question of True Value", *Proceedings of the GRI Seminar MQC/MQA and CQC/CQA of Geosynthetics*, pp. 29-35, 1991.
13. Poly-Flex, Inc. Reference Manual, 1995, pp. 43, 54.

14. EPA, Technical Guidance Document: "Quality Assurance and Quality Control for Waste Containment Facilities", EPA/530/SW-93/182/May 93.

5 Life Prediction

5.1 Viscoelasticity

Plastics are viscoelastic materials, with deformation and strength properties varying with temperature and duration of loading. They are also affected by certain environmental conditions. As the name implies, viscoelastic materials respond to stress by superposition of elastic and viscous elements. The springs in the highly simplified model of Fig. 48 represent the elastic elements of a polymer (e.g., chain rigidity, chemical bonds, and crystallinity), each spring having a different constant that represents a time-independent modulus of elasticity. The dashpots represent the viscous fluid elements (e.g., molecules slipping past each other), each having a different viscosity or time-dependent response.

When a constant load is applied and sustained on this model, it results in an initial deformation, which continues to increase indefinitely, Fig. 49. This phenomenon of continuing deformation, which also occurs in concrete, soft metals, wood, and structural metals at very high temperatures, is called creep. If the load is removed after a certain time (say, at point t_i in Fig. 49), there is a rapid initial strain recovery, followed by a continuing recovery that occurs at a steadily decreasing rate; in this model the recovery is never complete. However, if the creep strain does not cause irreversible structural changes and sufficient time is allowed, the strain recovery will be almost complete. The rate and extent of deformation and recovery are sensitive to temperature, and can also be influenced by environmental effects such as absorption of solvents or other materials with which the plastics may have come in contact while under stress. An analogous response of viscoelastic materials is stress-relaxation. The initial load required to achieve a certain deformation will tend to gradually relax when that deformation is kept constant, Fig. 50. Initially, stress-relaxation occurs rapidly and then steadily decreases with increasing time.

HDPE is a viscoelastic material for which the history of deformation has an effect on the response. For example, if a load is continuously applied, it creates an instantaneous initial deformation that then increases over time. The stress and strain are related by a modulus that depends on the duration of load and magnitude of the applied stress at a given temperature, Fig. 51. Viscoelastic behavior becomes nonlinear at high stress or strain or elevated temperatures, exhibiting logarithmic decay of the modulus over time, Fig. 52.

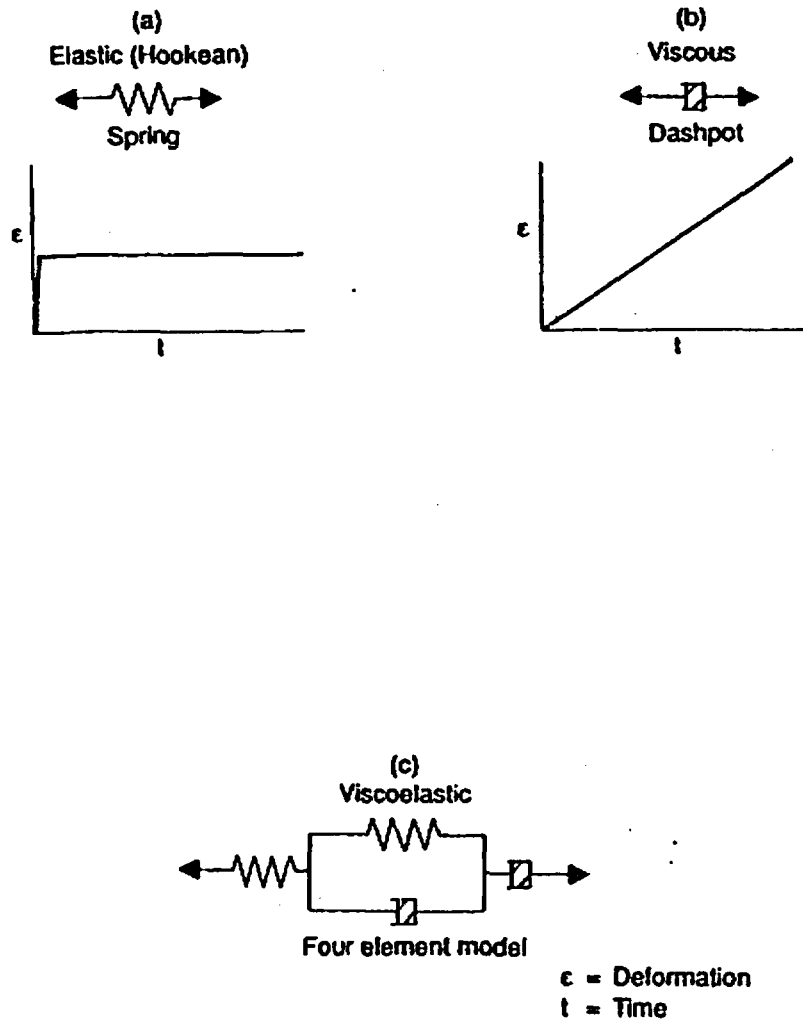


Figure 48: Model of viscoelastic behavior

Creep, expressed in terms of the increasing compliance contributing to increasing deformation, (i.e. loss of stiffness), and creep-rupture, expressed in terms of decreasing life with increasing stress and temperature, are important parameters for life prediction. The transition from ductile to brittle behavior enables the realistic estimation of life from the creep-rupture plot.

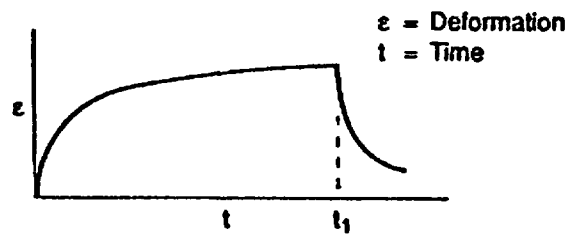


Figure 49: Viscoelastic response, creep (constant load)

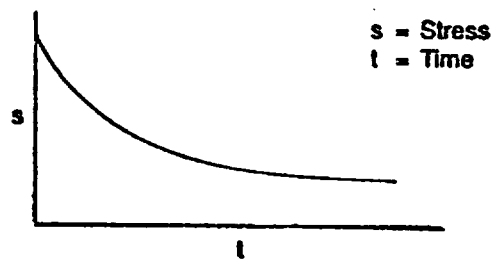


Figure 50: Viscoelastic response, stress relaxation (constant deformation)

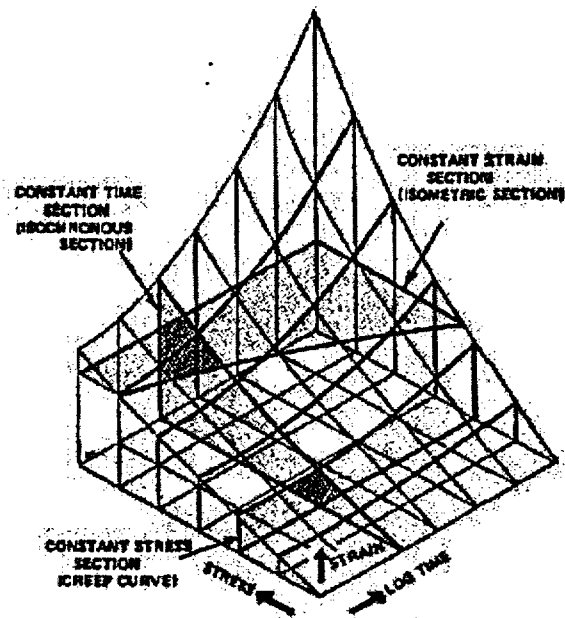


Figure 51: Constant stress-strain time coordinates (1)

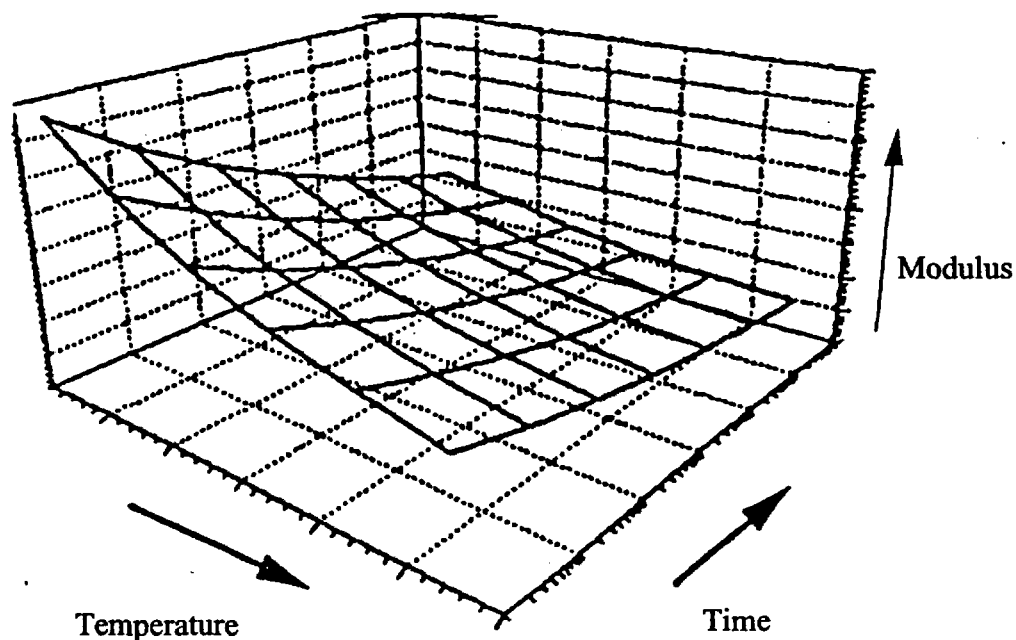


Figure 52: Schematic of the viscoelastic behavior of polymers

Woods et al. (2) conducted tensile creep-rupture testing on HDPE pipe material, based on ASTM D 638, and observed the occurrence of the ductile-brittle transition at a very early stage with a high stress level; no “knee” was seen in the tensile stress vs. time plot.

The predominant mode of premature failure of thermoplastic material, as indicated earlier is quasi-brittle fracture, initiated at stress concentrating surface notch geometries, imperfections (initial pinpoint depressions, etc.) and/or unexpected point stresses. Prediction of life, based on only long-term material properties, ignoring the geometry, would overestimate the predicted life. The creep and creep-rupture schematics for life prediction are shown in Fig. 53. It is necessary to identify unexpected failure-initiating defects, and to understand at what rate induced cracks will propagate, and how much they affect the reduction of service life.

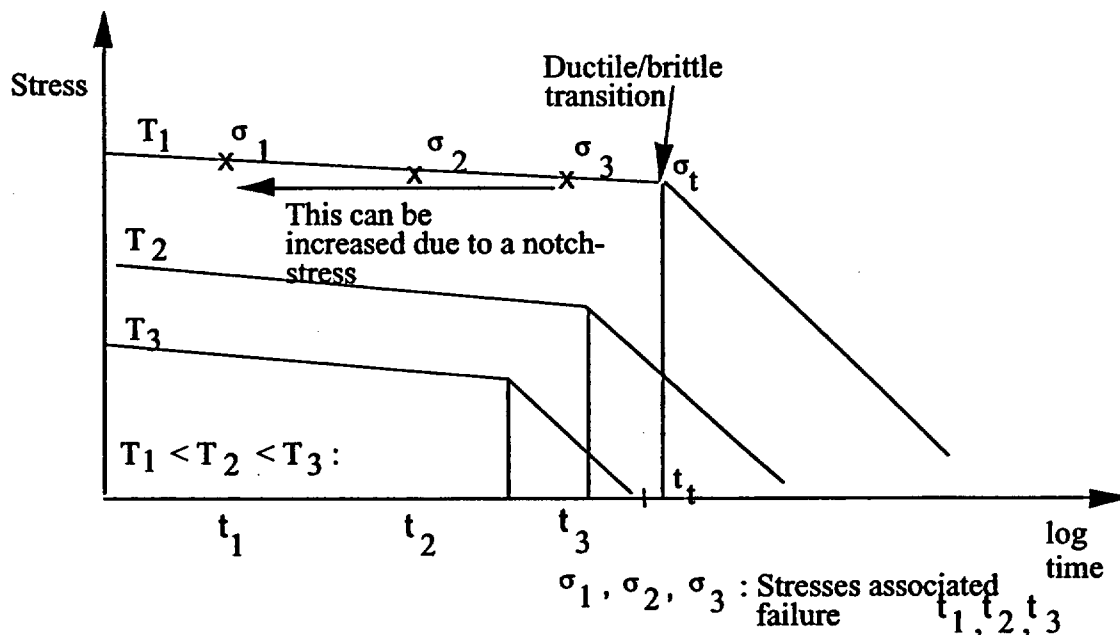


Figure 53: Creep-rupture behavior for semi-crystalline polymers (2)

5.2 Life Prediction

There is an identified need to investigate the long term behavior in relatively short laboratory time scale, by evaluating the effect of soil degradation mechanisms at field-related temperatures and stresses, compounded by synergistic effects, with accelerated testing, high stress, elevated temperatures, and/or aggressive liquids.

It is noteworthy that the type of thermoplastic material qualification testing, used for natural gas distribution piping has very effectively screened out one failure mode; ductile failure. This has been done by testing of pressurized pipe at temperatures and pressures that are well above the expected operating conditions. Because of the strong time and temperature dependence of polyethylene and other thermoplastic materials, it is both possible and necessary to accelerate the failure mechanism. The key is the use of time-temperature shifting functions that can reliably connect high temperature/high pressure performance to actual service conditions.

The long term properties can be predicted based on viscoelastic behavior: i) the time-temperature (WLF) superposition (3), which describes the equivalence of time and temperature, ii) the Arrhenius equation (4), which describes the temperature dependency of the degradation reaction on time and temperature, iii) the rate process method, describing which curve fits time-to-failure test data at elevated temperatures to enable predictions of times-to-failure at lower temperatures (5), and iv) the bidirectional shifting

method (5). Ahn and Reddy (8) have illustrated the application of WLF, Arrhenius, and Bidirectional Shifting Methods for HDPE piping.

5.2.1 WLF Method

Based on the time-temperature (WLF) superposition principle, for each of the three load levels, creep curves are plotted for different temperatures, and superposed by horizontal shifts along a logarithmic time scale to give a single curve covering a large range of times, termed a master curve. The shift factor, a_T' , is function of temperature and described as follows:

$$\log a_T' = [-C_1 \times (T - T_r)] / [C_2 + (T - T_r)] \dots \dots \dots [5.1]$$

where,

a_T' = shift factor

C_1 and C_2 = universal constants, which vary from polymer to polymer

T_r = reference temperature

T = absolute temperature.

The extended time-scale master curve enables the determination of the long term mechanical properties and service life, Fig. 54 (3). Fig. 55 shows the three master curves (modulus-time curves at three different stress levels) obtained by time shifting. The extrapolation equation for any other loading condition will be determined, similar to the procedure used for the Hydrostatic Design Basis (HDB) test described in the ASTM Standard D2837.

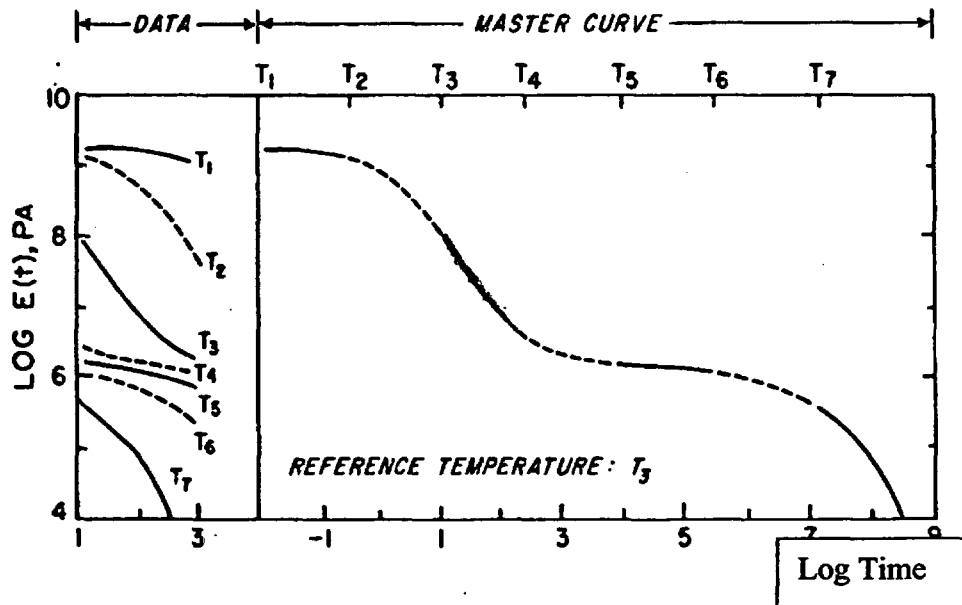


Figure 54: Master curve from experimentally measured modulus-time curves various temperatures (3)

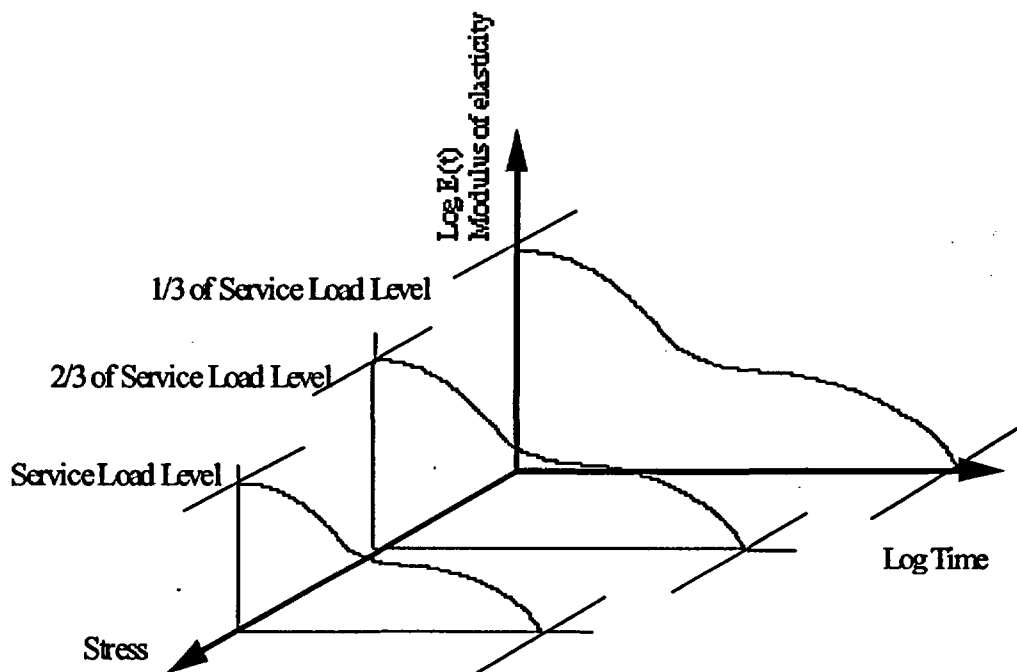


Figure 55: Master curves at different load levels

5.2.2 Arrhenius equation

A considerable amount of data shows that the rate of most chemical reactions has a strong dependence on the temperature and the concentration of reagents involved. In fact, such dependence can be used advantageously to develop relationships, which can be used for extrapolation purposes. A common form of this important extrapolation tool is as follows:

$$\ln (t/t_0) = (E_{act}/R)(1/T - 1/T_0) \dots\dots\dots [5.2]$$

where

t=time to given strength loss, usually 50%, at the test conditions

T=temperature of the test environment, in °K

t₀=time to the same given strength loss as for t, but in the in-situ environment

T₀=temperature of the in-situ environment, in °K

R=universal gas constant, which is 8.314 J/mole

E_{act}=effective activation energy, J/mole

In the Arrhenius plot, degradation is plotted as the logarithm of the reciprocal of time versus the reciprocal of temperature using the previous equation. A schematic plot is

provided in Fig. 56. It is noted that the temperature has an exponential effect on the time required for a specified level of degradation based on this model, and the data used in the previous equation is obtained at a constant level of degradation (indicated by the modulus decay) in the material. The extrapolation for failure time is similar to that used in the WLF Method. The WLF method and Arrhenius equation-based analyses are accurate for amorphous polymers, but catastrophic failure that occurs at ductile-brittle transition make the prediction difficult for semi-crystalline polymers. This problem should be addressed, and the life predictions given by the two methods compared, and their equivalence studied using the procedure developed by (6).

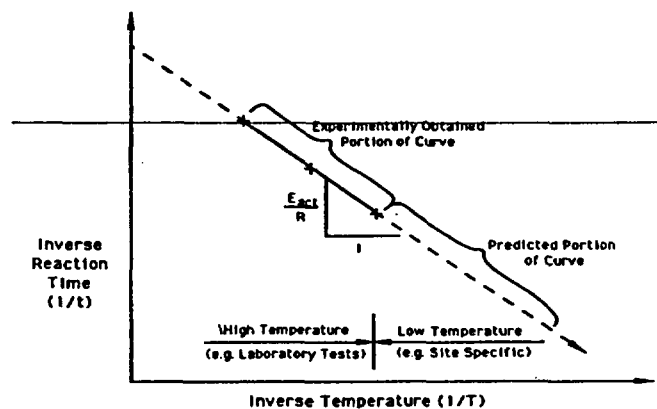


Figure 56: Generalized Arrhenius, for a specified stress level, used for life prediction from super-ambient temperature experimental data (7)

5.2.3 Rate Process Method (RPM)

The conventional time-temperature shifting procedure for pressurized pipe is the rate process method (RPM) which, in essence, curve fits time-to-failure test data at two elevated temperatures to enable predictions of times-to-failure at lower temperatures. The time to failure for thermoplastic pipe depends upon the operating temperature and the induced stress. The RPM has been used by the gas industry to extrapolate design parameters at the operating temperature from elevated temperature-based hydrostatic pressure tests of pipes (4) and (5). RPM, that has evolved from analyzing numerous test data, assumes that the time to failure is governed by an Arrhenius relation wherein the activation energy varies linearly with the logarithm of stress (4) and (5).

The RPM equation for the time to failure, t_f , at the absolute temperature, T , and hoop stress, σ , is expressed as follows:

$$\log t_f = A + (B/T) + (C/T) \log \sigma \dots \dots \dots [5.3]$$

An implication of this equation is that the data plots as a straight line in the $\log t - \log \sigma$ plane. The fitting of the previous equation requires that time-to-failure data be available for a minimum of two temperatures.

5.2.4 Bi-directional shifting method (BSM)

The bi-directional shifting method was introduced by Popelar and al. (5), as an alternative method to predict geosynthetic material's life. In this method no curve fitting is needed enabling a single data point, which represents any viscoelastic phenomenon determined at a given test temperature, to be shifted to another temperature.

Based on the time-temperature superposition principle, the horizontal and vertical shift functions, a_T and b_T , respectively, are given by the following equations:

$$a_T = \exp [-0.109(T-T_r)] \dots \dots \dots [5.4]$$

$$b_T = \exp [0.0116(T-T_r)] \dots \dots \dots [5.5]$$

5.3 REFERENCES

1. ASTM D 2990-93a: Standard Test Methods for Tensile, Compressive, and Flexural Creep, and Creep-Rupture of Plastics; Vol. 08.04, Plastic Pipe and Building Products, Annual Book of ASTM Standards, pp. 189-206, 1995.
2. Woods, D.W., Krause-Singh, J., and Hindman, J., "Estimation of Long-Term Stress Capacity of HDPE Materials by Tensile Stress-Rupture Testing," Technical Report, Hauser Laboratories, Boulder, CO, 1996.
3. Aklonis, J. J. and Macknight, W. J, "Introduction to Polymer Viscoelasticity", pp. 47-50, John Wiley and Sons, New York, 1983.
4. Koerner, R. M., "Design with Geosynthetics", Prentice Hall, Inc., 1994.
5. Popelar, C. H., "A Comparison of the Rate Process Method and the Bidirectional Shifting Method", Thirteenth Plastic Fuel Gas Pipe Symposium, San Antonio, TX, pp. 140-151, 1993.
6. Miyano, Yasushi "Long Term Prediction Method for Static, Creep, and Fatigue Strengths of CFRP Composites", Progress in Durability Analysis of Composite Systems, Fukuda and Reifsnider (eds.), 1996.
7. Koerner, R. M., Lord Jr., A. E., and Hsuan, Y. H., "Arrhenius Modeling to Predict Geosynthetic Degradation", Geotextiles and Geomembranes, Vol. 11, pp. 151-183, 1992.
8. Ahn W.S: "An Experimental and Analytical Investigation of Viscoelastic Pipe Soil interaction", PhD Dissertation supervised by D.V. Reddy, PhD, Florida Atlantic University, 1998.

6 Conclusions

Based on the review, the following conclusions are drawn for cost-effective use of landfill liner systems for long-term performance.

- 1) Creep can be considerably reduced using a resin, which is moderately affected by creep, and by proper design that limits the high stresses in the geomembrane.
- 2) Stress Cracking, the brittle fracture of a geosynthetic material under significantly lower stress than the material yield strength, can be minimized by using a UV and chemical resistant-resin and limiting high stress in the liner.
- 3) Static puncture, due to weight of the waste, can be prevented by using protective layers made of geonets and rounded soil particles, as well as stiff and thick geomembranes. Dynamic puncture, due to the fall of objects during construction, can be avoided by considerable care in construction (skilled workmanship is required).
- 4) Seam problems, mainly cracking, can be prevented by using proper equipment, proper seam geometry, adequate and constant temperature, skilled workmanship, and flaw inspection soon after the seam is completed.
- 5) Seismic and general stability of the landfill at the liner interface can be minimized by using a rough, stiff material under high vertical pressure, and by eliminating leakage at the interface level, since liquid decreases the shear properties of the interface.
- 6) Aging of geomembranes due to environmental conditions, such as temperature, UV, oxidation, and chemical agents, can be prevented or reduced by using proper material with adequate precaution to eliminate damage before installation.

Quality assurance and quality control procedures need to be developed and followed strictly to ensure safety of the liner systems. The criteria for design, construction, and maintenance are listed below:

- a) *Design*: Design a liner system with a composite liner made up of a geomembrane to prevent leaking, geogrids for leak collection; and a protection layer, comprised of either geosynthetics or fine aggregate material, to prevent puncture damage. Each material must be carefully chosen to reduce the creep, stress cracking, and aging phenomenon.
- b) *Installation*: Proper construction should be done with great care by skilled workmen and supervised following the design specifications.
- c) *Monitoring*: A proper and very detailed quality control plan should be followed throughout the entire life of the liner and landfill, to monitor the long-term performance with respect to liner integrity and landfill stability. This will significantly reduce liner damage-related risks.